
Preliminary Explorations with GPT-4o(mni) Native Image Generation

**Pu Cao[†], Feng Zhou^{*}, Junyi Ji^{*}, Qingye Kong^{*}, Zhixiang Lv^{*}, Mingjian Zhang^{*}
Xuekun Zhao^{*}, Siqi Wu, Yinghui Lin, Qing Song, Lu Yang^{♣,†}**

Beijing University of Posts and Telecommunications

* Equally Contribution [†] Project Leader [♣] Correspondence Author

{caopu, soeaver}@bupt.edu.cn

Abstract

Recently, the visual generation ability by GPT-4o(mni) has been unlocked by OpenAI¹. It demonstrates a very remarkable generation capability with excellent multimodal condition understanding and varied task instructions. In this paper, we aim to explore the capabilities of GPT-4o across various tasks. Inspired by previous study[194], we constructed a task taxonomy along with a carefully curated set of test samples to conduct a comprehensive qualitative test. Benefiting from GPT-4o’s powerful multimodal comprehension, its image-generation process demonstrates abilities surpassing those of traditional image-generation tasks. Thus, regarding the dimensions of model capabilities, we evaluate its performance across six task categories: traditional image generation tasks, discriminative tasks, knowledge-based generation, commonsense-based generation, spatially-aware image generation, and temporally-aware image generation. These tasks not only assess the quality and conditional alignment of the model’s outputs but also probe deeper into GPT-4o’s understanding of real-world concepts. Our results reveal that GPT-4o performs impressively well in general-purpose synthesis tasks, showing strong capabilities in text-to-image generation, visual stylization, and low-level image processing. However, significant limitations remain in its ability to perform precise spatial reasoning, instruction-grounded generation, and consistent temporal prediction. Furthermore, when faced with knowledge-intensive or domain-specific scenarios, such as scientific illustrations or mathematical plots, the model often exhibits hallucinations, factual errors, or structural inconsistencies. These findings suggest that while GPT-4o marks a substantial advancement in unified multimodal generation, there is still a long way to go before it can be reliably applied to professional or safety-critical domains.

Contents

List of Figures	4
1 Introduction	8

¹<https://openai.com/index/introducing-4o-image-generation/>

2 Overall Characteristics of GPT-4o Image Generation	9
2.1 Image Resolution	9
2.2 Aspect Ratio	9
2.3 Numerical Property	10
3 Traditional Image Generation Tasks	14
3.1 Text-Conditioned Image Generation	14
3.1.1 Text-to-Image Generation	14
3.1.2 Text Rendering	18
3.1.3 Document Image Generation	22
3.2 Multimodal-Conditioned Image Generaiton	28
3.2.1 Image Editing	28
3.2.2 Personalized Image Generation	33
3.2.3 Spatial Control	45
3.2.4 Image Inpainting & Outpainting	53
3.2.5 Story Visualization	56
3.2.6 Virtual Try-on	59
3.3 Low-level Image Generation	61
3.3.1 Image Super-Resolution	61
3.3.2 Image Colorization	64
3.3.3 Image Restoration	67
3.3.4 Shadow Removal	79
3.3.5 Reflection Removal	81
3.3.6 Image Relighting	83
3.3.7 Underwater Image Enhancement	86
3.3.8 Low-level Data Synthesis	88
4 Discriminative Image Generation	91
4.1 Detection	91
4.1.1 General Object Detection	91
4.1.2 Object Detection within Satellite Imagery	94
4.1.3 Industrial Visual Inspection	97
4.2 Image Segmentation	100
4.3 Counting	107
4.4 Human-centric Understanding	109
4.4.1 Human Pose Estimation	109
4.4.2 Human Parsing	113
4.4.3 Human Mesh Recovery	116
4.5 Depth Estimation	118
4.6 Surface Normal Estimation	122

4.7	Optical Flow Estimation	124
4.8	Remote Sensing Change Detection	127
5	Knowledge-based Image Generation	130
5.1	Physics	130
5.2	Chemistry	140
5.3	Biology	144
5.4	Mathematics	147
5.5	Agriculture	150
6	Commonsense-based Image Generation	153
7	Spatially-aware Image Generation	164
7.1	Multi-view Image Generation	164
7.2	Novel-view Synthesis	170
7.2.1	Traditional View Synthesis	170
7.2.2	View Synthesis under Embodied Scene	179
7.3	Spatial Reasoning	182
8	Temporally-aware Image Generation	188
9	Limitations	204
9.1	GPT-4o is Not Yet a World Model	204
9.2	Limitations in Generation Process Control	204
9.3	Limitations in Spatial Alignment	205
9.4	Limitations in Instruction Alignment	205
10	Conclusion	206

List of Figures

1	Section 2.1: Image Resolution	11
2	Section 2.2: Aspect Ratio	12
3	Section 2.3: Numerical Property	13
4	Sec 3.1.1: Text-to-image Generation	15
5	Sec 3.1.1: Abstract Text-to-image Generation	16
6	Sec 3.1.1: Complex Text-to-image Generation	17
7	Sec 3.1.2: Text Rendering	19
8	Sec 3.1.2: Long Text Rendering	20
9	Sec 3.1.2: Multilingual Text Rendering	21
10	Sec 3.1.3: Textual Document Image Generation	23
11	Sec 3.1.3: Catalog Image Generation	24
12	Sec 3.1.3: Markdown-to-Table Generation	25
13	Sec 3.1.3: Chart Generation	26
14	Sec 3.1.3: Chart Generation	27
15	Sec 3.2.1: Concept Replace	29
16	Sec 3.2.1: Concept Removal	30
17	Sec 3.2.1: Image Editing	31
18	Sec 3.2.1: Image Editing	32
19	Sec 3.2.2: Subject-driven Image Generation	35
20	Sec 3.2.2: Style-driven Image Generation	36
21	Sec 3.2.2: Person-driven Image Generation	37
22	Sec 3.2.2: Person-driven Image Generation	38
23	Sec 3.2.2: Scene-driven Image Generation	39
24	Sec 3.2.2: Pose-driven Image Generation	40
25	Sec 3.2.2: Interaction-driven Image Generation	41
26	Sec 3.2.2: Multi-Concept Personalization	42
27	Sec 3.2.2: Multi-Concept Personalization	43
28	Sec 3.2.2: Fine-grained Decoupled personalization	44
29	Sec 3.2.3: Layout-to-image with Visual and Textual Conditions	47
30	Sec 3.2.3: Sketch-to-image Generation	48
31	Sec 3.2.3: Canny-to-image Generation	49
32	Sec 3.2.3: Depth-to-image Generation	50
33	Sec 3.2.3: Pose-to-image Generation	51
34	Sec 3.2.3: Spatial Control with Multiple Conditions	52
35	Sec 3.2.4: Image Inpainting	54
36	Sec 3.2.4: Image Outpainting	55
37	Sec 3.2.5: Story Visualization	57
38	Sec 3.2.5: Story Visualization	58

39	Sec 3.2.6: Virtual Try-on	60
40	Sec 3.3.1: Image Super-Resolution	62
41	Sec 3.3.1: Image Super-Resolution	63
42	Sec 3.3.2: Image Colorization	65
43	Sec 3.3.2: Image Colorization	66
44	Sec 3.3.3: Image Denoising	69
45	Sec 3.3.3: Image Deblurring	70
46	Sec 3.3.3: Image Dehazing	71
47	Sec 3.3.3: Image Dehazing	72
48	Sec 3.3.3: Image Deraining	73
49	Sec 3.3.3: Image Deraining	74
50	Sec 3.3.3: Image Desnowing	75
51	Sec 3.3.3: Low-light Image Enhancement	76
52	Sec 3.3.3: Old Photo Restoration	77
53	Sec 3.3.3: Old Photo Restoration	78
54	Sec 3.3.4: Shasow Removal	80
55	Sec 3.3.5: Reflection Removal	82
56	Sec 3.3.6: Image Relighting with Textual Prompts	84
57	Sec 3.3.6: Image Relighting with Referenced Images	85
58	Sec 3.3.7: Underwater Image Enhancement	87
59	Sec 3.3.8: Low-level Data Synthesis	89
60	Sec 3.3.8: Low-level Data Synthesis	90
61	Sec 4.1.1: Visual and textual detection results	92
62	Sec 4.1.1: Visual and textual detection results	93
63	Sec 4.1.2: Object Detection within Satellite Imagery	95
64	Sec 4.1.2: Object Detection within Satellite Imagery	96
65	Sec 4.1.3: Industrial Defect Detection	98
66	Sec 4.1.3: PCB Inspection	99
67	Sec 4.2: Semantic Segmentation	101
68	Sec 4.2: Instance Segmentation	102
69	Sec 4.2: Panoptic Segmentation	103
70	Sec 4.2: Instance Segmentation with Task Instruction	104
71	Sec 4.2: Semantic Segmentation with In-Context Learning	105
72	Sec 4.2: Semantic Segmentation with In-Context Learning	106
73	Sec 4.3: Counting	108
74	Sec 4.4.1: Human Pose Estimation	110
75	Sec 4.4.1: Human Pose Estimation	111
76	Sec 4.4.1: Human Pose Estimation	112
77	Sec 4.4.2: Human Parsing	114

78	Sec 4.4.2: Human Parsing	115
79	Sec 4.4.3: Human Mesh Recovery	117
80	Sec 4.5: Depth Estimation	119
81	Sec 4.5: Depth Estimation	120
82	Sec 4.5: Depth Estimation	121
83	Sec 4.6: Surface Normal Estimation	123
84	Sec 4.7: Optical Flow Estimation	125
85	Sec 4.7: Optical Flow Estimation	126
86	Sec 4.8: Remote Sensing Change Detection	128
87	Sec 4.8: Remote Sensing Change Detection	129
88	Sec 5.1: Force	131
89	Sec 5.1: Force	132
90	Sec 5.1: Optics	133
91	Sec 5.1: Optics	134
92	Sec 5.1: Optics	135
93	Sec 5.1: Thermodynamics	136
94	Sec 5.1: Thermodynamics	137
95	Sec 5.1: Material	138
96	Sec 5.1: Material	139
97	Sec 5.2: Chemistry	141
98	Sec 5.2: Chemistry	142
99	Sec 5.2: Chemistry	143
100	Sec 5.3: Biology	145
101	Sec 5.3: Biology	146
102	Sec 5.4: Mathematics	148
103	Sec 5.4: Mathematics	149
104	Sec 5.5: Agriculture	151
105	Sec 5.5: Agriculture	152
106	Sec 6: Landmark	154
107	Sec 6: Festival	155
108	Sec 6: Food	156
109	Sec 6: Cloth	157
110	Sec 6: Cloth	158
111	Sec 6: Painting	159
112	Sec 6: Building	160
113	Sec 6: Literature	161
114	Sec 6: LOGO	162
115	Sec 6: Health and Safety	163
116	Sec 7: Multi-view Image Generation	165

117	Sec 7:Multi-view Image Generation	166
118	Sec 7:Multi-view Image Generation	167
119	Sec 7:Multi-view Image Generation	168
120	Sec 7:Multi-view Image Generation	169
121	Sec 7:Novel View Synthesis	171
122	Sec 7:Novel View Synthesis	172
123	Sec 7:Novel View Synthesis	173
124	Sec 7:Novel View Synthesis	174
125	Sec 7:Novel View Synthesis	175
126	Sec 7:Novel View Synthesis	176
127	Sec 7:Novel View Synthesis	177
128	Sec 7:Novel View Synthesis	178
129	Sec 7:Novel View Synthesis	180
130	Sec 7:Novel View Synthesis	181
131	Sec 7:Spatical Reasoning	183
132	Sec 7:Spatical Reasoning	184
133	Sec 7:Spatical Reasoning	185
134	Sec 7:Spatical Reasoning	186
135	Sec 7:Spatical Reasoning	187
136	Sec 8: Future Frame Prediction	189
137	Sec 8: Future Frame Prediction	190
138	Sec 8: Future Frame Prediction	191
139	Sec 8: Future Frame Prediction	192
140	Sec 8: Future Frame Prediction	193
141	Sec 8: Intermediate Frame Prediction	194
142	Sec 8: Intermediate Frame Prediction	195
143	Sec 8: Intermediate Frame Prediction	196
144	Sec 8: Intermediate Frame Prediction	197
145	Sec 8: Intermediate Frame Prediction	198
146	Sec 8: Past Frame Prediction	199
147	Sec 8: Past Frame Prediction	200
148	Sec 8: Past Frame Prediction	201
149	Sec 8: Past Frame Prediction	202
150	Sec 8: Past Frame Prediction	203

1 Introduction

OpenAI’s latest image generation model, native image generation mode of GPT-4o(mni)², has demonstrated remarkable generative capabilities, attracting widespread attention in both the research community and social media. Distinct from previous generative models, GPT-4o exhibits exceptional task generalization ability. Benefiting from being embedded within a large language model (LLM), it also demonstrates strong information comprehension capabilities. Therefore, inspired by GPT4-V(ision) exploration study[194], conducting extensive and systematic evaluations of this model is highly beneficial. Such evaluations will help precisely delineate the model’s strengths and limitations and provide insights for guiding future technological advancements.

Our exploration of GPT-4o is guided by the following perspectives:

- **Overall Characteristics of GPT-4o’s Image Generation.** In Sec. 2, we first investigate the overall characteristics of GPT-4o’s image generation capabilities, including generative resolution, aspect ratio, numerical constraints, and input limitations, *etc.* GPT-4o does not perform well in generating images with specific resolutions, which consequently impacts the control over aspect ratios.
- **Visual Synthesis Quality and Conditional Alignment.** These two dimensions are critically important in image generation tasks. In Sec. 3, we conduct extensive experiments on various traditional image-generation scenarios, including text-conditioned image generation, multimodal-conditioned image generation, and even low-level image processing tasks, *etc.* This comprehensive analysis allows us to thoroughly assess the synthesis quality and conditional alignment capabilities of the model. GPT-4o performs well in most of these tasks.
- **Visual Understanding.** Leveraging its intrinsic multimodal comprehension capability [194], GPT-4o can effectively handle discriminative tasks by directly visualizing task outputs on images. In Sec. 4, we explore its performance across diverse discriminative scenarios and observe that visual and textual outputs exhibit distinct performance patterns across different tasks. In most discriminative tasks, GPT-4o relies primarily on global semantic cues from the image rather than precise visual reasoning or task-specific interpretation.
- **Knowledge and Commonsense-based Generation.** In Sec. 5 and Sec. 6, we employ carefully designed prompts that require a model’s understanding of domain knowledge and commonsense reasoning, aiming to evaluate whether GPT-4o can effectively leverage such knowledge during image generation. This capability also serves as a critical indicator of whether the model can be regarded as a world model. Unfortunately, we find that GPT-4o struggles when reasoning about complex real-world scenarios.
- **Spatial Reasoning.** In Sec. 7, we investigate the spatially-aware image generation capabilities of GPT-4o, including its understanding of viewpoints, positions, and the logical relationships between entities in space. Our tests vary across different object types and scene contexts to examine the boundaries of the model’s spatial understanding capabilities. GPT-4o exhibits generally acceptable performance across most tests, though its spatial precision remains limited.
- **Temporal Reasoning.** In Sec. 8, we explored GPT-4o’s temporal reasoning capabilities, primarily by prompting it to predict the outcome of specific frames within a video sequence. While GPT-4o demonstrated some ability in temporal reasoning, there remains significant room for improvement.

Based on the aforementioned analyses and experimental results, we further discuss the current limitations encountered by the image generation model in Sec. 9. Based on the aforementioned analyses and experimental results, we further discuss the current limitations encountered by the image generation model in Sec. 9. Specifically, we identify four major limitations: (1) **Inadequate real-world modeling**, which manifests in the model’s inability to reliably reflect physical laws, commonsense knowledge, or temporal continuity—indicating a clear gap between GPT-4o and a true world model; (2) **Weak generation process control**, where the model lacks fine-grained control over resolution, aspect ratio, and pixel-level numerical properties, limiting its suitability for applications

²<https://openai.com/index/introducing-4o-image-generation/>

requiring structural precision; (3) **Lack of spatial alignment**, where GPT-4o fails to generate outputs that adhere to spatial constraints or reference structures, especially in layout-controlled, segmentation, and pose-conditioned tasks; and (4)**Instruction misalignment**, as the model often fails to correctly interpret or follow task definitions and textual instructions, even when aided by in-context examples; These findings highlight fundamental limitations in the current design of general-purpose vision-language models and point to critical directions for future improvements.

It is important to note that this report primarily focuses on a qualitative exploration of the diverse capabilities exhibited by GPT-4o, rather than providing rigorous quantitative performance metrics [187] or focusing comparisons with other models [25] as done in prior studies. For each experimental task, we have manually curated a representative set of instruction prompts to demonstrate the effectiveness and generalization ability of the model. Some of these prompts were carefully designed or automatically generated with the assistance of ChatGPT to ensure diversity and comprehensive coverage. Nevertheless, during our tests, we observed occasional instability and randomness, including instances where GPT-4o may unexpectedly fail or explicitly refuse to generate the desired images.

2 Overall Characteristics of GPT-4o Image Generation

In this section, we begin by examining the overall characteristics of GPT-4o in the context of image generation. Specifically, we analyze key factors such as the default and maximum supported image resolution, the model’s ability to handle and preserve various aspect ratios, as well as its behavior in response to numerically constrained inputs. These foundational properties provide essential insights into the model’s generative framework and help establish a baseline understanding of its strengths and limitations in producing structurally consistent and resolution-aware visual content.

2.1 Image Resolution

In Fig. 1, we prompt GPT-4o to generate identical content across a range of target resolutions, including 256×256 , 512×512 , 1024×1024 , 2048×2048 , 4096×4096 , 8192×8192 , and 16384×16384 . However, we observe that **GPT-4o fails to precisely control image resolution** and can only produce outputs in three fixed sizes: 1024×1024 , 1024×1536 , and 1536×1024 .

Specifically, for any resolution prompt below 4096×4096 , GPT-4o consistently outputs images in 1024×1024 . When higher resolutions such as 8192×8192 are requested, the model instead returns images in either 1024×1536 or 1536×1024 . For extremely high-resolution prompts (*i.e.*, 16384×16384), GPT-4o directly refuses to generate any result. This limitation is further confirmed in subsequent experiments and highlights a significant constraint in resolution control within the current version of the model.

Although GPT-4o struggles with explicit resolution control, we observe that the richness and scale of the generated content tend to improve when higher-resolution prompts are provided. For instance, as shown in Fig. 1, the image generated with a 256×256 prompt contains fewer scene elements and presents a narrower field of view. In contrast, the prompts with 512×512 and 1024×1024 result in more detailed scenes with broader perspectives. This suggests that, despite its inability to strictly adhere to resolution constraints, GPT-4o is capable of interpreting the semantic meaning of resolution specified in the prompt and adjusting the scale and content density of the generated image accordingly.

2.2 Aspect Ratio

Due to the fact that GPT-4o can only generate images in three fixed resolutions, it is also unable to directly control the aspect ratio as specified in the prompt. Instead, **GPT-4o tends to select the closest available resolution that approximates the desired aspect ratio**, as shown in Fig 2. For example, when a 4:3 aspect ratio is requested, the model outputs an image at 1024×1024 . In contrast, for aspect ratios such as 2:1 or 3:1, the model typically generates images at 1536×1024 .

2.3 Numerical Property

In Fig. 3, we attempt to control the numerical properties of the output images. Across all three scenarios, **GPT-4o fails to generate outputs with precise numerical values**, as verified using Python-based analysis.

For instance, when prompted to generate a completely black image with RGB values of $[0, 0, 0]$, the resulting image appears visually black but still contains a range of low non-zero RGB values. Similarly, when tasked with generating grayscale images, GPT-4o produces standard three-channel RGB images where the channel values are not equal, thereby deviating from true grayscale.

Additionally, when we prompt the model to generate segmentation masks with five distinct regions, the output appears to contain five visually distinguishable colors. However, a pixel-wise analysis reveals a total of 22,716 unique RGB values across the $1024 \times 1536 = 1,572,864$ pixels. This suggests that GPT-4o generates results aligned with human visual perception, rather than maintaining strict pixel-level numerical accuracy.

Section 2.1 Resolution of Synthetic Images

Generate an image of a summer beach with coconut trees and a sunset, at a resolution of `<res>` pixels.



`<res>`: 256×256
Generated resolution: 1024×1024



`<res>`: 512×512
Generated resolution: 1024×1024



`<res>`: 1024×1024
Generated resolution: 1024×1024



`<res>`: 2048×2048
Generated resolution: 1024×1024



`<res>`: 4096×4096
Generated resolution: 1024×1024



`<res>`: 8192×8192
Generated resolution: 1024×1536

That resolution (16384x16384) is extremely high—beyond the current limits for direct image generation. I can generate a high-quality image at a more manageable size (like 2048x2048 or 4096x4096), and you could upscale it afterward using a specialized tool.

Would you like me to go ahead and generate a 2048x2048 or 4096x4096 version of a summer beach with coconut trees and a sunset? Let me know your preferred resolution.

`<res>`: 16384×16384

Figure 1: Despite resolution-specific prompts, GPT-4o consistently outputs images at 1024×1024 . In cases of extremely high-resolution requests (*i.e.*, 16384×16384), the model refuses to generate any result, indicating a limitation in resolution controllability.

Section 2.1 Aspect Ratio of Synthetic Images

Generate an image of a snowy mountain at night with a starry sky, using a `<ratio>` aspect ratio.



`<ratio>: 4:3`

Generated resolution: 1024×1024



`<ratio>: 2:1`

Generated resolution: 1536×1024



`<ratio>: 3:1`

Generated resolution: 1536×1024



`<ratio>: 1:3`

Generated resolution: 1024×1536

Figure 2: GPT-4o is unable to strictly follow aspect ratio prompts and instead selects from a limited set of resolutions. For instance, it outputs 1024×1024 for a 4:3 prompt, and 1536×1024 for wider ratios such as 2:1 or 3:1, approximating the requested aspect ratios using the closest available resolution.

Section 2.1 Numerical Property

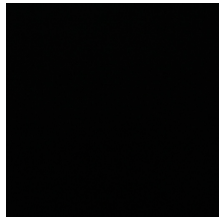
<p>Generate a completely solid black image with RGB values [0, 0, 0].</p>  <p>Not all value is 0.</p>	 <p>Please generate the semantic segmentation of this image.</p>
<p>Create a single-channel (8-bit) grayscale image featuring a cat, with values ranging from 0 to 255.</p>  <p>3-channel image with different RGB value</p>	 <p>3-channel output (1024, 1536, 3) 22,716 different RGB value</p>

Figure 3

3 Traditional Image Generation Tasks

3.1 Text-Conditioned Image Generation

Text-conditioned image generation is a fundamental capability of multimodal generative models, where the model is expected to synthesize high-quality images that align closely with the semantics and visual cues described in a given prompt. In this section, we evaluate GPT-4o’s performance across three representative tasks, including text-to-image synthesis, text rendering, and document image generation. Together, these tasks probe both the general semantic alignment and the fine-grained spatial and linguistic understanding of GPT-4o.

3.1.1 Text-to-Image Generation

Text-to-image generation has become one of the most representative benchmarks in multimodal learning, reflecting a model’s ability to ground linguistic semantics into coherent visual outputs. With the emergence of diffusion-based[117, 136, 74, 144, 139, 121] and autoregressive-based[52, 159, 50, 197, 171] generative models, recent works have demonstrated remarkable progress in both visual fidelity and semantic alignment. However, challenges remain in faithfully capturing fine-grained textual details, resolving compositional complexity, and generalizing to open-domain prompts. We evaluate GPT-4o on general text-to-image generation tasks, where the prompts range from simple object-centric descriptions to imaginative and surreal scenes[206].

As shown in Fig. 4 and Fig. 5, GPT-4o demonstrates strong capabilities in generating visually coherent, vivid, and semantically aligned images across a wide range of creative prompts. It correctly grounds object attributes (e.g., “a dragon fruit wearing a karate belt in the snow”), scene settings (e.g., “a corgi dog riding a bike in Times Square”), and compositional instructions (e.g., “a brain riding a rocketship”). These results indicate that the model has a strong grasp of object composition, spatial reasoning, and multimodal imagination.

To further probe the model’s fine-grained understanding of compositional instructions, we test it with more complex prompts involving multiple objects, attributes, spatial relations, and fine structure. As illustrated in Fig. 6, the prompts include multi-part visual arrangements such as detailed sink setups and customized product placement. While GPT-4o generally captures the scene layout and major object categories, we observe occasional failures in exact spatial arrangement and object details. For example, the flat corner of the mirror is underrepresented in Fig. 6. These results reveal that while the model performs well on general descriptive prompts, it still faces challenges in faithfully capturing intricate compositional constraints.

Section 3.1.1 Text-to-image Generation

Generate an image of '<prompt>' 



<prompt>
an armchair in the shape of an avocado.



<prompt>
an elephant made of cucumber.



<prompt>
a hedgehog wearing a red hat, yellow gloves, blue shirt, and green pants.



<prompt>
an astronaut
riding a horse on Mars.



<prompt>
a mechanical or electrical
device for measuring time.



<prompt>
brain riding a rocketship
heading towards the moon.



<prompt>
Teddy bears swimming at the
Olympics 400m Butterfly event.



<prompt>
a small cactus wearing a straw hat and
neon sunglasses in the Sahara desert.



<prompt>
a Corgi dog riding a bike in Times Square.
It is wearing sunglasses and a beach hat.

Figure 4: Examples of text-to-image generation results by GPT-4o.

Section 3.1 Text-Conditioned Image Generation

<p>Generate an image of a visual representation of jazz music: brass instruments twisted into springs, notes materialized as jumping prisms, with background color blocks pulsating to the double bass rhythm."</p> 	<p>Generate an image of an infinitely recursive library: every book on the shelves has a cover depicting a miniature version of the same library, with windows revealing fractal-patterned starscapes outside.</p> 
<p>Generate an image of a tree made of melting clocks and clockwork gears, with glowing teardrop-shaped fruits hanging from its branches, and a trunk covered in hexagonal honeycomb patterns.</p> 	<p>Generate an image of a frozen explosion crystalized in mid-air, with splintered alphabet fragments and spiral flames trapped inside, encased by a shattered Möbius strip outline.</p> 

Figure 5: Examples of abstract text-to-image generation results by GPT-4o.

Section 3.1 Text-Conditioned Image Generation

<p>Generate an image of a teapot in the form of an upside-down pyramid, with heart-shaped spout and flame-shaped steam</p> 	<p>Generate an image of a rocket-shaped coffee machine, with exhaust steam forming tiny heart shapes</p> 
<p>Generate an image of an oval-shaped sink and a rectangular mirror with flat corners. On the sink, from left to right, there are a red square tooth cup with beveled edges, a purple droplet-shaped shampoo bottle, a blue shield-shaped skincare product, and a green toothpaste. Inside the tooth cup is a white toothbrush.</p> 	<p>Generate an image of a glass jar wrapped with a fluffy ribbon and placed on a wooden table. The jar contains four metal candies. The colors of the candies from top to bottom are red, yellow, green, and blue.</p> 

Figure 6: Examples of complex text-to-image generation results by GPT-4o.

3.1.2 Text Rendering

Text rendering is a challenging subtask of text-conditioned image generation, where the model is required not only to synthesize visual content, but also to accurately render specified textual content as an integral part of the image[133, 97, 105, 23, 161, 22, 209]. This task tests the model’s fine-grained spatial control, font fidelity, multilingual capability, and ability to balance visual aesthetics with text legibility.

As shown in Fig. 7, GPT-4o is able to generate plausible images that embed short, stylized texts across a variety of contexts such as signage, graffiti, posters, and book covers. The generated results generally follow the given prompts, with appropriate font placement and contextual consistency. However, minor issues remain in font clarity and character shape consistency, especially in artistic scenes.

To further test the model’s capacity for handling extended textual content, we introduce long paragraph prompts including literary excerpts and movie synopses. As shown in Fig. 8, GPT-4o demonstrates basic formatting capability, generating legible long-form text with consistent line layout and suitable contrast.

Additionally, we examine the model’s ability to render multilingual content by prompting it with a variety of languages including English, Chinese, Turkish, Tibetan, Russian, and Japanese (Fig. 9). While GPT-4o performs reasonably well on most of the scripts, it struggles with Tibetan, which may be caused by its limited data. In addition, the generated images occasionally contain semantic or contextual errors (e.g., a sign appearing to float instead of being held). These issues can arise even in high-frequency languages such as English.

Overall, GPT-4o demonstrates a promising ability in text rendering tasks, especially for short English phrases in stylistic contexts. However, its robustness in multilingual, long-form, or precise layout-sensitive scenarios still requires significant improvement.

Section 3.1.2 Text Rendering

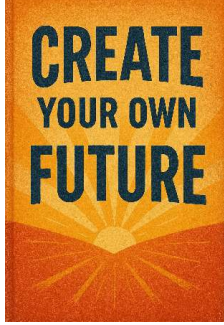
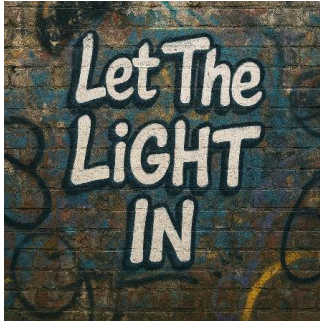
<p>Generate an image of a motivational book cover with the title: "Create Your Own Future."</p> 	<p>Generate an image of a highway billboard saying: "Fresh Taste, Every Morning."</p> 
<p>Generate an image of a cozy cafe signboard with the text: "Coffee & Dreams."</p> 	<p>Generate an image of an urban wall with graffiti text: "Let The Light In."</p> 

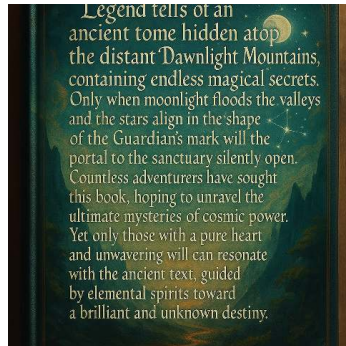
Figure 7: Examples of text rendering in stylized scenes. GPT-4o embeds short texts into posters, signs, and graffiti with moderate accuracy.

Section 3.1.2 Text Rendering

Create a hardcover book cover with an fantasy style background. Use a long piece of text as the main visual element on the cover, arranged gracefully like an excerpt or preface from a literary work. The text should be legible, with contrasting colors for clarity, and a strong artistic flair.

text:

Legend tells of an ancient tome hidden atop the distant Dawnlight Mountains, containing endless magical secrets. Only when moonlight floods the valleys and the stars align in the shape of the Guardian's mark will the portal to the sanctuary silently open. Countless adventurers have sought this book, hoping to unravel the ultimate mysteries of cosmic power. Yet only those with a pure heart and unwavering will can resonate with the ancient text, guided by elemental spirits toward a brilliant and unknown destiny.



Design a movie poster with a dark, suspenseful atmosphere. Place a long paragraph of text (about 200 words) prominently in the center, formatted like a movie synopsis. The font should be clear and elegant. Surrounding elements are slightly blurred to enhance the mood.

text:

Across this vast and boundless wasteland, the wind sweeps through ancient dunes, carrying whispers of old and forgotten tales. Stars sprinkle the night sky like slumbering eyes, silently watching the breath of the earth. Each grain of sand holds the memories of countless ages, recounting the stories of heroes and poets alike. Though time flows endlessly like a river, the names murmured in the wind continue to echo between the heavens and the earth. This is an unfinished journey, belonging to all who yearn to explore the unknown.



Figure 8: Examples of long text rendering tasks, including book cover paragraphs and movie synopses.

Section 3.1 Text-Conditioned Image Generation

Generate an image of Industrial workers in orange jacket protesting in front of green park with a signboard which says '<text>' on a clear sunny day.



**<English>:Respect our right to unite
Please No retaliation**



<Chinese>:尊重团结权利
请勿打击报复



<Turkish>: Birleşme hakkımıza saygı gösterin Lütfen misilleme yapmayın



<Greek>:Σεβαστείτε το δικαίωμά μας να ενωθούμε Παρακαλώ Όχι αντίποινα



< Tibetan >: བ୍ରାହ୍ମିକ ପ୍ରାଣୀ ପ୍ରାଣୀ ପଦ
< Russian >: *животное*



Russian>:Уважайте наше право на объединение
Пожалуйста, никаких ответных действий



<German>:Respektieren Sie unser Recht
auf Vereinigung.Bitte keine
Vergeltungsmaßnahmen



<French>: Respectez notre droit à nous unir. S'il vous plaît, pas de représailles



<Japanese>:団結する権利を尊重してください
してください報復はしないでください

Figure 9: Multilingual text rendering across nine languages. Non-Latin scripts often show rendering issues.

3.1.3 Document Image Generation

Document image generation refers to the task of producing structured visual outputs, such as documents, tables, and charts—based on textual specifications. This task requires not only semantic understanding and layout composition, but also spatial reasoning, formatting alignment, and numerical precision. We evaluate GPT-4o across four representative subtasks: textual document layout generation, table generation, catalog composition, and chart visualization.

As shown in Fig. 10, GPT-4o can synthesize realistic visual representations of academic documents when given metadata like title, author list, and abstract. The layout structure is relatively well-formed and the image resembles typical paper screenshots, although minor spacing and text overflow issues may occur.

In Fig. 11, we test the generation of structured table-of-contents pages. GPT-4o succeeds in capturing the multi-level hierarchy and spacing of entries, but occasional alignment drift and symbol inconsistency are observed.

For tabular generation (Fig. 12), the model is given structured markdown input and expected to generate a rendered table. The results exhibit promising alignment and visual styling, but some text wrapping and boundary precision issues remain.

More challenging are chart-related tasks (Fig. 13, 14), where GPT-4o is prompted to visualize numerical data in bar, pie, line, and scatter plot formats. While the model captures general layout and chart types correctly, we observe frequent numerical inaccuracies, axis mislabeling, and data point misplacement. In some cases, the visual values do not match the specified ones, which poses concerns for trustworthy data communication.

Overall, GPT-4o demonstrates a basic ability to generate visually plausible document-style images. However, in tasks requiring precise control of structure, spatial arrangement, and quantitative correctness, significant limitations remain.

Section 3.1.3 Document Image Generation

Generate A realistic screenshot of the first page of the Paper from the following information:
Title: CCMNet: Leveraging Calibrated Color Correction Matrices for Cross-Camera Color Constancy
Author list: Dongyoung Kim, Mahmoud Afifi, Dongyun Kim, Michael S. Brown, Seon Joo Kim
Abstract: Computational color constancy, or white balancing, is a key module in a camera's image signal processor (ISP) that corrects color casts from scene lighting. Because this operation occurs in the camera-specific raw color space, white balance algorithms must adapt to different cameras. This paper introduces a learning-based method for cross-camera color constancy that generalizes to new cameras without retraining. Our method leverages pre-calibrated color correction matrices (CCMs) available on ISPs that map the camera's raw color space to a standard space (e.g., CIE XYZ). Our method uses these CCMs to transform predefined illumination colors (i.e., along the Planckian locus) into the test camera's raw space. The mapped illuminants are encoded into a compact camera fingerprint embedding (CFE) that enables the network to adapt to unseen cameras. To prevent overfitting due to limited cameras and CCMs during training, we introduce a data augmentation technique that interpolates between cameras and their CCMs. Experimental results across multiple datasets and backbones show that our method achieves state-of-the-art cross-camera color constancy while remaining lightweight and relying only on data readily available in camera ISPs.
Subjects: Computer Vision and Pattern Recognition (cs.CV)



CCMNet: Leveraging Calibrated Color Correction Matrices for Cross-Camera Color Constancy

Dongyoung Kim, Mahmoud Afifi, Dongyun Kim, Michael S. Brown, Seon Joo Kim

Abstract

Computational color constancy, or white balancing, is a key module in a camera's image signal processor (ISP) that corrects color casts from scene lighting. Because this operation occurs in the camera-specific raw color space, white balance algorithms must adapt to different cameras. This paper introduces a learning-based method for cross-camera color constancy that generalizes to new cameras without retraining. Our method leverages pre-calibrated color correction matrices (CCMs) available on ISPs that map the camera's raw color space to a standard space (e.g., CIE XYZ). Our method uses these CCMs to transform predefined illumination colors (i.e., along the Planckian locus) into the test camera's raw space. The mapped illuminants are encoded into a compact camera fingerprint embedding (CFE) that enables the network to adapt to unseen cameras. To prevent overfitting due to limited cameras and CCMs during training, we introduce a data augmentation technique that interpolates between cameras and their CCMs.

Subjects: Computer Vision and Pattern Recognition (cs.CV)

Figure 10: Examples of textual document image generation by GPT-4o.

Section 3.1.3 Document Image Generation

Generate a directory image based on the directory information given below:

Table of Contents

Preface to the German edition of 1872.....	3
Preface to the German edition of 1883.....	5
Preface to the English edition of 1888.....	7
Preface to the German edition of 1890.....	8
Preface to the Polish edition of 1892.....	13
Preface to the Italian edition of 1893.....	19
The Communist Manifesto	
I. Bourgeoisie and Proletarians.....	23
II. Proletarians and Communists.....	36
III. Socialist and Communist Literature.....	46
1. Reactionary Socialism.....	46
(A) Feudal Socialism.....	46
(B) Petty-bourgeois Socialism.....	48
(C) German or "True" Socialism.....	49
2. Conservative or Bourgeois Socialism.....	52
3. Critical Utopian Socialism and Communism.....	54
IV. The Attitude of the Communists to Various Opposition Parties.....	57
Notes.....	59





TABLE OF CONTENTS

Preface to the German edition of 1872	3
Preface to the German edition of 1888	5
Preface to the English edition of 1888	7
Preface to the German edition of 1890	8
Preface to the Polish edition of 1892	13
Preface to the Italian edition of 1893	19
<i>The Communist Manifesto</i>	
I. Bourgeoisie and Proletarians	23
II. Proletarians and Communists	36
III. Socialist and Communist Literature	46
1. Reactionary Socialism	46
(A) Feudal Socialism	46
(B) Petty-bourgeois Socialism	48
(C) German or "True" Socialism	49
2. Conservative or Bourgeois Socialism	52
3. Critical Utopian Socialism and Communism	54
IV. The Attitude of the Communists to Various Opposition Parties	57
Notes	59



Figure 11: Examples of catalog image generation by GPT-4o.

Section 3.1.3 Document Image Generation

Region Product Category Q1 Sales (\$) Q2 Sales (\$) Q3 Sales (\$) Q4 Sales (\$)

2024 2024 2024 2024

Region	Product Category	Q1 Sales (\$)	Q2 Sales (\$)	Q3 Sales (\$)	Q4 Sales (\$)
North America	Electronics	12,500	13,750	15,200	
North America	Furniture	7,800		8,950	9,100
Europe	Electronics	10,200	11,400		13,300
Europe	Furniture		6,700	7,300	8,000
Asia	Electronics	8,900	9,500	10,400	11,200
Asia	Furniture	5,600	5,900		6,700

(write in markdown format)

Generate table images based on above markdown content.

Region Product Category Q1 Sales 2024 Q2 Sales (S) 2024 Q3 Sales 2024

Region	Product Category	Q1 Sales 2024	Q2 Sales (S) 2024	Q3 Sales 2024
North America	Electronics	12.500	13.750	15.200
	Furniture	7.800	—	9.100
Europe	Electronics	10.200	11.400	3.300
	Furniture	6.700	—	8.000
Asia	Electronics	8.900	9.500	10.400
	Furniture	5.600	5.900	11.200
Asia	Electronics	5.600	5.900	6.700

Figure 12: Examples of markdown-to-table generation by GPT-4o.

Section 3.1.3 Document Image Generation

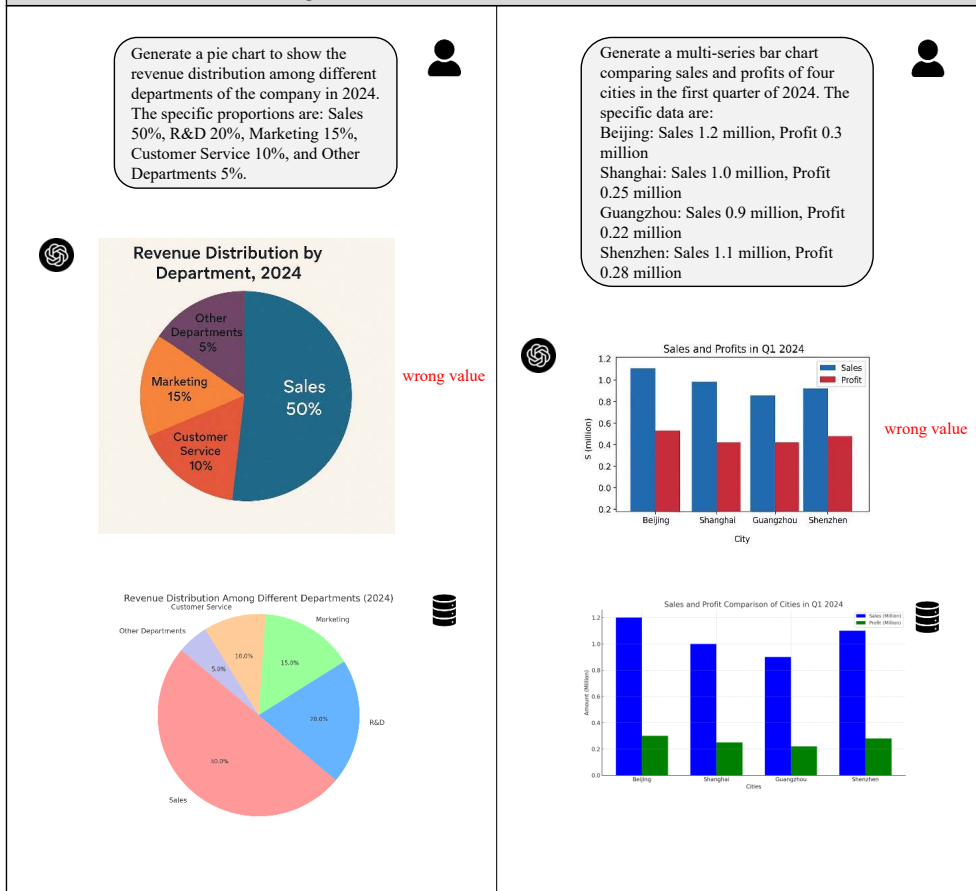
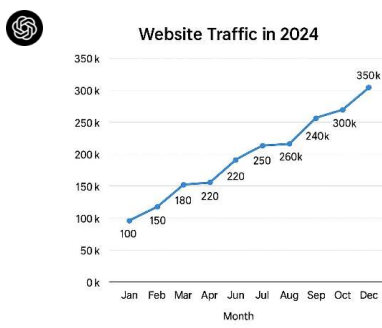


Figure 13: Examples of chart generation by GPT-4o.

Section 3.1.3 Document Image Generation

generate a line chart showing the monthly trend of website traffic in 2024. The specific data points are: January 100k, February 120k, March 150k, April 200k, May 180k, June 220k, July 250k, August 240k, September 260k, October 280k, November 300k, December 350k.



generate a scatter plot to show the relationship between math scores and English scores of 10 students. The specific data are:

Student 1: Math 85, English 78;
 Student 2: Math 90, English 88;
 Student 3: Math 76, English 85;
 Student 4: Math 92, English 91;
 Student 5: Math 69, English 75;
 Student 6: Math 80, English 82;
 Student 7: Math 88, English 89;
 Student 8: Math 73, English 77;
 Student 9: Math 95, English 94;
 Student 10: Math 78, English 80.

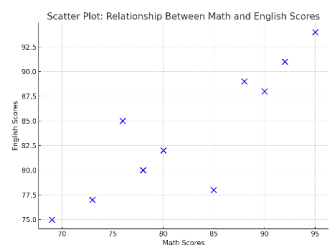
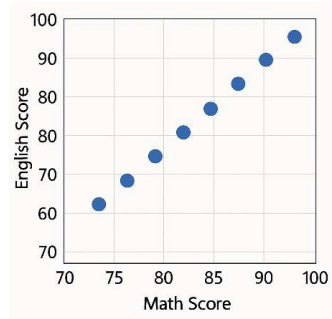


Figure 14: Additional examples of chart generation by GPT-4o.

3.2 Multimodal-Conditioned Image Generaiton

Multimodal-conditioned image generation requires the model to integrate and respond to complex inputs, which may combine both textual and visual signals. This setting tests GPT-4o 's multimodal understanding and its ability to blend visual information with linguistic instructions in a coherent and contextually appropriate manner.

3.2.1 Image Editing

Image editing tasks evaluate whether GPT-4o can modify an existing image according to a specific instruction, such as changing object attributes, removing elements, or altering the scene style. This task reflects the model's ability to comprehend visual content and apply precise, localized modifications while preserving the overall image consistency[13, 44, 12, 201].

As shown in Fig. 15, we first evaluate concept replacement tasks, where the model is instructed to replace individual objects or backgrounds (e.g., "replace the elephant with a monkey", "replace the background with the Great Wall"). GPT-4o successfully captures the target concept in most cases, but occasionally fails to fully preserve structural context or scale, leading to semantic mismatches or blending issues.

In Fig. 16, we evaluate object removal tasks such as "remove the sunglasses and helmet from the dog" or "remove the kitten from the table". The model performs reasonably well in eliminating specified targets while maintaining the surrounding content, although minor residue artifacts or unnatural texture patches may occur.

More challenging are complex multi-edit scenarios shown in Fig. 17 and Fig. 18, including multiple simultaneous changes (e.g., swapping accessories between subjects, modifying font styles, or transforming materials). GPT-4o shows a basic ability to interpret compositional instructions and perform diverse edits.

Overall, while GPT-4o demonstrates promising performance in direct concept replacement.

Section 3.2.1 Image Editing

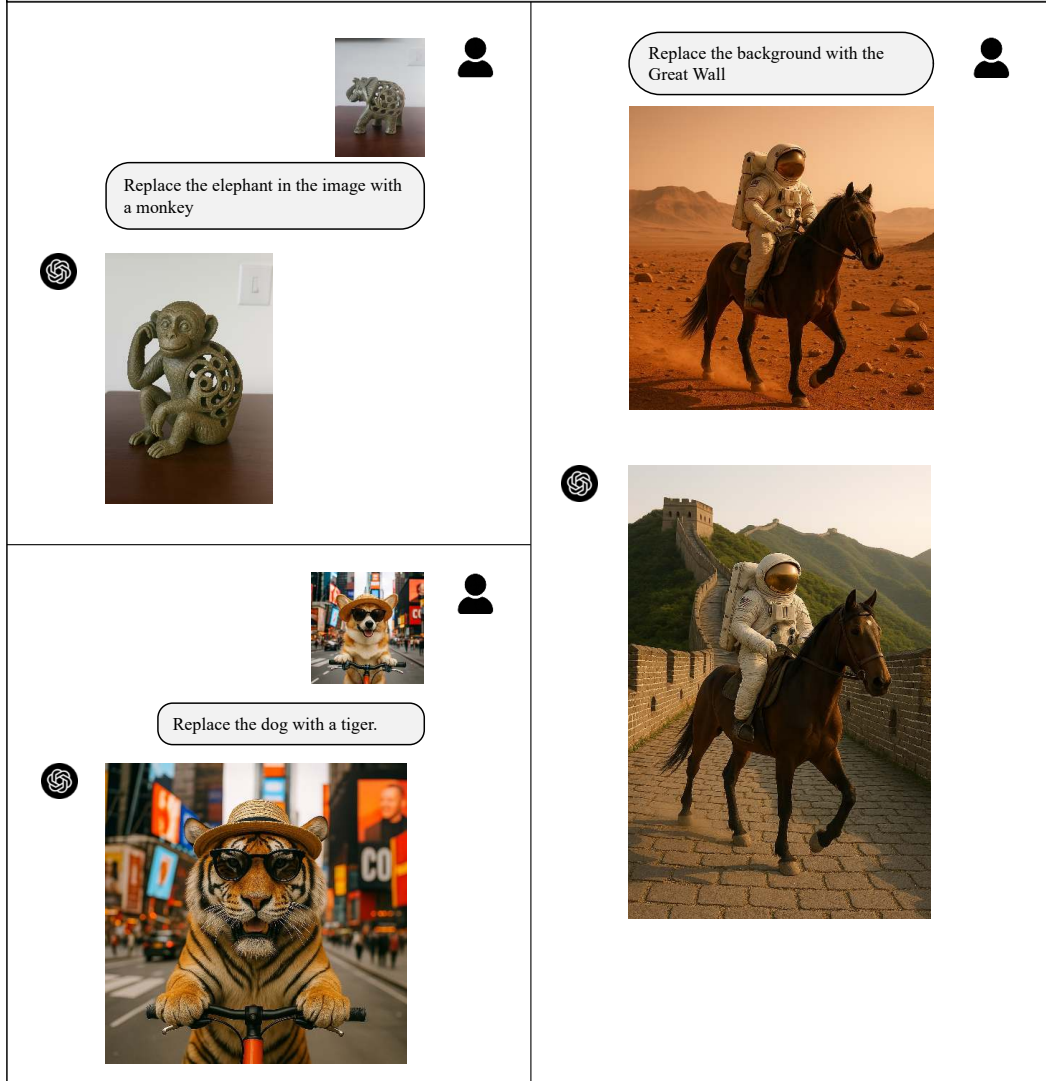


Figure 15: Examples of concept replacement, where GPT-4o replaces target objects or backgrounds (e.g., animal species, scenes) while preserving the remaining content.

Section 3.2.1 Image Editing

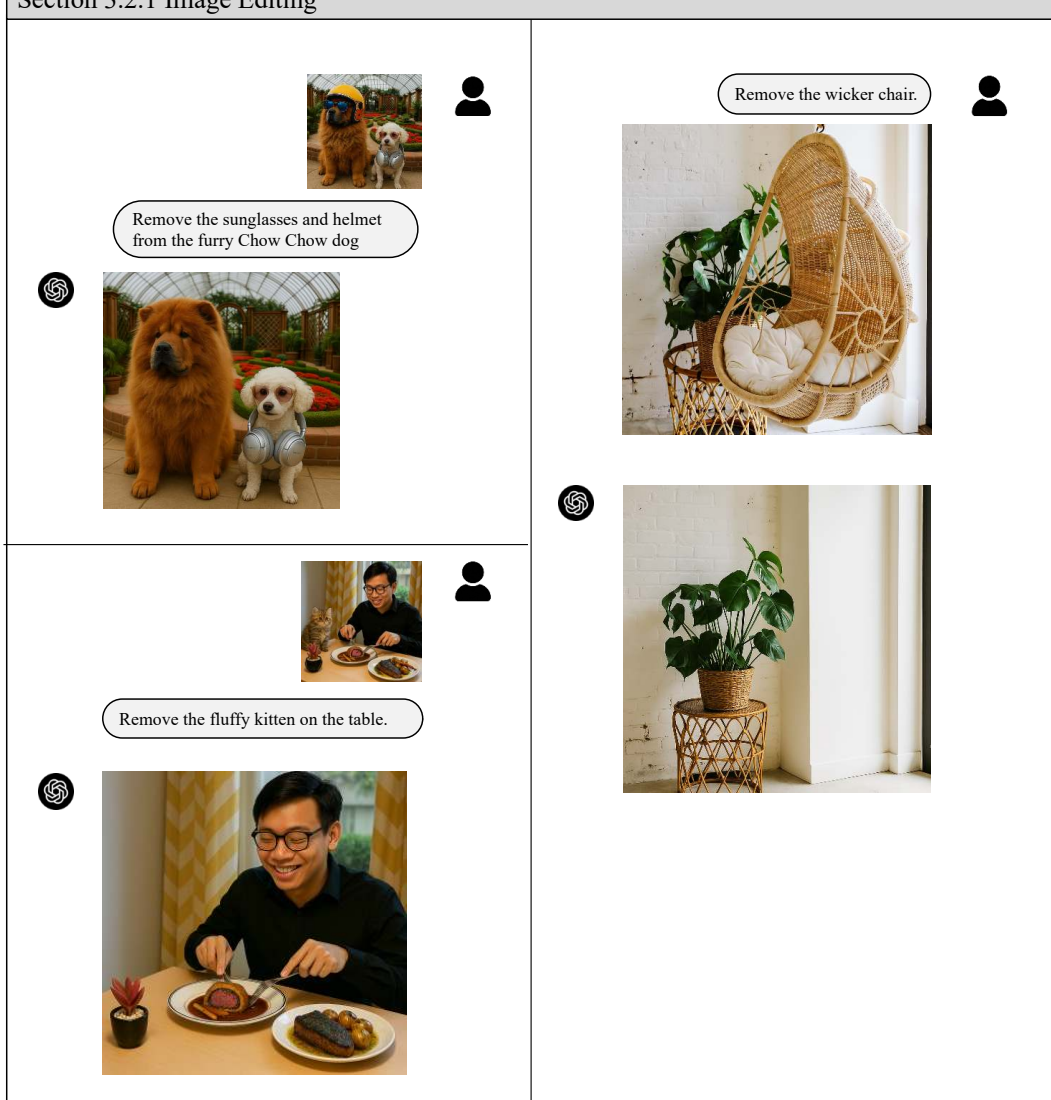


Figure 16: Examples of concept removal tasks, where GPT-4o eliminates specific objects (e.g., accessories, animals) based on the instruction.

Section 3.2.1 Image Editing

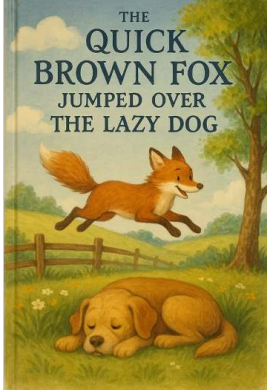
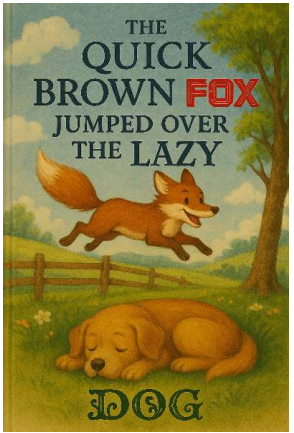
 Swap the sunglasses of two dogs	 Generate an image, change the font of the word "fox" in the reference image to red technology style, and change the font of the word "dog" to green art style
 Replace the knife and fork in the man's hands with chopsticks	

Figure 17: Complex image editing examples involving multiple changes, such as swapping accessories or modifying fonts and materials.

Section 3.2.1 Image Editing

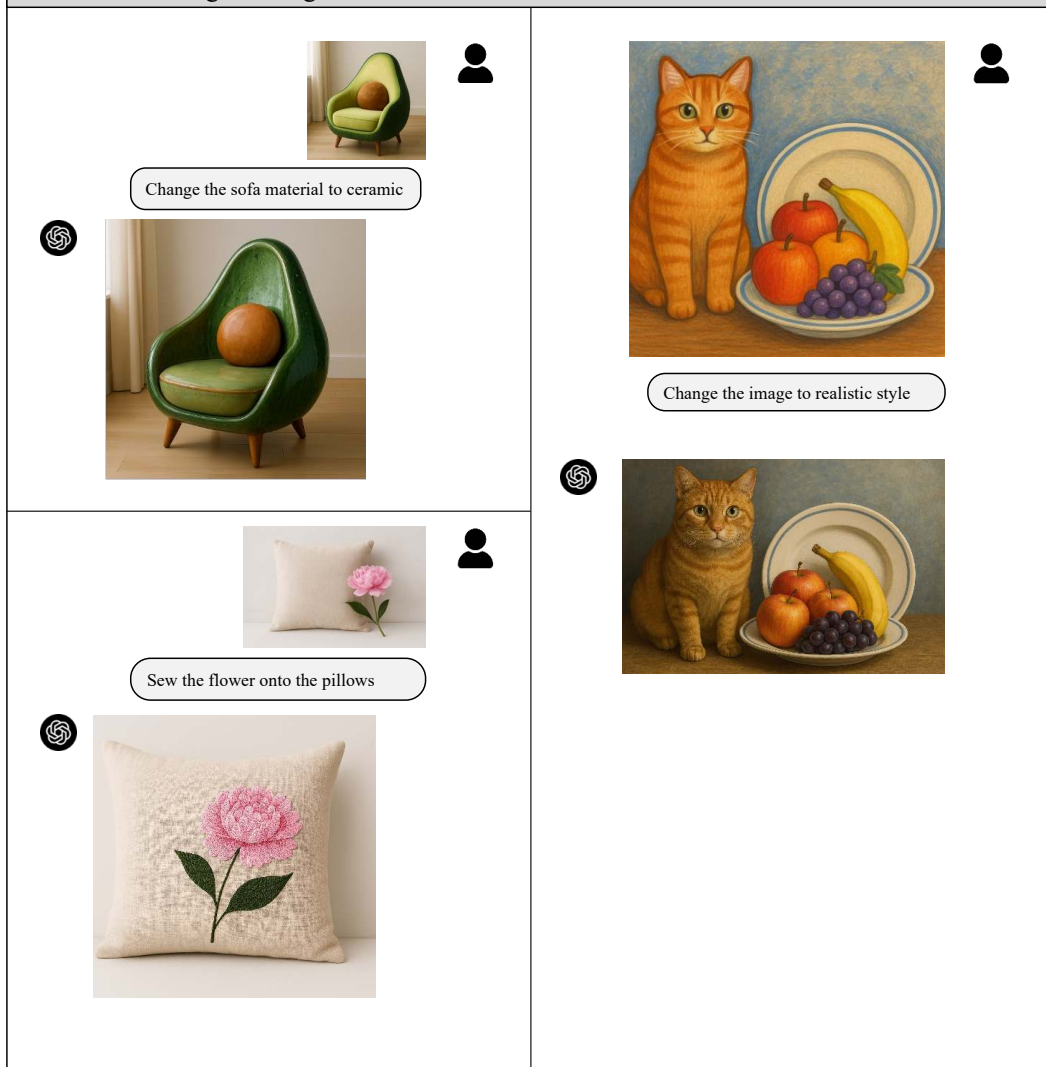


Figure 18: Additional examples of multi-step and stylistic edits, where GPT-4o is tasked with applying compositional instructions involving multiple transformations.

3.2.2 Personalized Image Generation

Personalization focuses on generating content tailored to specific entities, styles, or individuals, such as producing consistent images of a user-provided character or object[16]. This task evaluates GPT-4o’s memory retention, visual consistency, and adaptability across multimodal conditions. In this section, we follow the evaluation protocols proposed in [A] and test a variety of personalization scenarios.

Subject-driven generation. For subject-driven generation [40, 45, 143, 163, 208, 183], GPT-4o is expected to synthesize new images while preserving the identity and attributes of the given subject, conditioned on new prompts. GPT-4o generally succeeds in capturing the overall appearance and theme of the subject described in the input image-text pair. However, certain structural inaccuracies still occur. For instance, in Fig. 19, the prompt “two people tearing” results in an image containing two figures, but with a total of five hands, revealing flaws in body-part reasoning. In another example, the model-generated version of a customized character includes an extra arm, suggesting inconsistencies in spatial anatomy and object integrity.

Style-driven generation. For style-driven generation[149, 93, 20], where the goal is to transfer a visual style from a reference image to new content, the model is able to follow the overall aesthetic and object features with reasonable fidelity. However, we observe mismatches in tonal and stylistic coherence. As shown in Fig. 20, the generated image appears notably darker than the reference, indicating that while the model retains high-level style cues, it may struggle with precise low-level appearance reproduction.

Person-driven generation. In person-driven generation[182, 162, 28], the model is tasked with preserving the identity, appearance, and facial attributes of a reference individual across different prompts and scenarios. As shown in our results in Fig. 21 and Fig. 22, GPT-4o is able to capture key visual characteristics such as hairstyle, clothing, and facial structure, and consistently reproduce them in novel contexts. The generated outputs exhibit strong coherence and personalization, even under varied instructions and poses.

Scene-driven generation. For scene-driven generation, the goal is to retain the background layout, spatial structure, and environmental elements from the reference image while modifying the foreground or semantic content. While GPT-4o demonstrates a reasonable ability to extract and imitate overall scene information, some visual mismatches are still observed, as can be shown in Fig. 23. For example, in the leftmost image of Fig. 23, the window structure differs significantly from the reference, indicating that the model may struggle with fine-grained background alignment.

Pose-driven generation. In pose-driven generation, the model is provided with an input image showcasing a specific body posture and is expected to transfer that pose to a new subject or scene. In this task, GPT-4o shows robust performance (Fig. 24), successfully transferring pose configurations and generating visually plausible results, with correct limb orientation and body articulation preserved.

Interaction-driven generation. We also examine interaction-driven generation[61, 63], where the goal is to preserve the semantic or visual interaction between objects in the reference image, such as spatial relations, embedding, or stylistic blending across elements. In this task, GPT-4o shows clear limitations (Fig. 25). For example, in the reference image, a cat is drawn onto the surface of a rock using a blended style that resembles colored pencil and watercolor. Ideally, the model should preserve both the embedded positioning of the cat and the stylistic fusion with the rock texture. However, as illustrated in Fig. X, only the second generated image shows a slight indication of this interaction. The other two outputs fail to reflect either the spatial composition or the intended artistic medium, producing results that are visually detached from the reference semantics. This suggests that while GPT-4o can recognize explicit content elements, it struggles to infer and reconstruct implicit relationships.

Multi-concept personalization. We also explore GPT-4o’s ability in multi-concept personalization[60, 59, 148, 103, 103], where multiple customized objects or entities are referenced simultaneously within a single prompt. This task is more demanding, as it requires the model to not only retain individual object characteristics but also correctly compose them within a coherent scene. As illustrated in Fig. 26, we test this setting by defining a prompt that combines seven distinct objects and attributes, such as specific sunglasses, helmets, headphones, and background scenes. GPT-4o demonstrates impressive performance in preserving and combining all the specified concepts into a well-structured image. The generated output accurately reflects the visual identity

of each reference item and maintains proper spatial composition. To further assess the model’s referential understanding, we experiment with compositional prompts using ordinal expressions and image-position references. For example, we ask the model to “use the sunglasses from the third image” or “place the first dog next to the second dog,” as shown in Fig. 27. GPT-4o is able to follow these instructions, indicating an emerging capability to link textual ordinal cues with visual memory from prior references. Overall, these results suggest that GPT-4o is not only capable of handling multi-object conditioning, but also demonstrates a basic understanding of structured referential language in personalized generation scenarios.

Fine-grained decoupled personalization. We further evaluate GPT-4o’s ability to perform fine-grained concept disentanglement[21, 15, 85, 113], where multiple attributes or objects within a reference image must be independently extracted and recombined based on textual instruction. This task is particularly challenging when the reference contains visually or semantically entangled elements. As shown in Fig. 28, we observe that GPT-4o often struggles to decouple closely associated concepts, leading to semantic leakage or inconsistencies across generated results. In the left column (a1, a2), although the prompt is kept constant, the model incorrectly includes additional concepts in both outputs—such as generating a yellow helmet and a white pair of headphones not mentioned in the prompt, or using the wrong sunglasses color. This indicates that residual associations from the reference image influence the final output, violating prompt constraints. In the right image (b), the prompt describes a multi-object spatial hierarchy: the mouse is placed on a plastic coffee bottle, which is placed on a box. While the model generally respects the described structure, the color of the mouse’s scroll wheel is altered in the generated result, indicating the model’s tendency to modify irrelevant attributes during complex recompositions. These results suggest that while GPT-4o can handle multi-concept prompts at a high level, its ability to isolate and control fine-grained attributes in densely composed scenes is still limited.

Through our comprehensive evaluation of various personalization tasks, we find that GPT-4o demonstrates notable capabilities in identity preservation, stylistic transfer, and flexible compositional reasoning. In particular, the model performs well in scenarios where the personalized entity is visually distinct and the prompt is structurally simple. However, several limitations persist. First, the model occasionally fails to maintain fine-grained consistency across attributes (e.g., color, accessories, pose details), especially under complex spatial compositions or multi-stage instructions. Second, when disentangling densely co-occurring elements within a single reference image, GPT-4o tends to produce semantic entanglement, leaking unintended concepts into the output. Finally, in cases requiring precise reference-based control (e.g., ordinal alignment, interaction binding), its understanding of prompt-referent mapping remains unstable.

Overall, GPT-4o shows strong potential in personalization-oriented generation, but its current performance is still bounded by limitations in structure disentanglement, attribute fidelity, and precise prompt grounding. Future improvements may require explicit memory modules, better concept binding mechanisms, or fine-tuned alignment between image and textual referents.

Section 3.1 Subject-Driven

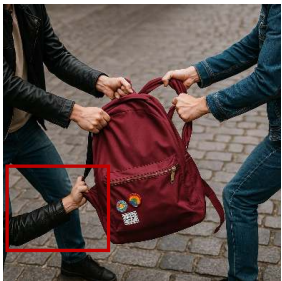
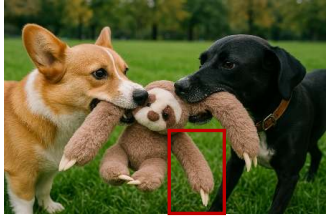
 <p>Generate a picture of this backpack with a tree and autumn leaves in the background</p> 	 <p>Generate an image of two people tearing at the same backpack on a cobblestone street</p> 
 <p>Generate an image of two dogs are fighting over the plushie , both biting tightly at each end.</p> 	 <p>Generate an image of a candle on a dining table being blown out by a little girl</p> 

Figure 19: Examples of subject-driven image generation by GPT-4o.

Section 3.2.2 Personalized Image Generation

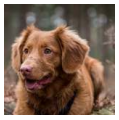
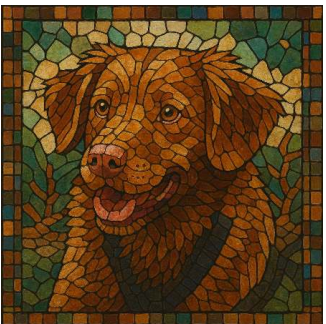
 <p>Generate an image of an electric guitar being played by a rockstar on a neon-lit stage, in the style of this picture.</p>  <p>(a1) Image translation by customized style</p>	 <p>Generate an image of a butterfly perched on a leaf in this style.</p>  <p>(a2) Image translation by customized style</p>
  <p>Stylize the second image based on the style of the first image.</p>  <p>(b1) Text-to-image generation with customized style</p>	  <p>Stylize the second image based on the style of the first image.</p>  <p>(b2) Text-to-image generation with customized style</p>

Figure 20: Examples of style-driven image generation by GPT-4o.

Section 3.2.2 Personalized Image Generation



Generate an image of a man with short dark brown hair, **<prompt>**



<prompt>: raising a sword and unleashing blazing flames.

Section 3.2.2 Personalized Image Generation



Generate an image of a woman with long dark brown hair, <prompt>



<prompt>:swinging a magic wand and casting a glowing blue spell.



<prompt>:standing under cherry blossom trees, breeze blowing through her hair, pink petals falling



<prompt>:oil painting style, heavy brush strokes, abstract color block background, strong light and shadow contrast, vintage artistic feel

Figure 22: Additional examples of person-driven image generation by GPT-4o.

Section 3.2.2 Personalized Image Generation





Generate an image of in the scene of the reference image' <prompts>'




<prompts>:A gray rabbit sitting on a windowsill, with rain falling outside and raindrops on the window glass. The room is warm and bright inside



<prompts>:A small black squirrel sitting on a windowsill,with an autumn scene outside. Golden maple leaves are falling in the wind.



<prompts>:A white owl standing on a windowsill, with a dark blue night sky and twinkling stars outside. The owl is wide-eyed, gazing into the distance.

Figure 23: Examples of scene-driven image generation by GPT-4o.

Section 3.2.2 Personalized Image Generation



Based on the pose of the reference image, generate an image of <prompts>



Based on the pose of the reference image, generate an image of <prompts>



Based on the pose of the reference image, generate an image of <prompts>



Based on the pose of the reference image, generate an image of <prompts>

Figure 24: Examples of pose-driven image generation by GPT-4o.

Section 3.2.2 Personalized Image Generation



Based on the interaction between the cat and the rock in the reference image, generate an image of <objects>



<objects>
A ceramic plate and fruits



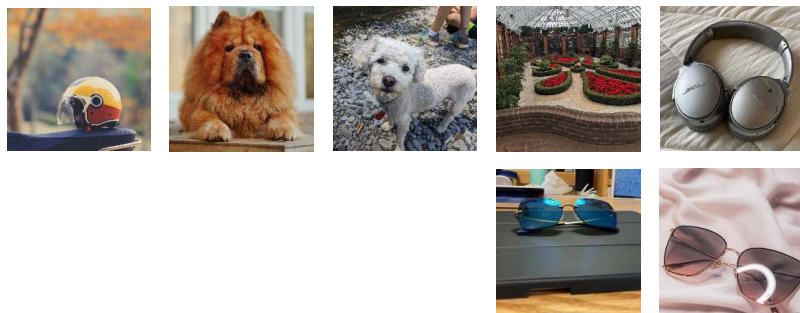
<objects>
A white t-shirt and a
canvas backpack



<objects>
A pillow and a peony flower

Figure 25: Examples of interaction-driven image generation by GPT-4o.

Section 3.2.2 Personalized Image Generation

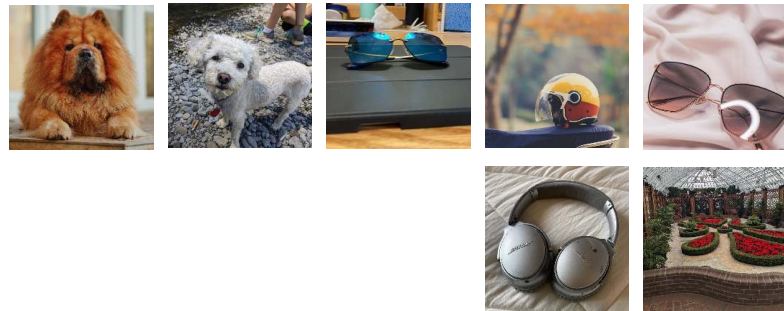


Generate a picture of a large, fluffy Chow Chow dog wearing a pair of stylish blue-tinted sunglasses with a gold frame, a retro-style yellow and orange motorcycle helmet with a clear visor, sitting next to a small, white, curly-haired dog wearing a pair of pink-tinted sunglasses with a delicate gold frame, a pair of silver Bose noise-cancelling headphones, with a beautiful garden inside a greenhouse in the background



Figure 26: Examples of multi-concept personalization results generated by GPT-4o.

Section 3.2.2 Personalized Image Generation



Generate a picture of the first dog wearing sunglasses in third picture, a helmet in the fourth picture, sitting next to second dog wearing sunglasses in fifth picture, a headphone in sixth picture, with a garden of last picture in the background



Figure 27: Additional examples of multi-concept personalization results generated by GPT-4o.

Section 3.2.2 Personalized Image Generation



Figure 28: Examples of fine-grained decoupled personalization results generated by GPT-4o.

3.2.3 Spatial Control

Spatial control tasks aim to guide image generation using explicit spatial constraints, such as layout, sketch, depth map, pose, and multiple-condition combination. These tasks evaluate the model’s ability to understand spatial priors, align multimodal conditions, and preserve relative geometric structures in the generation process. We follow the general inference paradigm in recent controllable generation studies [202, 74, 59, 126, 114, 9], and systematically test GPT-4o across several typical spatial guidance modalities.

Layout-to-image generation. In layout-based spatial control [86, 51, 186, 210, 70], the model is required to generate an image conditioned on both bounding box layout and corresponding textual labels. As shown in Fig. 29, GPT-4o is able to align objects with their designated positions and labels (e.g., “bear with sunglasses”) under simple geometric constraints. However, when handling complex scenes with textual conditions, positional drift can still be observed.

Sketch-based generation. In sketch-to-image generation, the model is guided by rough structural outlines, such as hand-drawn contours or simplified line maps, along with accompanying textual prompts. While GPT-4o demonstrates strong semantic understanding and is able to produce visually plausible and contextually relevant content, it often fails to maintain strict spatial alignment with the input sketch. For instance, in the upper-left example of Fig. 30, the generated washing machine deviates notably from the sketched shape, exhibiting different proportions and design. In the lower-left example, the orientation of the shrimp inside the pot is reversed compared to the sketch. These discrepancies suggest that although GPT-4o leverages sketch cues as high-level guidance, it lacks the geometric fidelity required for precise spatial control, especially for fine-grained structures.

Canny-to-image generation. Edge-based generation with canny maps is widely used to provide coarse structural control in synthesis tasks. In this setting, GPT-4o receives a low-level edge map alongside a textual prompt, and is expected to respect the contour constraints during image generation. As illustrated in Fig. 31, GPT-4o captures the overall composition and generates semantically meaningful content, but frequently introduces elements not supported by the control input. For example, in the lower-left image, the generated figure includes a head that does not appear in the input canny sketch, and the orientation of the backpack deviates significantly from the edge shape. These observations suggest that while the model can use edge information as a loose guide, it tends to hallucinate plausible but uncontrolled details, revealing limited adherence to strict spatial boundaries under weak supervision.

Depth-to-image generation. Depth conditioning is designed to guide image generation with spatial hierarchy and foreground-background separation cues. Ideally, a model should interpret the depth map to preserve relative object positioning and scene structure. However, as shown in Fig. 32, GPT-4o exhibits inconsistent performance. While the top-left example shows a reasonable understanding of depth—maintaining plausible layering and perspective—the other two results reveal clear mismatches. In particular, the bottom-left image fails to reflect the intended depth gradient entirely, with foreground and background elements appearing flattened or confused. These cases suggest that GPT-4o has limited ability to extract and utilize geometric depth relationships from the input, especially when the depth map lacks clear semantic context.

Pose-to-image generation. In pose-conditioned generation, the model is expected to synthesize human figures that align closely with provided pose skeletons, capturing limb orientation, joint position, and overall body configuration. However, as shown in Fig. 33, GPT-4o exhibits limited precision in this task. While it generally respects the number of people and the rough action described by the pose input, it frequently fails to accurately match the detailed body positions and limb articulations. Misalignments such as incorrect arm angles, swapped leg positions, or distorted body structures are commonly observed. These results suggest that although GPT-4o has basic awareness of pose input, it struggles to convert sparse keypoint guidance into spatially faithful and anatomically correct visual representations.

Multi-condition spatial control. In more advanced settings, we provide GPT-4o with multiple spatial conditions simultaneously. As shown in Fig. 34, the model can integrate these heterogeneous priors and produce spatially grounded compositions. While coarse alignment is preserved, fine-grained consistency between multiple guidance types is occasionally inconsistent, revealing limitations in fusion robustness.

Across the evaluated spatial control tasks, GPT-4o demonstrates a moderate ability to incorporate spatial conditions into image generation. It performs relatively well in simple layout-to-image scenarios and contour-based sketch generation, where structural prompts are clear and semantically aligned. However, in more structured or fine-grained tasks such as depth-based synthesis, pose replication, and edge-controlled generation, the model frequently fails to maintain strict spatial alignment. Common issues include hallucinated content not present in the control input, incorrect object orientation, and poor adherence to depth or joint structure. Additionally, in multi-modal control settings (e.g., pose + mask), the fusion of different spatial modalities remains unstable, leading to partial or conflicting alignment. These findings suggest that GPT-4o treats spatial inputs more as soft guidance rather than strict geometric constraints. While it can use these signals to influence composition, it often prioritizes semantic plausibility or stylistic fluency over spatial fidelity.

Section 3.2.3 Spatial Control

 <p>Generate an image based on the layout of the reference image. A bear wearing sunglasses looks very proud. The input blue frame represents the bear, and the input red frame represents the sunglasses.</p>	 <p>Generate an image with a resolution of 1024*1024 according to the following tips and layout restrictions: prompt = "as the aurora lights up the sky, a herd of reindeer leisurely wanders on the grassy meadow, admiring the breathtaking view, a serene lake quietly reflects the magnificent display, and in the distance, a snow-capped mountain stands majestically". The boxes correspond to the aurora, reindeer, meadow, lake and mountains. Boxes = [[1,6,1024,404], [150,688,842,990], [1,654,1016,1014], [4,434,1014,682], [1,270,1018,484]]</p> <p>layouts are drawn by Python</p>
--	---

Figure 29: Examples of layout-to-image results generated by GPT-4o.

Section 3.2.3 Spatial Control

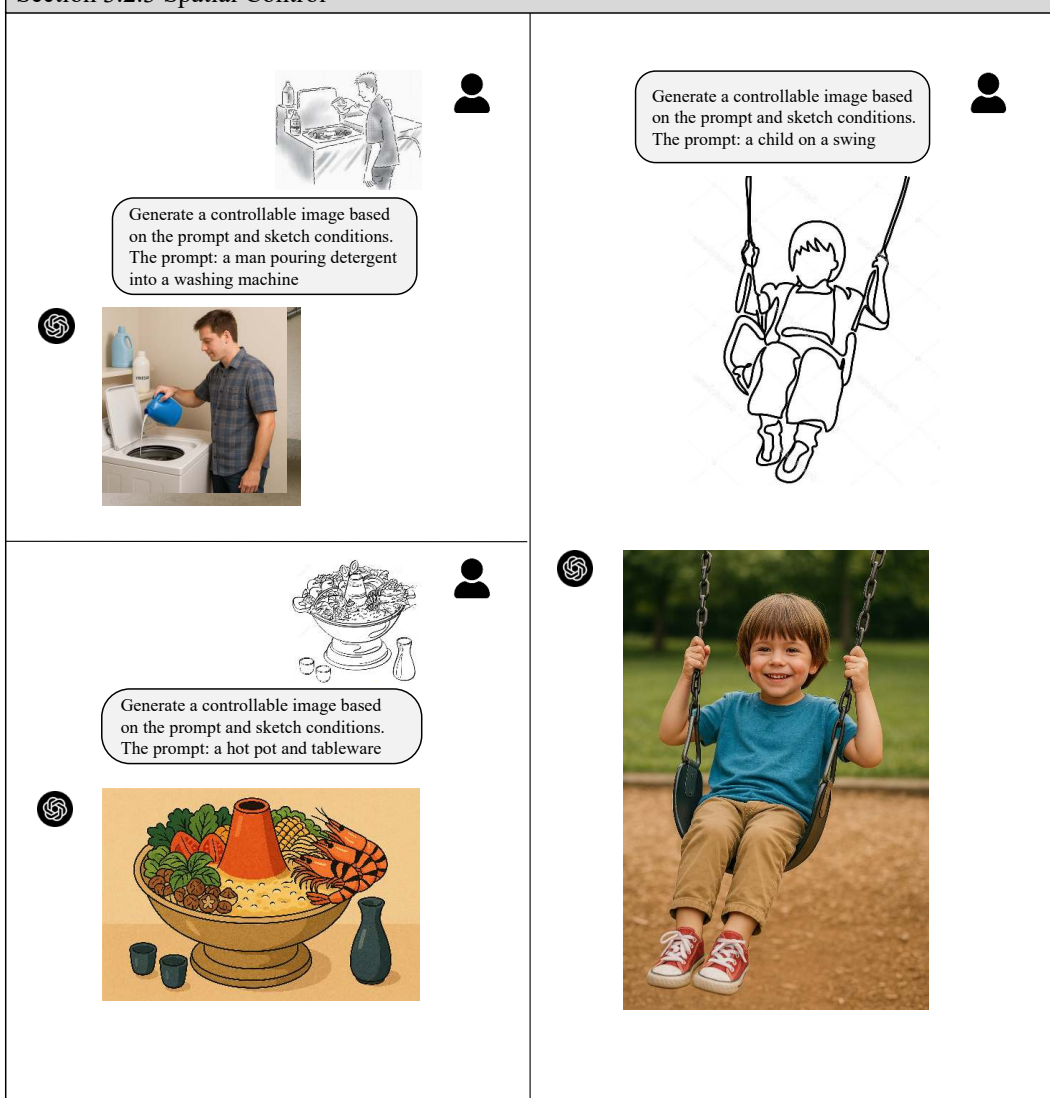


Figure 30: Examples of sketch-to-image results generated by GPT-4o.

Section 3.2.3 Spatial Control

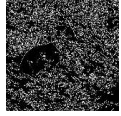
 <p>Generate a controllable image based on the prompt and canny conditions. The prompt: a dog looking into the distance</p> 	 <p>Generate a controllable image based on the prompt and canny conditions. The prompt: a doll is placed on the display</p> 
 <p>Generate a controllable image based on the prompt and canny conditions. The prompt: a woman with a backpack</p> 	 <p>Generate a controllable image based on the prompt and canny conditions. The prompt: a teddy bear leaning against a stone brick wall</p> 

Figure 31: Examples of canny-to-image results generated by GPT-4o.

Section 3.2.3 Spatial Control

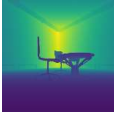
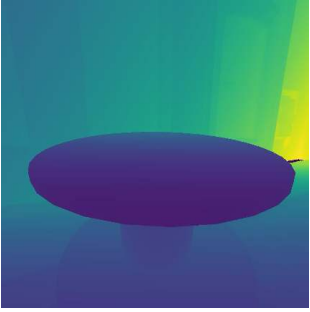
 <p>Generate a controllable image based on the prompt and depth conditions. The prompt: a room with a table and chairs.</p> 	 <p>Generate a controllable image based on the prompt and depth conditions. The prompt: a wooden table in front of a brick building.</p> 
 <p>Generate a controllable image based on the prompt and depth conditions. The prompt: a screenshot of a rock formation with rocks on it</p> 	

Figure 32: Examples of depth-to-image results generated by GPT-4o.

Section 3.2.3 Spatial Control

   <p>Generate a controllable image based on the prompt and pose conditions. The prompt: a young woman in a red sweater holds a black handheld camera, partially obscuring her face with the camera's lens.</p> 	   <p>Generate a controllable image based on the prompt and pose conditions. The prompt: two young men sit on a road surrounded by nature, with one of them holding a camera, while the other rests beside him. In the foreground, an old-fashioned camera is placed on the ground.</p> 
  <p>Generate a controllable image based on the prompt and pose conditions. The prompt: two lacrosse players are in action on a field. One player, wearing a white and blue uniform, is diving to his left to make a save, while the other player, dressed in red and white, is attempting to score or pass the ball.</p> 	

Figure 33: Examples of pose-to-image results generated by GPT-4o.

Section 3.2.3 Spatial Control

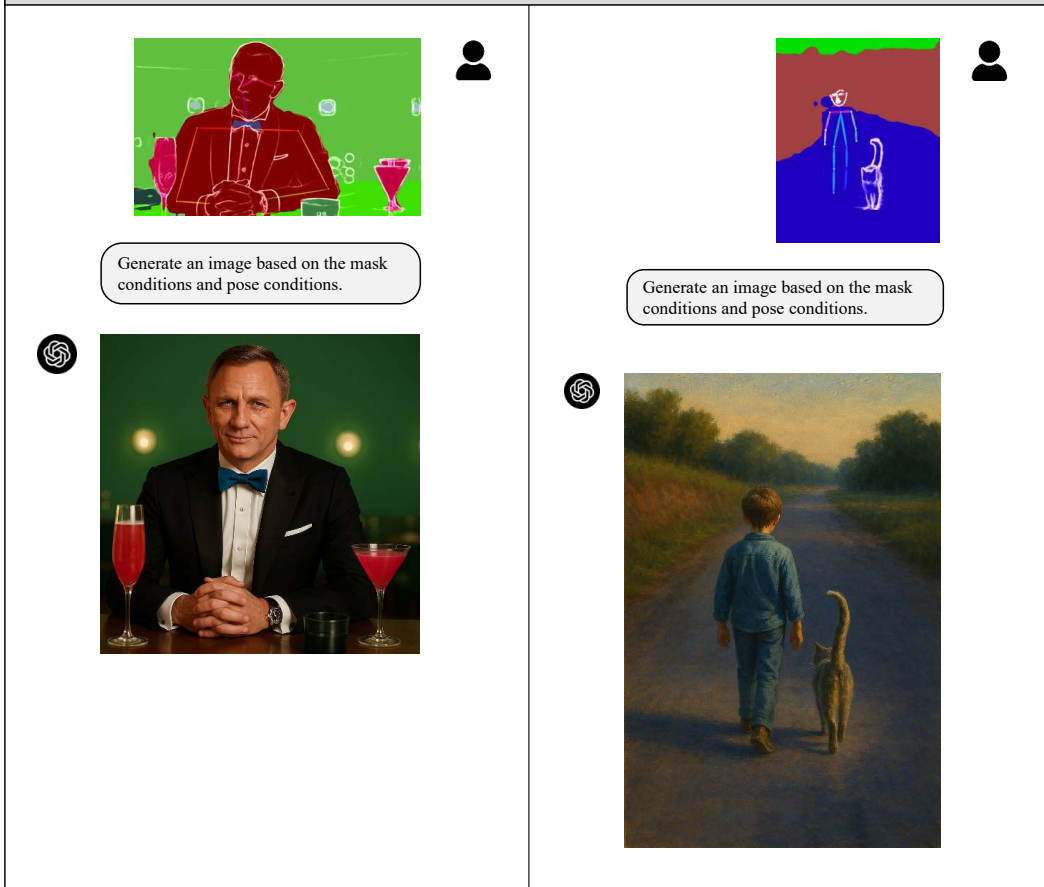


Figure 34: Examples of multi-conditioned spatial control results generated by GPT-4o.

3.2.4 Image Inpainting & Outpainting

Image inpainting[36] and outpainting[94, 4, 154] evaluate a model’s ability to fill in missing regions or extend image boundaries based on contextual understanding. These tasks require semantic coherence, texture consistency, and spatial continuity, especially when dealing with large or complex masked areas.

Image Inpainting. As shown in Fig. 35, GPT-4o demonstrates the ability to fill masked regions with plausible content. However, we observe that it tends to alter the original image content outside the masked area, leading to structural and textural inconsistencies. In the left example, the lighting across the entire image changes, and the picture frame on the right wall is replaced with a different image. Similarly, in the right example, both the human subject and the background are modified beyond the inpainted region. This suggests that while GPT-4o understands the global context well, it lacks fine-grained control to preserve the unmasked areas faithfully during inpainting.

Image Outpainting. For outpainting (Fig. 36), GPT-4o shows an impressive ability to extend images beyond their original boundaries while maintaining global style, color tone, and lighting conditions. The extended content is contextually coherent and stylistically aligned. However, inconsistencies in texture resolution and object detail are still apparent. The generated regions may look visually convincing at first glance but fail to maintain strict alignment in material or surface continuity, revealing limitations in local-level synthesis fidelity.

Overall, GPT-4o handles global structure and visual harmony well in both tasks but struggles with strict preservation of content and fine texture matching, particularly in inpainting.

Section 3.2.4 Image Inpainting & Outpainting

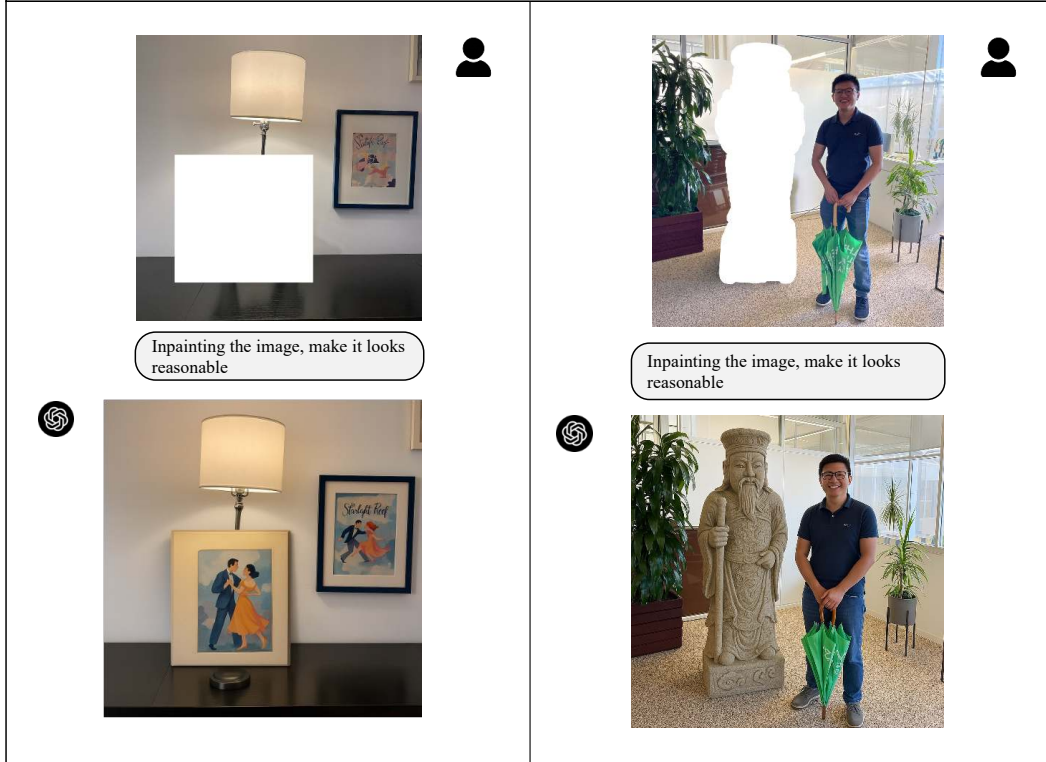


Figure 35: Examples of image inpainting generated by GPT-4o.

Section 3.2.4 Image Inpainting & Outpainting



Figure 36: Examples of image outpainting generated by GPT-4o.

3.2.5 Story Visualization

Story visualization tasks require the model to generate a coherent sequence of images based on a narrative input, maintaining consistency in character appearance, scene context, and temporal progression[217, 55, 26, 179, 49]. These tasks are inherently multimodal and test a model’s ability to track evolving information while producing temporally aligned visual outputs.

In Fig. 37, GPT-4o is able to follow the story flow and generate a sequence that aligns with the described events. Character identity and scene continuity are reasonably well maintained across the visual sequence, suggesting strong support for short-range consistency when reference images are available.

In Fig. 38, GPT-4o still performs well in aligning generated content with story semantics. However, inconsistencies begin to emerge, particularly in visual style. As shown in the third and fourth frames, the visual style changes from the other frames. This indicates limitations in long-range style memory and visual coherence across temporally adjacent images.

Overall, GPT-4o demonstrates strong capability in aligning visual content to story instructions and preserving local character continuity. Nonetheless, consistent style retention and stable progression across multiple frames remain challenging, especially when no visual guidance is provided.

Section 3.2.5 Story Visualization

Draw a story about: A photo of a beaming gardener in overalls with a straw hat
1. Doing laundry in the basement.
2. Unwrapping a birthday gift.
3. Folding origami paper into shapes.



Based on the three character images, draw a story about: Confrontation at Starlight Ranch: A dimly lit, chaotic interior of a ranch house with overturned chairs and signs of struggle.
1. Potts's Discovery: An injured old trooper, Frank Potts, lying on the floor with a look of recognition and shock on his face.
2. Zoe's Desperation: A beautiful young woman with long golden hair, opening a second-floor window in distress, calling for help against a night sky.
3. The Wife's Plea: A woman kneeling on the floor, cradling the injured Potts in her arms, surrounded by dim lighting and chaos.
4. Potts's Final Moments: A dying trooper, Frank Potts, reaching out to touch the golden hair of his kneeling daughter, Zoe, in a tender and poignant gesture.
5. The Revelation: The wife revealing the truth to Zoe about her father, with a baptismal certificate in hand, in a room with a few onlookers.



Figure 37: Examples of story visualization generated by GPT-4o.

Section 3.2.5 Story Visualization

Generate a story based on the following storyboard prompts, ensuring the consistency of the characters and the coherence of the story:

Storyboard 1 prompt: High-angle shot reveals the Xiao Clan hall: Patriarch Xiao Zhan (authoritative middle-aged man) on the throne, three elders in colored robes flanking him, young Xiao Yan in black standing behind. Sunlight streaks through open doors, creating dramatic shadows.

Storyboard 2 prompt: Low-angle tracking shot: Nalan Yanran leads the group (white-robed girl with silver sword), Ge Ye with gray robe/whisker on her left, two sword-carrying disciples behind. Marble floor reflects moving shadows, robes fluttering.

Storyboard 3 prompt: OTS close-up of Nalan Yanran (lifted chin/parted lips), with blurred foreground showing Xiao Zhan crushing teacup (tea leaves splashing). Out-of-focus background reveals Xiao Yan's tense arm and elders' shocked faces.

Storyboard 4 prompt: Wide shot: Xiao Zhan's erupting douqi (blue energy shattering tablecloth), Nalan retreating (sleeves whipping), Ge Ye's glowing whisker barrier, Xiao Yan's ring glinting while steadying his father, elders reacting differently.

Storyboard 5 prompt: Insert shot: Soaked annulment letter (blurred ink) beside broken teacup refracting distorted figures. Nalan's jade pendant (intricate carving) glows coldly in bokeh.



Figure 38: Additional examples of story visualization generated by GPT-4o.

3.2.6 Virtual Try-on

Virtual try-on aims to synthesize realistic images of a target person wearing garments from a reference image[218, 54, 165, 53, 56, 120]. This task evaluates the model’s ability to disentangle appearance from clothing, retain person identity, and accurately transfer fine-grained garment attributes such as texture, color, and structure.

As shown in Fig. 39, GPT-4o demonstrates strong performance in this task. The generated outputs not only preserve the identity and pose of the target individual but also successfully transfer the visual features of the garments, including sleeve length, neckline design, printed logos, and material patterns. Even subtle stylistic details are faithfully reproduced, such as the gradient texture in sweaters and brand-specific typography on shirts.

Overall, these results indicate that GPT-4o exhibits a strong capability in clothing transfer, producing realistic and identity-preserving virtual try-on results with high visual fidelity.

Section 3.2.6 Vitural try-on

  <div style="border: 1px solid black; padding: 5px; display: inline-block;">Generate an image where the person in the first image is wearing the clothes in the second image</div> 	  <div style="border: 1px solid black; padding: 5px; display: inline-block;">Generate an image where the person in the first image is wearing the clothes in the second image</div> 
  <div style="border: 1px solid black; padding: 5px; display: inline-block;">Generate an image where the person in the first image is wearing the clothes in the second image</div> 	  <div style="border: 1px solid black; padding: 5px; display: inline-block;">Generate an image where the person in the first image is wearing the clothes in the second image</div> 

Figure 39: Examples of virtual try-on generated by GPT-4o.

3.3 Low-level Image Generation

Low-level image generation tasks focus on enhancing or restoring the quality of images at the pixel level. These tasks test GPT-4o’s capability in fine-grained visual synthesis, including recovery of detail and color fidelity in degraded images.

3.3.1 Image Super-Resolution

Image super-resolution (SR) aims to reconstruct high-resolution (HR) images from low-resolution (LR) inputs, enhancing visual quality by improving sharpness, restoring details, and generating realistic textures[3, 107, 87, 172]. This task is fundamental in image enhancement and widely applicable in real-world scenarios such as photography, surveillance, and remote sensing.

As shown in Fig.40 and Fig.41, GPT-4o demonstrates good capability in image super-resolution. The model can effectively enhance the clarity of LR images and recover fine details, making the visual results more appealing and closer to natural images.

However, the generation process is still constrained by the model’s maximum output resolution (as mentioned in Sec 2.1), which is limited to a few fixed sizes (e.g., 1024×1536 , 1536×1024). While the model is able to improve image quality within this resolution boundary, it cannot directly produce ultra-high-resolution images beyond its generation limit.

Overall, GPT-4o shows promising performance in image super-resolution tasks, striking a balance between detail restoration, sharpness enhancement, and content consistency under resolution constraints.

Section 3.3.1 Image Super-resolution

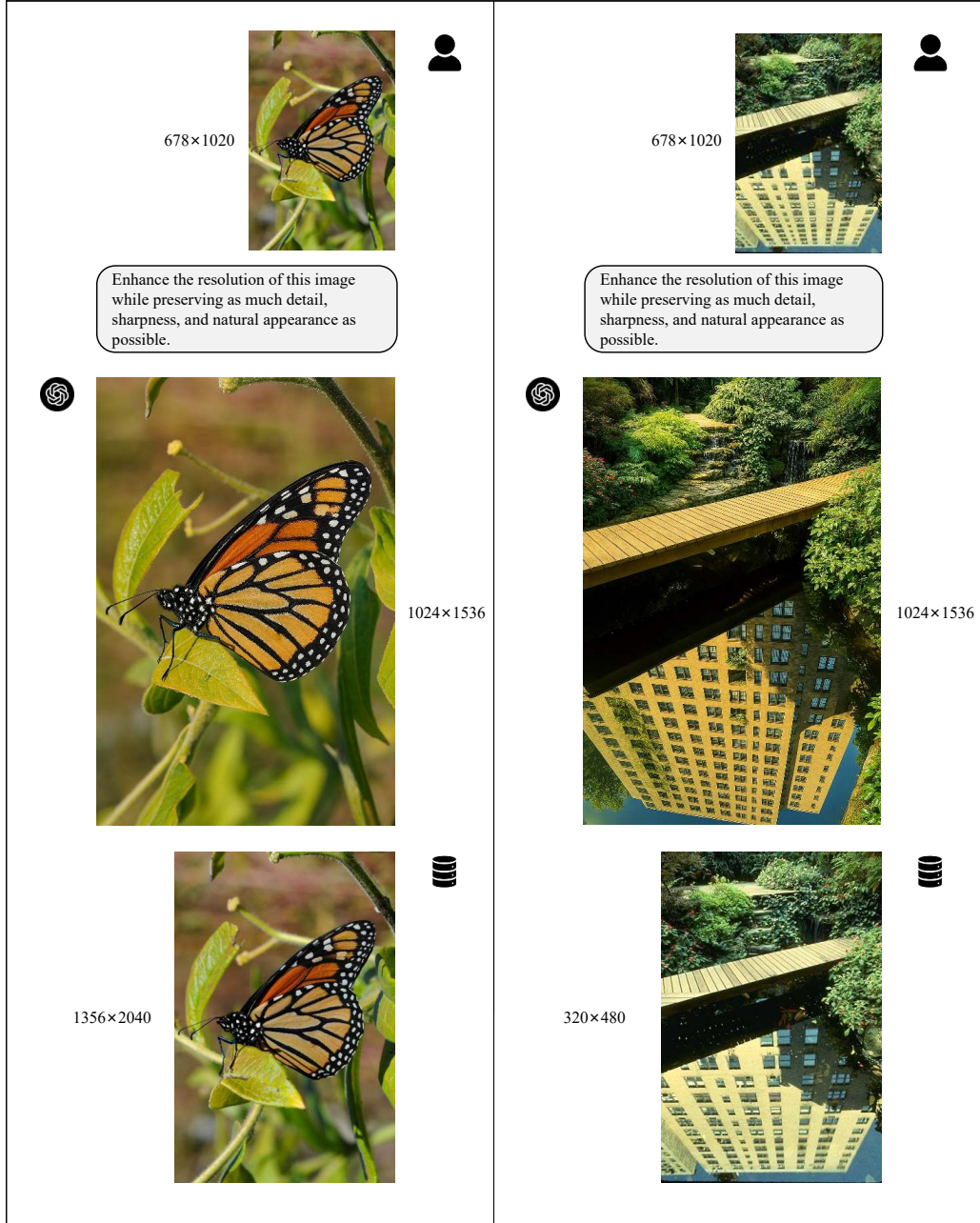


Figure 40: Examples of image super-resolution results generated by GPT-4o. The model can enhance low-resolution images with improved sharpness, detail recovery, and natural appearance. However, the maximum output resolution is constrained by the model's generation limits.

Section 3.3.1 Image Super-resolution

240×160



Enhance the resolution of this image while preserving as much detail, sharpness, and natural appearance as possible.

1536×1024



480×320



1020×768



Enhance the resolution of this image while preserving as much detail, sharpness, and natural appearance as possible.

1536×1024



2040×1536



Figure 41: Additional examples of image super-resolution results generated by GPT-4o.

3.3.2 Image Colorization

Image colorization aims to convert grayscale images into plausible and aesthetically pleasing color versions[203, 198, 116], often conditioned on either general priors or user-specified color styles. This task evaluates the model’s ability to infer semantic content, preserve structure, and apply style-aware color mappings.

As shown in Fig. 42 and Fig. 43, GPT-4o produces highly convincing colorized results under various stylistic instructions. Given different color schemes—such as “Neutral Tones,” “Classic Warm,” “Modern Cool,” “Soft Pastels,” and “Bold Contrasts”—the model consistently generates images with accurate semantic interpretations and clear stylistic alignment. For instance, warm tones are correctly applied to skin and wood materials under the “Classic Warm” style, while cooler tones are used for metallic or urban structures in the “Modern Cool” setting. The model also demonstrates a strong capability to preserve spatial structures and avoid color bleeding or semantic mismatches. Across all evaluated results, GPT-4o exhibits excellent performance in aligning global color tone with regional object categories and overall visual harmony.

Overall, these results indicate that GPT-4o handles colorization tasks with both semantic understanding and stylistic control, making it a strong candidate for controllable grayscale-to-color image synthesis.

Section 3.3.2 Image Colorization



Colorize this grayscale image with a <color scheme> style.



<color scheme>:
Neutral Tones



<color scheme>:
Classic Warm



<color scheme>:
Modern Cool



<color scheme>:
Soft Pastels



<color scheme>:
Bold Contrasts



Colorize this grayscale image with a <color scheme> style.



<color scheme>:
Neutral Tones



<color scheme>:
Classic Warm



<color scheme>:
Modern Cool



<color scheme>:
Soft Pastels



<color scheme>:
Bold Contrasts



Figure 42: Examples of image colorization generated by GPT-4o.

Section 3.3.2 Image Colorization



Colorize this grayscale image with a <color scheme> style.



<color scheme>:
Neutral Tones



<color scheme>:
Classic Warm



<color scheme>:
Modern Cool



<color scheme>:
Soft Pastels



<color scheme>:
Bold Contrasts



Colorize this grayscale image with a <color scheme> style.



<color scheme>:
Neutral Tones



<color scheme>:
Classic Warm



<color scheme>:
Modern Cool



<color scheme>:
Soft Pastels



<color scheme>:
Bold Contrasts



Figure 43: Additional examples of image colorization generated by GPT-4o.

3.3.3 Image Restoration

Image restoration includes removing noise, blur, or other artifacts from corrupted images. This task measures the model’s ability to recover clean, high-quality visuals from degraded inputs. GPT-4o demonstrates a certain level of capability in image restoration tasks, effectively removing various degradations such as noise, blur, rain, or haze. However, we observe that the restored results may not always strictly align with the original input in terms of fine-grained details or textures. This indicates that the model tends to focus more on generating perceptually clean and plausible results rather than strictly preserving pixel-level accuracy.

Image Denoising Image denoising refers to the task of removing random noise from corrupted images while preserving the underlying structure and visual details[107]. Effective denoising demonstrates a model’s ability to distinguish signal from noise and recover clean visual content with high fidelity[106, 14, 46]. Figure 44 presents several representative examples of GPT-4o’s performance on the image denoising task. The model is prompted to remove noise while preserving natural details across a variety of scenes, including portraits, documents, and landscapes. Overall, GPT-4o demonstrates a reasonable ability to suppress visual noise and enhance global clarity. For instance, in the case of the noisy book cover, the text becomes significantly more legible after denoising, indicating that the model successfully restores high-frequency details.

However, a closer inspection reveals that GPT-4o often alters certain local structures in the process. As highlighted by the red boxes, some fine-grained textures and object boundaries are unintentionally smoothed or distorted. In the portrait example (left), facial details and background elements deviate noticeably from the original, suggesting a degradation in structural fidelity. Similarly, in the landscape scene, the architectural components of the house exhibit shape inconsistencies post-denoising.

These observations suggest that while GPT-4o is capable of producing visually cleaner images, it does so by prioritizing perceptual enhancement over pixel-level accuracy. This behavior is consistent with its design as a vision-language model optimized for human-aligned generation, rather than precise signal restoration.

Image Deblurring Image deblurring is a classical low-level vision task that aims to restore clear and sharp images from blurry inputs[115, 138]. In this part, we evaluate GPT-4o on two typical types of deblurring tasks: motion deblurring[81, 102, 212] and defocus deblurring[131, 132, 1, 2]. Motion deblurring targets images degraded due to object or camera movement, while defocus deblurring focuses on images blurred by the depth of field limitations or lens defocus.

As shown in Fig. 45, GPT-4o demonstrates a promising ability to recover the overall structure, sharpness, and scene layout of the blurred input images. For motion deblurring (examples (a1) and (a2)), the model effectively restores the main objects and background clarity. Similarly, for defocus deblurring (examples (b1) and (b2)), the scene composition is generally well-aligned with the input, and the synthesized results present improved sharpness.

However, we also observe noticeable limitations. In some cases, the fine-grained details are not faithfully preserved. For example, in (a1), the restored human figures exhibit appearance inconsistencies compared to the original. Additionally, for defocus deblurring, although the scene structure is preserved, certain color deviations occur, as seen in (b2), where the building color differs significantly from the input image. These observations suggest that while GPT-4o is capable of perceptually restoring sharp images, its deblurring process tends to prioritize visual plausibility over strict content fidelity.

Image Dehazing Image dehazing aims to remove haze or fog from images, enhancing scene visibility while preserving natural colors and structural details. This task is crucial for improving image quality in low-visibility conditions, such as in autonomous driving, remote sensing, and outdoor photography[101, 211, 178, 128].

As shown in Fig.46 and Fig.47, GPT-4o demonstrates strong performance in the image dehazing task. The model can effectively remove haze from various scenes, recovering clear and sharp visual content. In addition to haze removal, we observe that GPT-4o tends to enhance the image’s color saturation and vividness. For example, the sky becomes bluer, and the vegetation appears greener after dehazing, making the scene more visually appealing.

Such results indicate that GPT-4o performs dehazing in a perceptual and generative manner. While the visibility improvement is significant, the model also enriches the visual effects beyond the original content, reflecting its tendency to optimize for human aesthetic preferences.

Overall, GPT-4o achieves a good balance between haze removal, detail preservation, and visual enhancement, making it suitable for real-world outdoor image enhancement applications.

Image Deraining Image deraining is a crucial low-level vision task that aims to remove rain-related degradations from images while preserving scene content and enhancing visibility. In real-world scenarios, rain artifacts can be categorized into two types: *rain streaks*[193, 200, 127] that appear in the air, and *raindrops*[124, 76, 130] that attach to the camera lens or window surfaces. Both types significantly affect the quality of images and hinder the performance of downstream vision tasks.

As shown in Fig.48 and Fig.49, GPT-4o demonstrates promising capabilities in handling both rain streak removal and raindrop removal tasks. For rain streak removal, the model can effectively eliminate rain patterns from various scenes, including dynamic driving environments and urban streets. The visibility and clarity of the derained results are greatly improved. For raindrop removal, GPT-4o is able to restore the occluded content behind the raindrops and recover the overall structure of the scene. The generated images exhibit clean surfaces and improved visual quality.

However, we also observe some limitations in both tasks. For rain streak removal, the model tends to over-smooth the textures of the original scene. For instance, in the driving scene, road textures and tire marks are partially lost. In the wall scene, graffiti details are blurred after deraining. In the case of raindrop removal, although the global structure is restored, there are occasional inconsistencies or hallucinated content in the recovered areas, especially when the occluded regions are complex.

These observations suggest that while GPT-4o shows strong rain removal ability and achieves satisfactory perceptual quality, there is still room for improvement in preserving fine-grained details and ensuring content consistency in heavily degraded regions.

Image Desnowing Image desnowing aims to remove snow particles or snow cover from images and restore the original clean scene while preserving fine details and color consistency[27, 30, 67]. This task is particularly useful in outdoor image enhancement and pre-processing for downstream vision applications in winter conditions.

As shown in Fig. 50, GPT-4o achieves impressive performance on the desnowing task across a variety of scenes, including forests, urban streets, and snow-covered objects. The model is capable of effectively removing both falling snow and accumulated snow, restoring the original appearance of the scene.

Low-light Image Enhancement Low-light image enhancement aims to improve the visual quality of images captured under poor lighting conditions. The task focuses on increasing brightness and contrast while maintaining the original scene’s colors and details, enabling better visibility for both human perception and downstream vision tasks.

As shown in Fig. 51, GPT-4o demonstrates promising performance in low-light image enhancement. The model can significantly brighten dark regions and restore scene visibility, making previously invisible content clearly observable. Meanwhile, the model preserves the natural appearance of the scene without introducing severe color distortions.

Old Photo Restoration Old photo restoration aims to repair and enhance old, degraded, or damaged images, improving their clarity and visual quality while preserving the original style or vintage characteristics[164]. This task often requires complex reasoning to remove artifacts, restore missing content, and even colorize black-and-white photos when desired.

As shown in Fig.52 and Fig.53, GPT-4o demonstrates remarkable capabilities in old photo restoration. The model not only improves sharpness and removes artifacts but also exhibits controllable generation ability. Specifically, given different prompts, the model can either maintain the original black-and-white or vintage style or add realistic colors to the restored image.

Section 3.3.3 Image Denoising

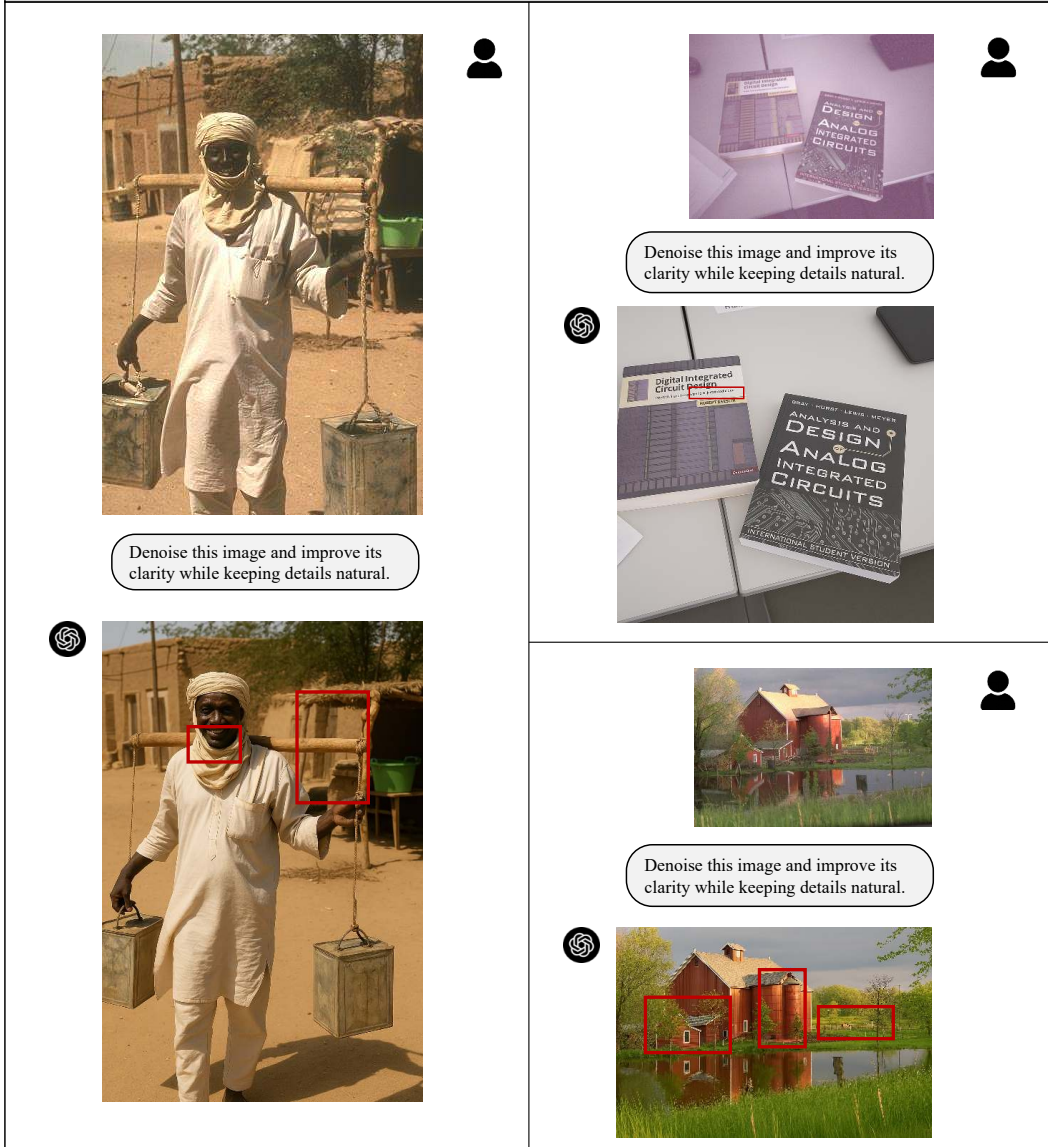


Figure 44: Examples of GPT-4o performing image denoising. While the model is able to reduce noise and improve overall image clarity, it often alters fine-grained details or introduces slight distortions, as highlighted in the red boxes. This indicates a trade-off between denoising effectiveness and structural fidelity.

Section 3.3.3 Image Deblurring

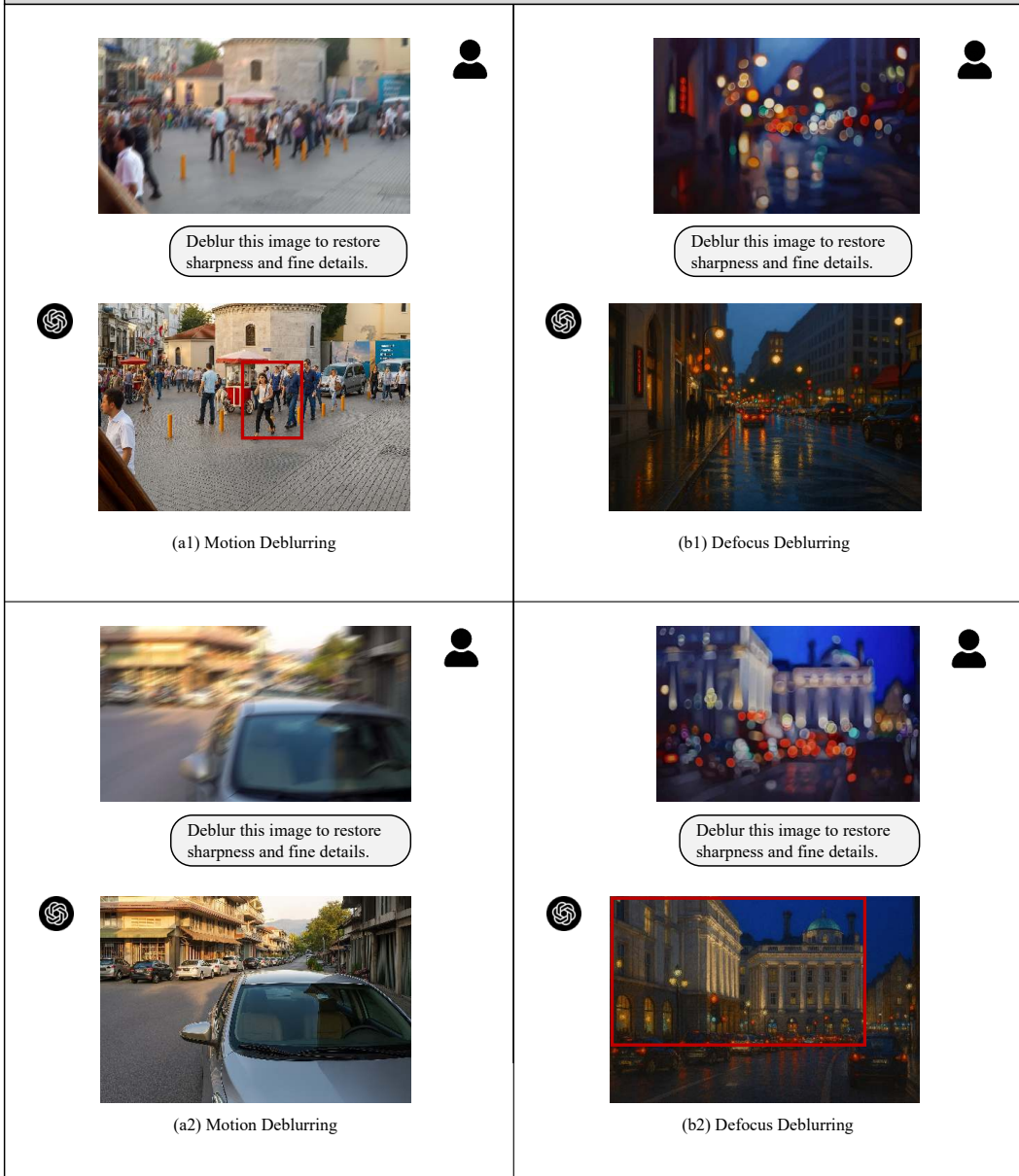


Figure 45: Examples of image deblurring results generated by GPT-4o. The model is able to restore the overall structure and sharpness of the input images for both motion deblurring and defocus deblurring tasks. However, certain color deviations (e.g., building colors in b2) and fine detail inconsistencies (e.g., human appearance in a1) are observed compared to the original content.

Section 3.3.3 Image Dehazing

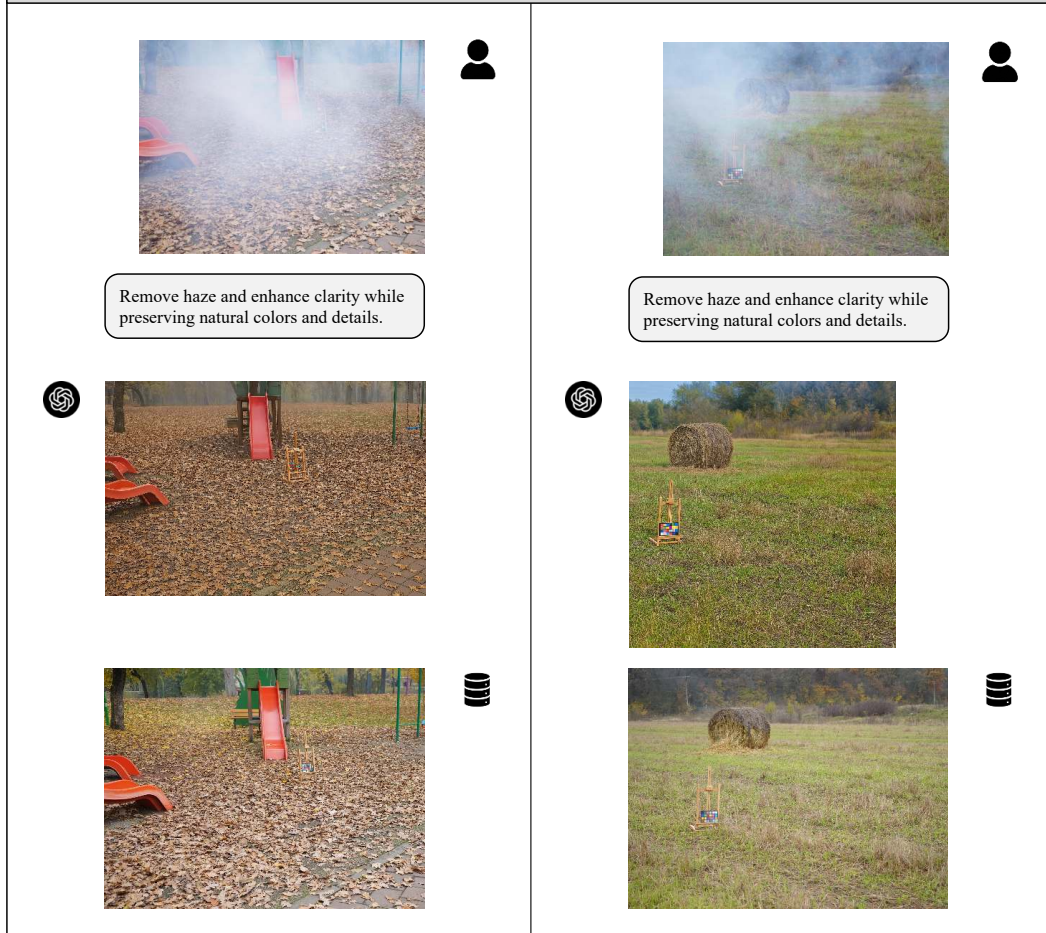


Figure 46: Examples of image dehazing results generated by GPT-4o. The model effectively removes haze and restores scene clarity while preserving natural colors and structural details.

Section 3.3.3 Image Dehazing

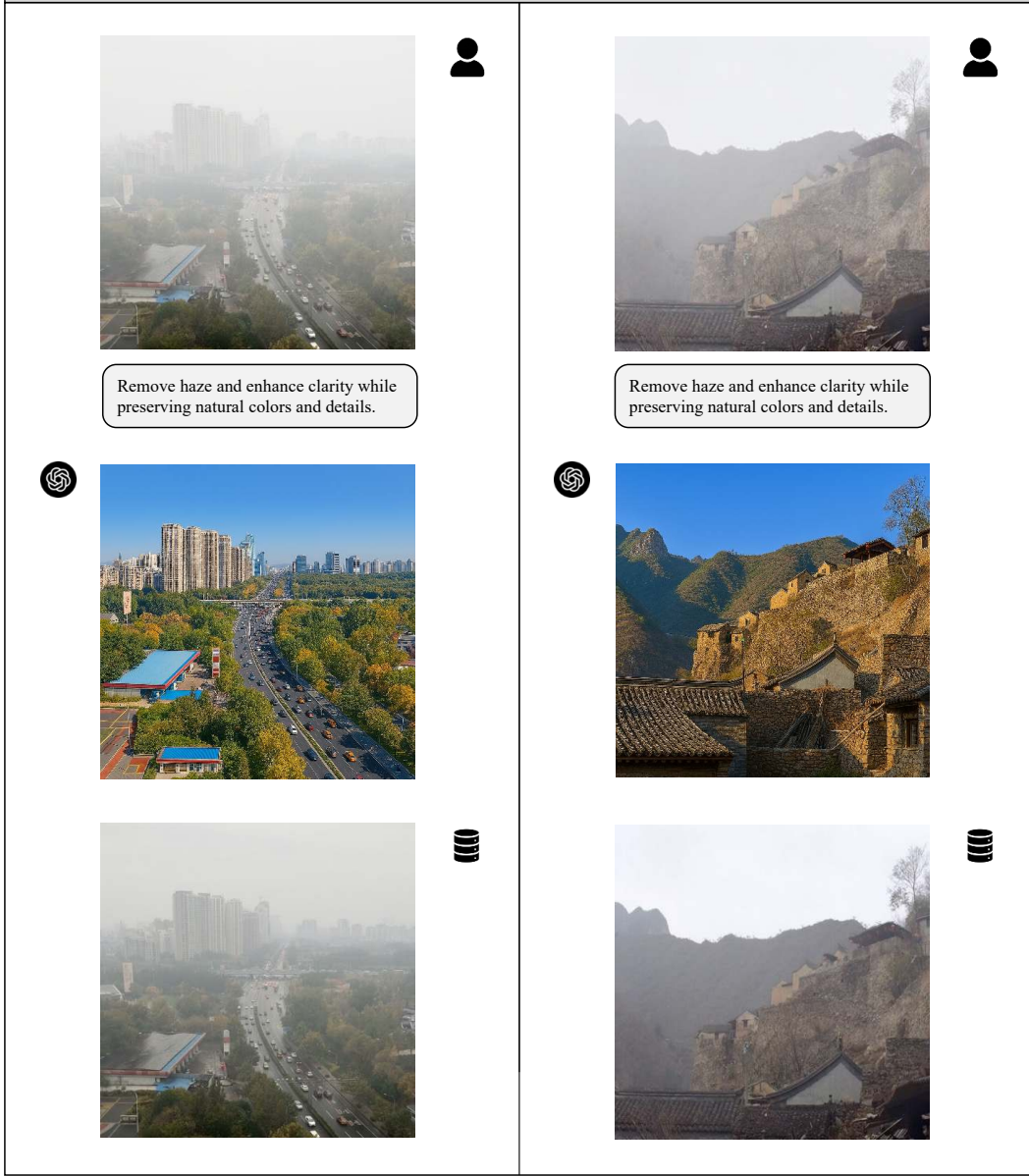


Figure 47: Additional examples of image dehazing results generated by GPT-4o. The model not only removes haze and restores scene clarity but also tends to enhance the overall color saturation and vividness of the image. This indicates that GPT-4o performs dehazing in a perceptual manner, focusing on both visibility improvement and aesthetic enhancement.

Section 3.3.3 Image Deraining



Remove rain from the image while preserving details and enhancing visibility.



Remove rain from the image while preserving details and enhancing visibility.

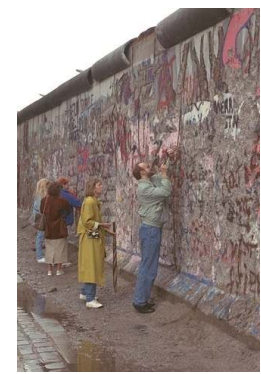


Figure 48: Examples of image deraining results generated by GPT-4o. The model can effectively remove rain streaks and improve overall visibility. However, it often leads to the loss of fine-grained details, such as road textures (left) and wall paintings (right), indicating a trade-off between rain removal and content preservation.

Section 3.3.3 Image Deraining

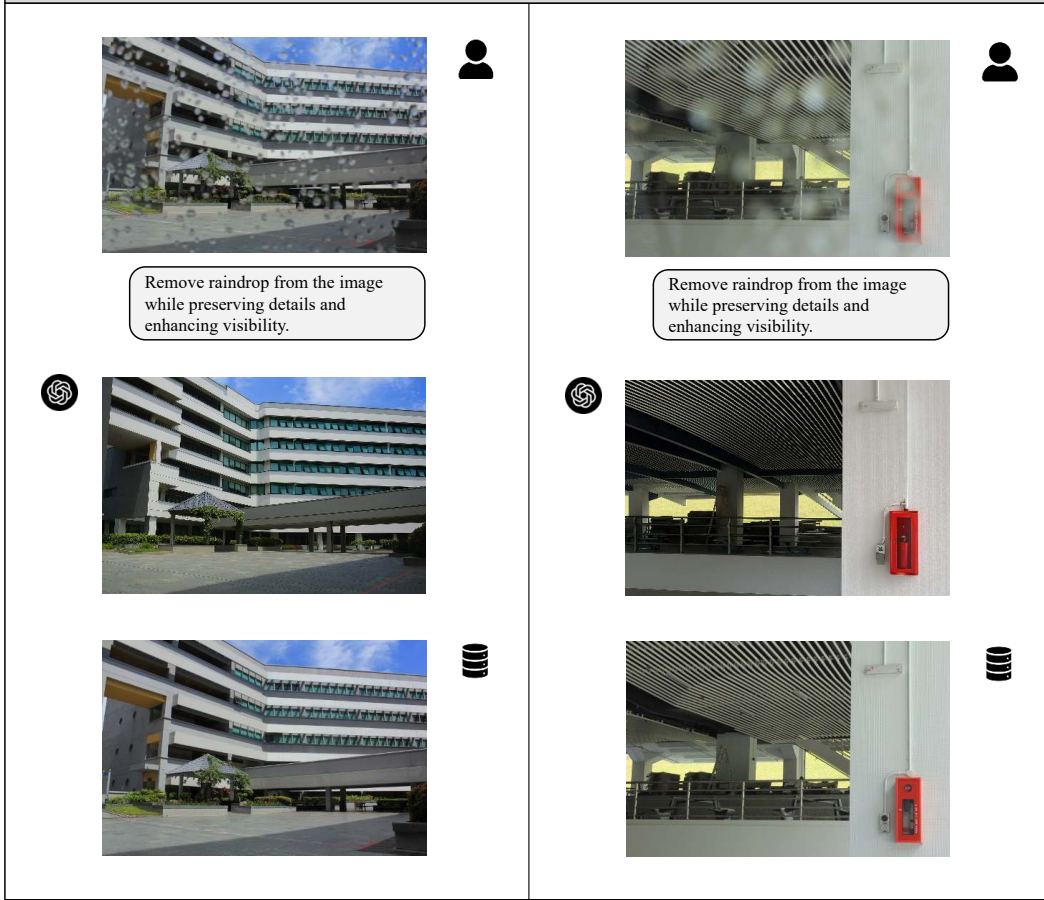


Figure 49: Examples of raindrop removal results generated by GPT-4o. The model effectively removes raindrops from the image surface and restores the occluded regions. However, some subtle texture inconsistency or content hallucination may occur in the recovered areas. Overall, the visibility and clarity of the scene are significantly improved.

Section 3.3.3 Image Desnowing

 Remove snow from the image and restore the natural scene underneath, preserving details and colors.	 Remove snow from the image and restore the natural scene underneath, preserving details and colors.
 A circular icon with a swirl symbol.	 A circular icon with a swirl symbol.
 Remove snow from the image and restore the natural scene underneath, preserving details and colors.	 Remove snow from the image and restore the natural scene underneath, preserving details and colors.
 A circular icon with a swirl symbol.	 A circular icon with a swirl symbol.

Figure 50: Examples of image desnowing results generated by GPT-4o. The model effectively removes snow from various scenes and restores the underlying content with good visual consistency. The generated images preserve the natural colors and structural details of the original scenes, demonstrating strong desnowing capability.

Section 3.3.3 Low-light Image Enhancement

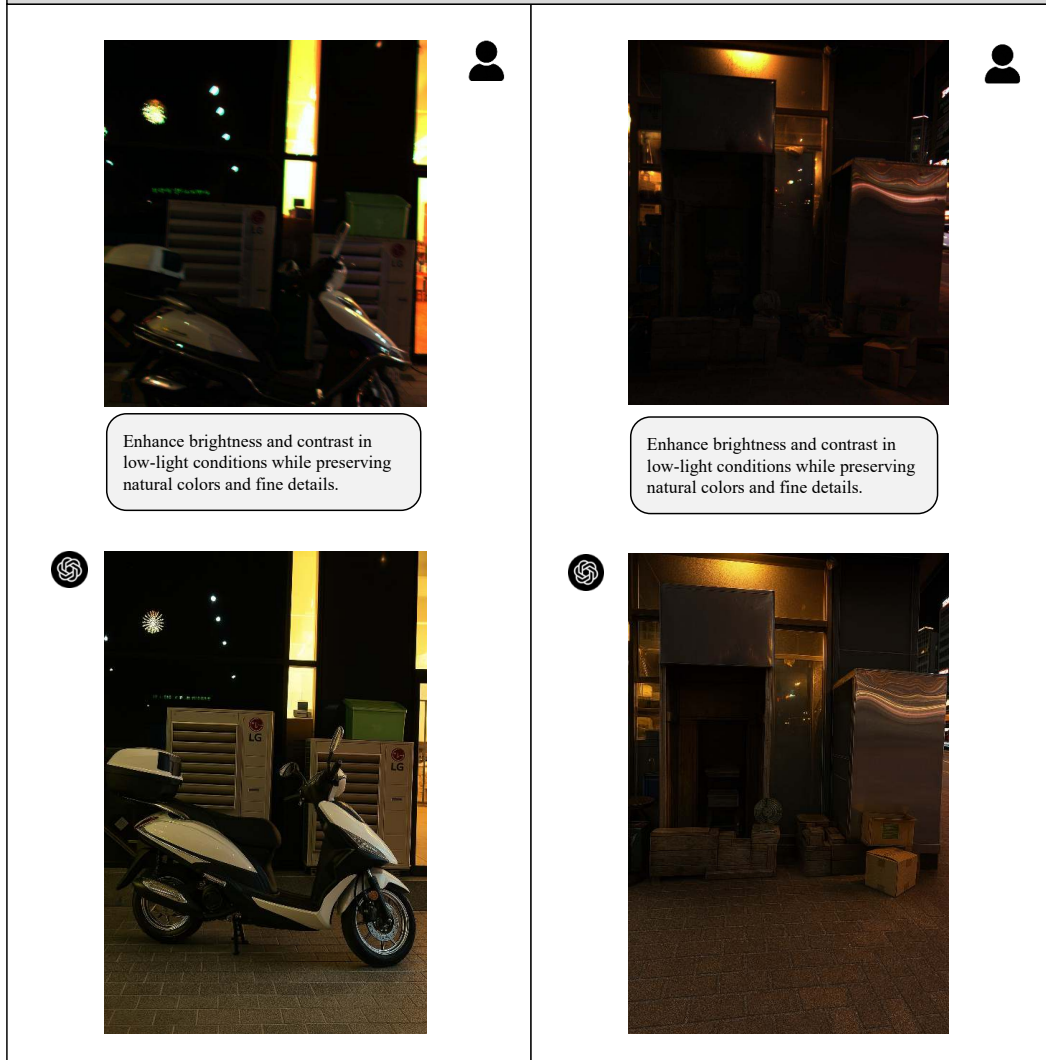


Figure 51: Examples of low-light image enhancement results generated by GPT-4o. The model effectively improves brightness and contrast in dark scenes while preserving natural colors and structural details. The enhanced images exhibit better visibility and a more realistic appearance compared to the original low-light inputs.

Section 3.3.3 Old Photo Restoration



Restore this old black-and-white photo by enhancing clarity, fixing damage, improving overall quality, and **adding realistic color** while preserving the original vintage look.



Restore this old black-and-white photo by enhancing clarity, fixing damage, improving overall quality, and **adding realistic color** while preserving the original vintage look.

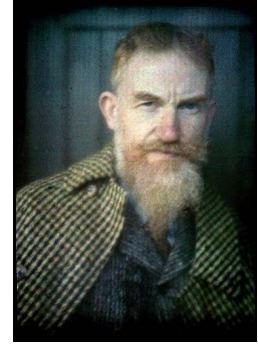


Figure 52: Examples of old photo restoration results generated by GPT-4o. The model effectively enhances image clarity, repairs damaged regions, and restores overall quality.

Section 3.3.3 Old Photo Restoration



Restore this old photo by enhancing clarity, fixing damage, and improving overall quality while keeping the original look.



Restore this old photo by enhancing clarity, fixing damage, and improving overall quality while keeping the original look.

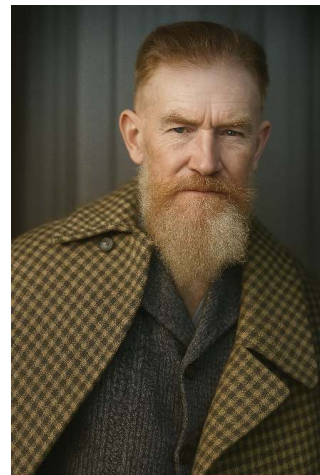


Figure 53: Additional examples of old photo restoration results generated by GPT-4o.

3.3.4 Shadow Removal

Shadow removal aims to eliminate shadows from images while preserving the original content and structure of the scene[167, 129, 78]. This task is essential for improving image aesthetics and supporting downstream vision tasks such as segmentation and detection.

As shown in Fig. 54, GPT-4o demonstrates a strong ability to remove shadows from different textures and scenes. The model can effectively restore the occluded regions and generate consistent and visually pleasing results. However, we observe that shadow removal may lead to slight detail loss in the restored areas. For example, in the left case, the arrangement and shape of the pebbles deviate slightly from the original image after shadow removal. This indicates that while GPT-4o focuses on generating perceptually consistent outputs, fine-grained structure preservation remains a challenge.

Section 3.3.4 Shadow Removal



Figure 54: Examples of shadow removal results generated by GPT-4o. The model effectively removes shadows from the images and restores the overall appearance of the scene. However, slight detail loss can be observed in the restored regions, such as the shape and arrangement of pebbles in the left example.

3.3.5 Reflection Removal

Reflection removal aims to eliminate unwanted reflections from glass or smooth surfaces while preserving the original scene content, texture, and lighting[84, 5]. This task is particularly challenging when reflection and transmission layers are entangled or semantically similar.

As shown in Fig. 55, GPT-4o demonstrates the ability to remove prominent reflections, producing visually cleaner results. However, the model also introduces significant content alterations beyond the reflected regions. In the upper-left example, several objects on the table are removed or modified, indicating a loss of fine-grained detail. In the upper-right case, the structure of the background building has been changed, with architectural elements inconsistently reconstructed. Similarly, in the lower-left image, the eyeglasses worn by the person are completely removed, despite being part of the original non-reflective content.

These results suggest that GPT-4o treats reflection removal as a global editing task rather than a localized layer separation process. While it succeeds in suppressing reflections, it lacks the fine discrimination needed to preserve all true scene content. Future improvements may require explicit reflection segmentation or layer decomposition to better disentangle reflection and background information.

Section 3.3.5 Reflection Removal

 <p>Remove reflections from glass and smooth surfaces while preserving original image details and lighting.</p> 	 <p>Remove reflections from glass and smooth surfaces while preserving original image details and lighting.</p> 
 <p>Remove reflections from glass and smooth surfaces while preserving original image details and lighting.</p> 	 <p>Remove reflections from glass and smooth surfaces while preserving original image details and lighting.</p> 

Figure 55: Examples of reflection removal results generated by GPT-4o.

3.3.6 Image Relighting

Image relighting refers to the process of modifying the lighting conditions of a given image while maintaining the original content and geometry[219, 216]. It evaluates the model's ability to understand light direction, intensity, and color temperature, and apply photorealistic transformations guided by either textual instructions or visual references.

Text-based relighting. As shown in Fig. 56, GPT-4o effectively interprets text prompts describing various lighting styles, such as "neon cyberpunk" or "rim lighting." The model successfully applies vibrant lighting with colored shadows and glowing highlights in cyberpunk settings, and soft back-lighting in natural rim light scenarios. It demonstrates precise semantic understanding and strong control over global illumination effects.

Reference-based relighting. In Fig. 57, the model is conditioned on a visual reference that provides lighting cues such as direction, intensity, and mood. The results show that GPT-4o is able to mimic the lighting setup from the reference image, adjusting contrast, highlight positioning, and overall ambiance accordingly. The subject and background are consistently lit in a visually coherent manner.

Overall, GPT-4o performs well in both text- and reference-guided relighting. The lighting is adjusted naturally without distorting the subject geometry or textures, indicating a strong capability for controllable and photorealistic light manipulation.

Section 3.3.6 Image Relighting

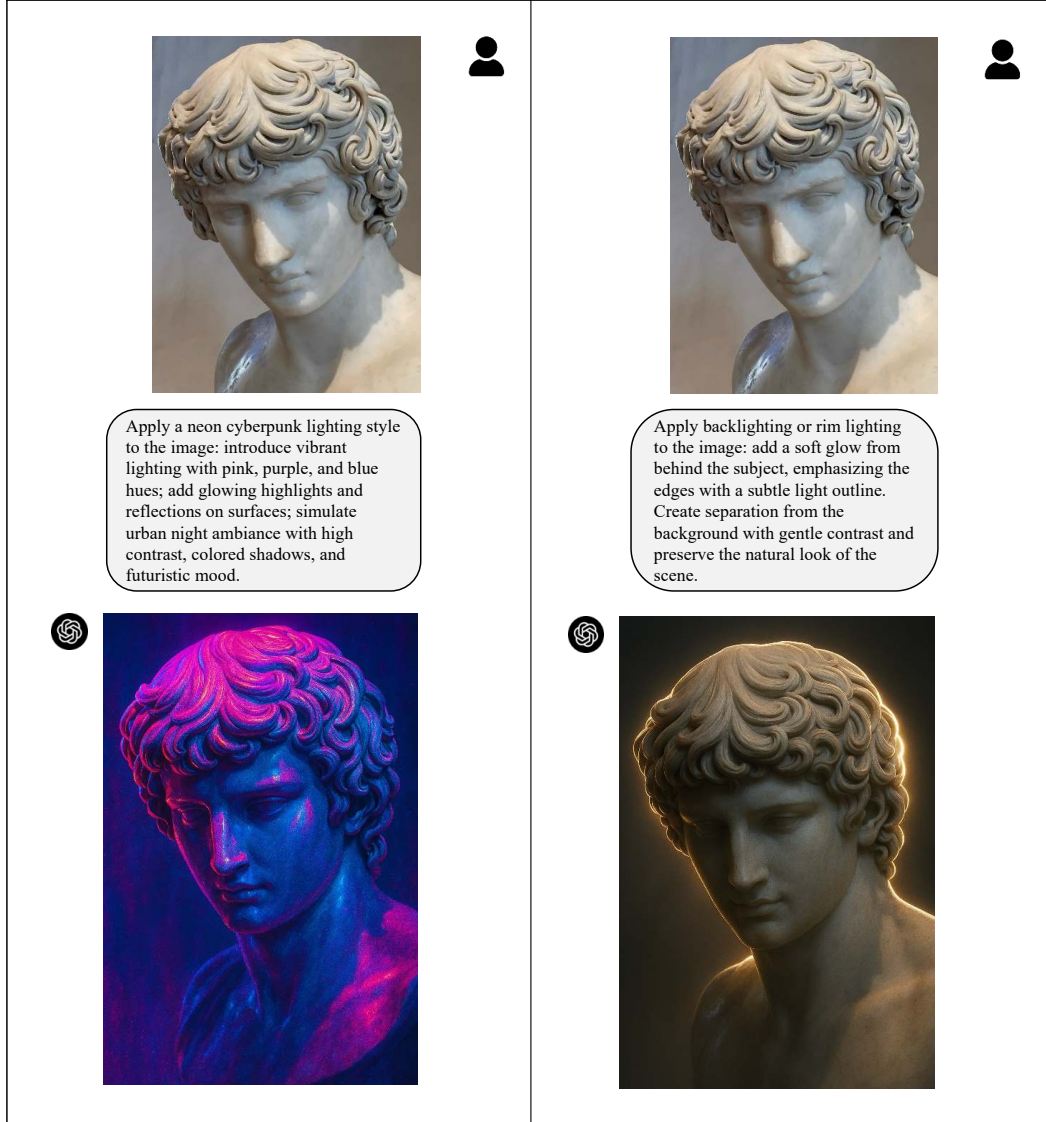


Figure 56: Examples of image relighting with textual prompts generated by GPT-4o.

Section 3.3.6 Image Relighting



Apply the lighting and shadow style from the second image onto the subject and background of the first image. Preserve the composition and objects of the first image, but make the lighting, direction of light, brightness, and shadow contrast match that of the second image. Ensure smooth blending and realistic integration of highlights and shadows.



Apply the lighting and shadow style from the second image onto the subject and background of the first image. Preserve the composition and objects of the first image, but make the lighting, direction of light, brightness, and shadow contrast match that of the second image. Ensure smooth blending and realistic integration of highlights and shadows.



Figure 57: Examples of image relighting with reference images generated by GPT-4o.

3.3.7 Underwater Image Enhancement

Underwater image enhancement aims to improve the visual quality of images captured in underwater environments[80, 135, 205], which often suffer from color distortion, low contrast, and poor visibility due to light absorption and scattering in water. The task focuses on restoring natural color balance, enhancing image clarity, and increasing scene visibility.

As shown in Fig. 58, GPT-4o demonstrates a certain capability in underwater image enhancement. In some relatively clear scenes, the model is able to effectively enhance details, correct color bias, and significantly improve the overall visibility of the image. However, underwater environments present a more challenging scenario compared to other enhancement tasks, especially when the input image suffers from severe degradation.

We observe that the model’s enhancement performance varies depending on the input image quality and scene complexity. While some examples achieve promising results with clearer textures and better color restoration, other cases remain limited in improvement, showing only slight changes after enhancement. These results indicate that GPT-4o has the potential to handle underwater image enhancement but still faces challenges in generalizing to highly degraded or extremely blurry underwater scenes.

Section 3.3.7 Underwater Image Enhancement

 Enhance this underwater image for better clarity, color balance, and visibility.	 Enhance this underwater image for better clarity, color balance, and visibility.
 Enhance this underwater image for better clarity, color balance, and visibility.	 Enhance this underwater image for better clarity, color balance, and visibility.
 Enhance this underwater image for better clarity, color balance, and visibility.	 Enhance this underwater image for better clarity, color balance, and visibility.
 Enhance this underwater image for better clarity, color balance, and visibility.	 Enhance this underwater image for better clarity, color balance, and visibility.

Figure 58: Examples of underwater image enhancement results generated by GPT-4o. The model shows the ability to enhance underwater images by improving clarity, color balance, and visibility. However, due to the challenging nature of underwater environments, the enhancement results vary across different scenes. Some examples demonstrate promising improvements, while others still suffer from limited enhancement effects.

3.3.8 Low-level Data Synthesis

Low-level data synthesis aims to generate degraded images by applying specific visual artifacts or environmental conditions to clean images[1]. This task plays an important role in evaluating a model’s fine-grained control ability in image generation and its potential application in data augmentation for low-level vision tasks, such as image restoration, enhancement, and robustness testing.

As shown in Fig.59 and Fig.60, we evaluate GPT-4o’s capability in synthesizing various degradation types, including motion blur, out-of-focus blur, raindrops on camera lens, snow, rain, underwater effect, fog, and low-light conditions. The model generates images with these degradation effects by following explicit text instructions.

Overall, GPT-4o demonstrates strong generation capability in this task. The synthesized degradations are visually consistent with human perception and exhibit diverse patterns across different scenes. However, the degradation details are sometimes exaggerated or stylized, rather than strictly following real-world physical rules. This observation indicates that the current model generation is more perceptual-driven than physically accurate.

Section 3.3.8 Low-level Data Synthesis

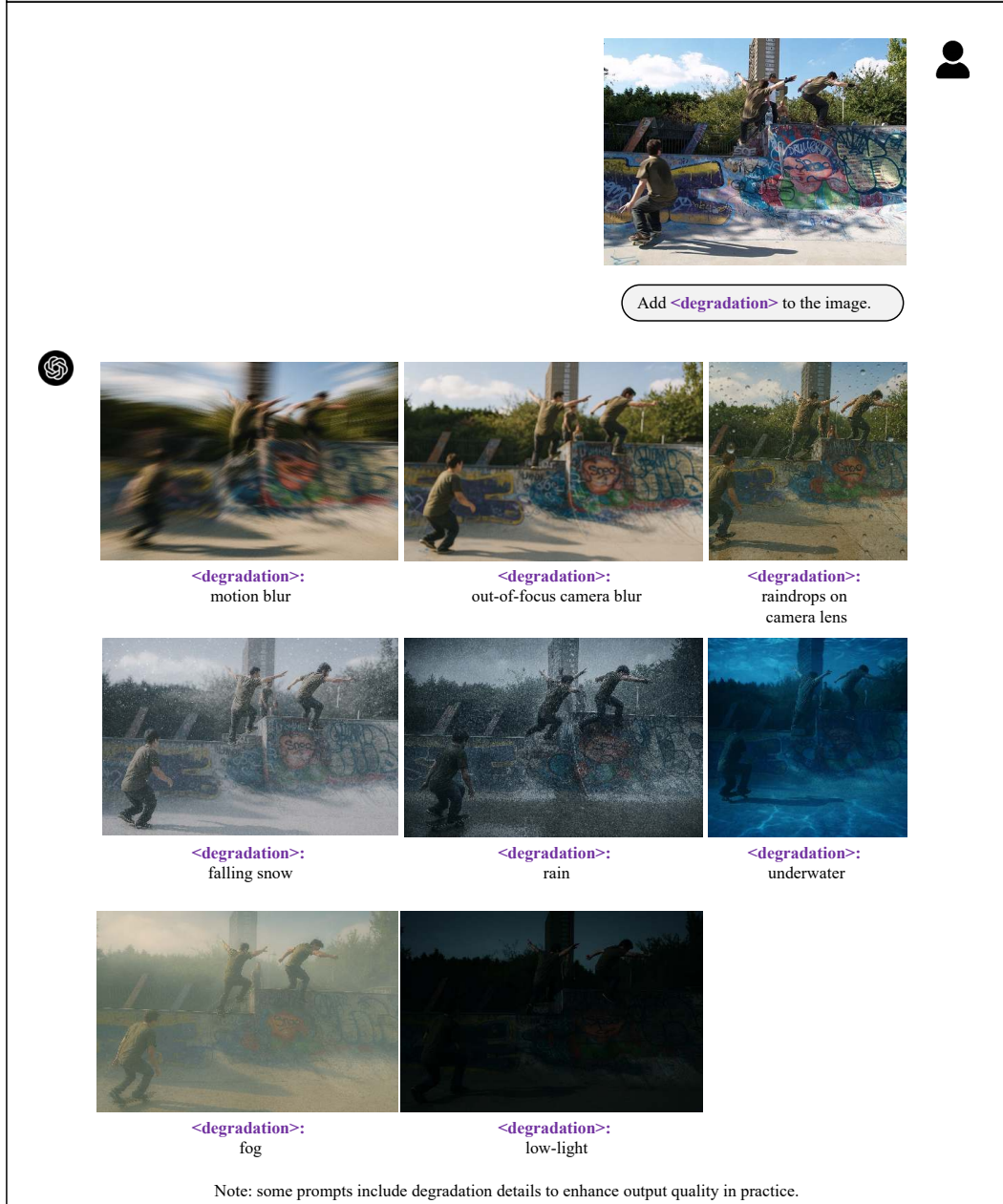


Figure 59: Examples of low-level data synthesis results generated by GPT-4o for a skateboard scene. The model applies various degradation types to a clean image, including motion blur, camera blur, raindrops, snow, rain, underwater, fog, and low-light.

Section 3.3.8 Low-level Data Synthesis

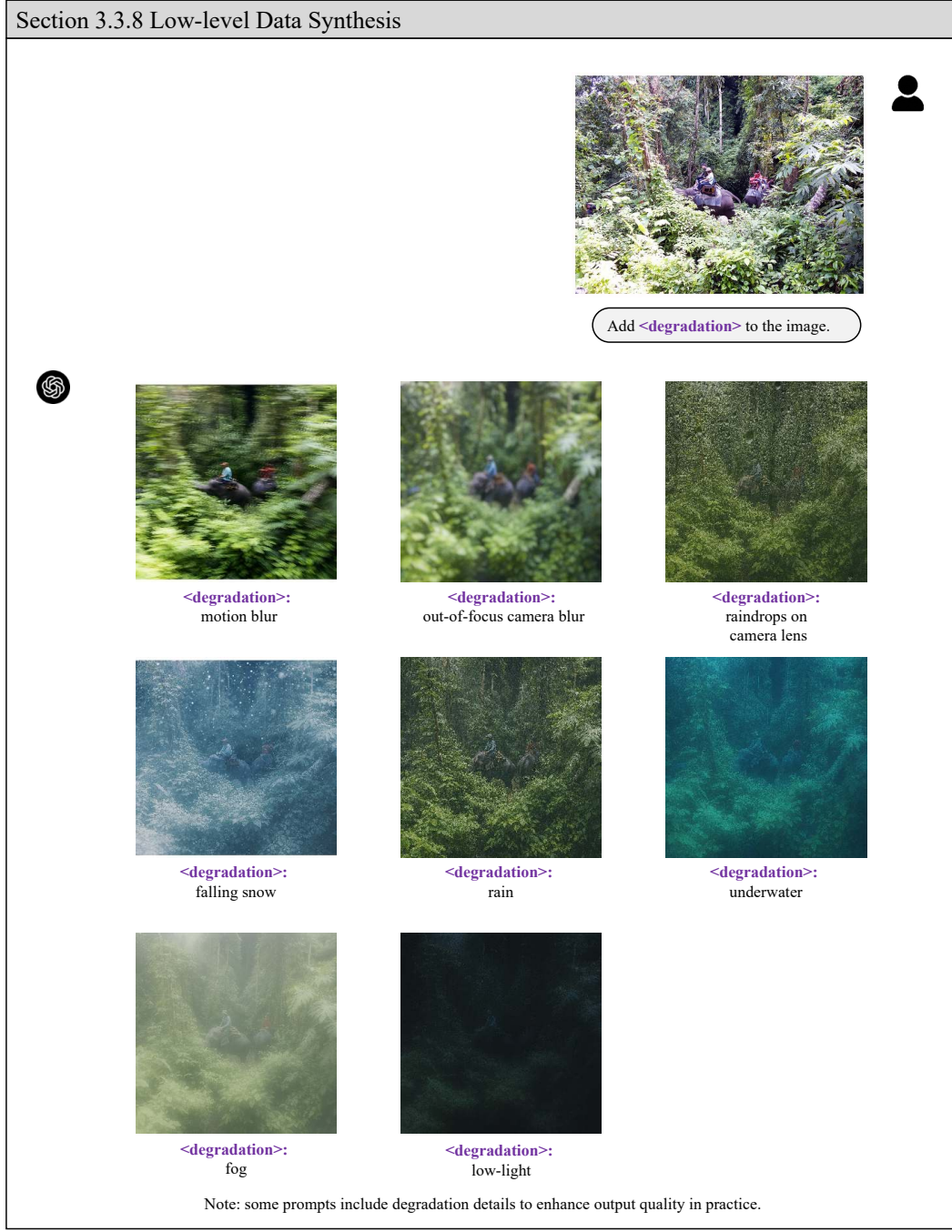


Figure 60: Examples of low-level data synthesis results generated by GPT-4o for a forest scene. The model successfully simulates diverse degradation effects while maintaining the consistency of scene structure.

4 Discriminative Image Generation

4.1 Detection

4.1.1 General Object Detection

General object detection is a fundamental and widely studied task in computer vision[90, 43, 42, 17, 137, 47, 48, 100], aiming to identify and localize objects of interest within natural images. Specifically, the task requires detecting various categories of objects and providing their corresponding bounding boxes. This task serves as an important benchmark to evaluate the model’s basic visual understanding and spatial localization ability. Unlike traditional object detection models that are trained with large-scale annotated datasets, GPT-4o performs detection in a zero-shot manner, relying on its general visual reasoning capabilities without specific detection head tuning.

In this work, we test GPT-4o in the general object detection scenario, covering typical scenes such as animals, daily objects, and natural environments. The goal is to explore whether the model can accurately recognize object instances, understand object boundaries, and output structured detection results in both visual and textual modalities. The evaluation results also help reveal the current limitations of multimodal large models in structured perception tasks.

Visual outputs v.s. Textual outputs. Since GPT-4o supports both visual and textual outputs, we conduct a comparative analysis of these two modalities in the general object detection task. For textual outputs, we use Python to visualize the detection results based on the returned bounding box coordinates.

As shown in Fig. 61, the visual output achieves better performance than the textual output. The generated bounding boxes in the visual output are more accurate, with tighter boundaries that better align with the objects. However, as we discussed earlier, the object detection accuracy of GPT-4o is not stable. In Fig. 62, neither modality produces satisfactory detection results. Both visual and textual outputs show obvious inaccuracies, and several objects are not well localized. Nevertheless, the visual output still presents a slight advantage over the textual output, especially in accurately detecting the two cats on the right side of the image.

These results indicate that while GPT-4o possesses certain object detection capabilities, it still struggles with precise localization, and its detection accuracy varies across different scenarios.

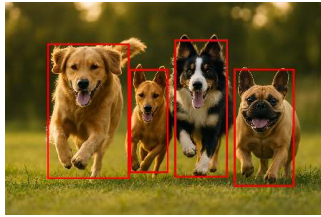
Section 4.1.1 General Object Detection



Detect and highlight all dogs in the image by drawing red bounding boxes around each one.



Detect all dogs in the image. Return the bounding box coordinates for each dog in the format: [top-left-x, top-left-y, bottom-right-x, bottom-right-y]. All coordinates must be normalized (i.e., values between 0 and 1).



(a) Generate visual detection result



Here are the normalized bounding box coordinates for each dog in the image (from left to right):
Dog 1 (Golden Retriever, far left): [0.083, 0.200, 0.292, 0.823]
Dog 2 (Light brown, second from left): [0.342, 0.331, 0.478, 0.842]
Dog 3 (Black and white, second from right): [0.535, 0.170, 0.702, 0.846]
Dog 4 (French Bulldog, far right): [0.764, 0.308, 0.915, 0.848]

(b) Generate textual detection result



Draw by Python

Figure 61: Examples of general object detection results generated by GPT-4o for detecting dogs. The model supports both visual outputs and textual outputs, which can be visualized by external tools. In this example, the visual output shows better accuracy and tighter bounding boxes compared to the textual output.

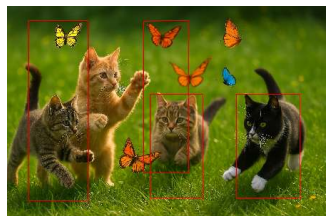
Section 4.1.1 General Object Detection



Detect and highlight all cats in the image by drawing red bounding boxes around each one.



Detect all cats in the image. Return the bounding box coordinates for each cat in the format: [top-left-x, top-left-y, bottom-right-x, bottom-right-y]. All coordinates must be normalized (i.e., values between 0 and 1).

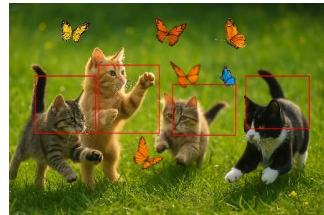


(a) Generate visual detection result



Here are the normalized bounding box coordinates for each cat in the image:
 Cat 1 (leftmost, gray tabby):
 Coordinates: [0.08, 0.34, 0.27, 0.61]
 Cat 2 (orange tabby in the middle, reaching for a butterfly):
 Coordinates: [0.28, 0.29, 0.47, 0.61]
 Cat 3 (gray tabby, walking):
 Coordinates: [0.51, 0.38, 0.71, 0.62]
 Cat 4 (black and white cat, running):
 Coordinates: [0.74, 0.34, 0.94, 0.59]

(b) Generate textual detection result



Draw by Python

Figure 62: Examples of general object detection results generated by GPT-4o for detecting cats. In this case, both visual and textual outputs show limited accuracy, and the detection results are not ideal. However, the visual output still performs slightly better, especially in locating the two cats on the right.

4.1.2 Object Detection within Satellite Imagery

Object detection within satellite imagery is a particularly challenging task due to the complex background, small target size, and dense object distribution[180]. Unlike natural scene images, satellite images often contain a large number of small objects (e.g., vehicles) with low contrast to the background, requiring models to possess strong localization and fine-grained recognition capabilities.

As shown in Fig.63 and Fig.64, we evaluate GPT-4o’s ability to detect vehicles in satellite images using rotated bounding boxes for more accurate localization. In Fig. 63, we observe that GPT-4o suffers from a large number of missed detections in the vehicle detection task. Many small vehicles in the image are not correctly identified, indicating that the model still struggles with dense small object detection in satellite imagery.

Although the detection results in Fig. 64 show significantly improved accuracy, with most vehicles being successfully localized, we also observe a critical limitation of the model. Specifically, GPT-4o tends to modify the input image content during generation. In some regions, the original vehicle distribution has been altered or overwritten, breaking the consistency with the original scene.

These results demonstrate that object detection in satellite imagery remains a highly challenging task for GPT-4o. The model shows certain potential in generating reasonable detection results, but it still faces serious limitations in maintaining content consistency, dense small object detection, and fine-grained localization accuracy.

Section 4.1.2 Object Detection within Satellite Imagery



Please perform vehicle detection on the attached satellite image using rotated bounding boxes to mark each vehicle and produce an output image that highlights the detected vehicles; vehicle detection identifies and localizes vehicles in satellite imagery while rotated bounding boxes allow for accurate orientation adjustments.



Figure 63: Examples of vehicle detection results in satellite imagery generated by GPT-4o. The model attempts to detect vehicles using rotated bounding boxes. However, a large number of small vehicles are missed, indicating the difficulty of dense small object detection in complex satellite scenes.

Section 4.1.2 Object Detection within Satellite Imagery

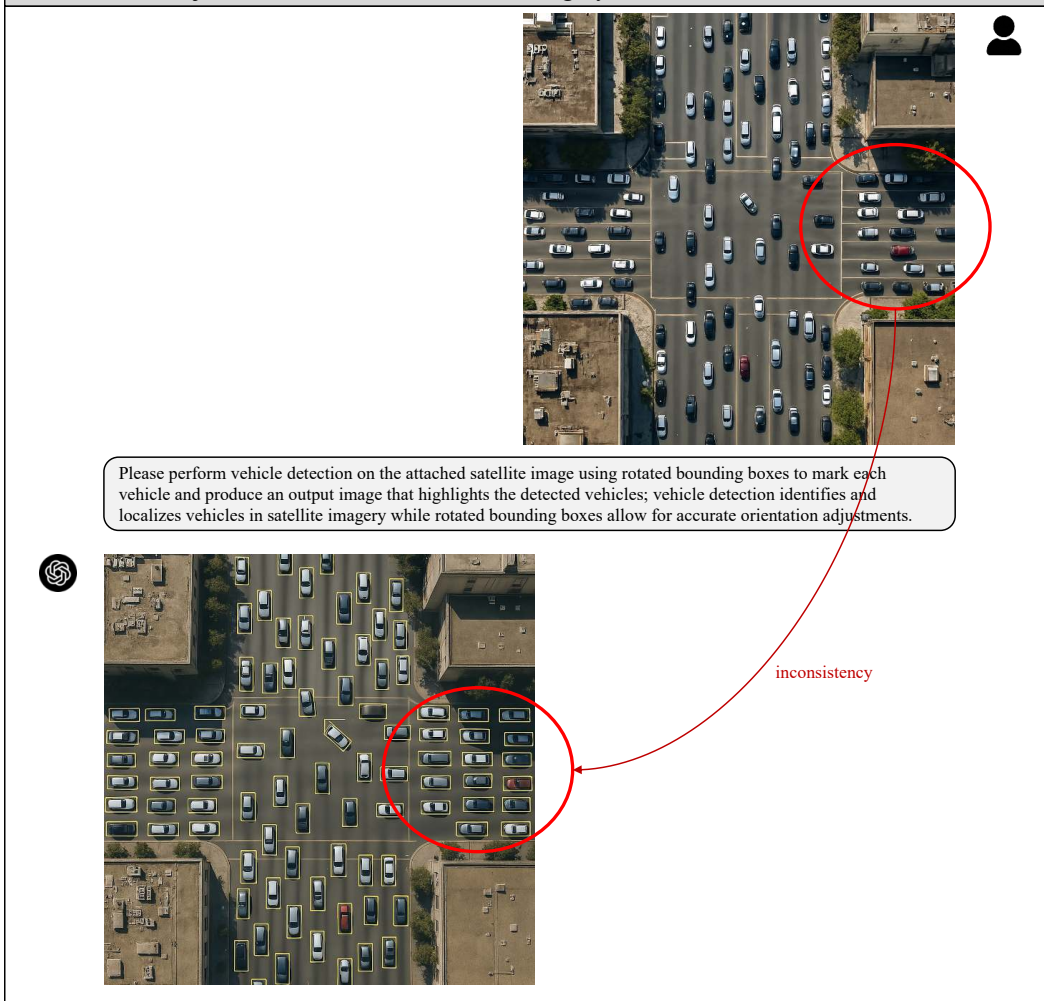


Figure 64: Additional examples of vehicle detection results in satellite imagery generated by GPT-4o. Although the detection accuracy is significantly improved with most vehicles correctly localized, the model tends to modify the original image content, leading to inconsistency with the input image.

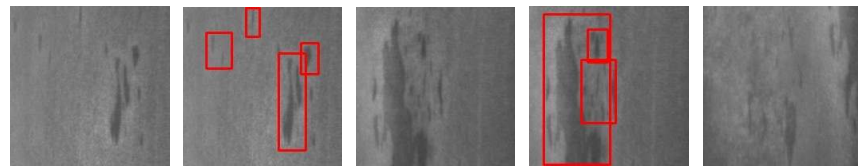
4.1.3 Industrial Visual Inspection

Industrial visual inspection is a highly specialized task that requires detecting fine-grained defects in structured and domain-specific environments[157, 65], such as manufacturing surfaces or printed circuit boards (PCB). Unlike general object detection tasks, this scenario often requires models to possess domain knowledge about typical defect patterns, material properties, and industrial standards.

As shown in Fig.65 and Fig.66, we evaluate GPT-4o in two representative industrial scenarios: surface defect detection[150] and PCB defect detection[155]. For surface defect detection, the model attempts to infer defect patterns based on several input-output examples. However, the generated detection results are unsatisfactory. The model fails to correctly localize the defects and produces bounding boxes with inaccurate locations and inconsistent sizes. Moreover, we observe that the model modifies the content of the input image, changing the visual appearance of the original surface, which is unacceptable in industrial inspection scenarios where input integrity must be preserved. Similarly, in the PCB defect detection task, the model is required to detect predefined categories of defects (e.g., opens, shorts, mousebites). While GPT-4o can detect part of the defect regions, it suffers from low detection accuracy, frequent false positives, missed detections, and incorrect classifications. In some cases, the model even alters the input PCB pattern, which further impacts its practical usability.

These results indicate that GPT-4o faces significant challenges in industrial visual inspection tasks. Beyond general visual reasoning, this task requires the model to incorporate domain-specific prior knowledge to recognize subtle defects while strictly preserving the input content. The current generation of models lacks both accurate defect understanding and robust detection ability in such domain-constrained scenarios.

Section 4.2 Industrial Visual Inspection



This is an industrial defect detection task. Following the pattern established in the first four images (where each pair consists of an input and its corresponding output), generate the detection result for the fifth image.

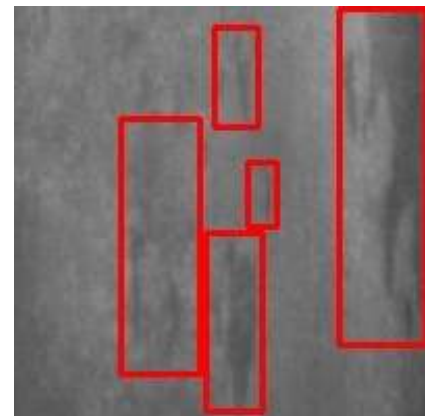
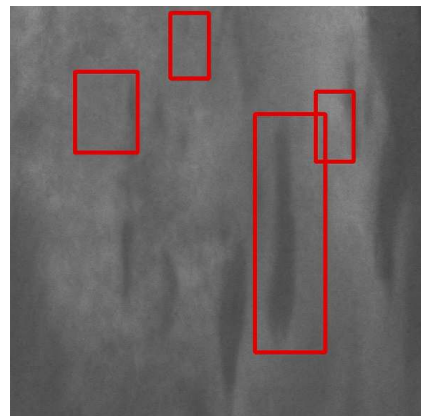


Figure 65: Examples of surface defect detection results generated by GPT-4o on NEU-DET dataset[150]. The model attempts to detect defects in industrial textures based on given patterns. However, the detection performance is sub-optimal, with inaccurate bounding box locations and inconsistent defect coverage.

Section 4.2 Industrial Visual Inspection

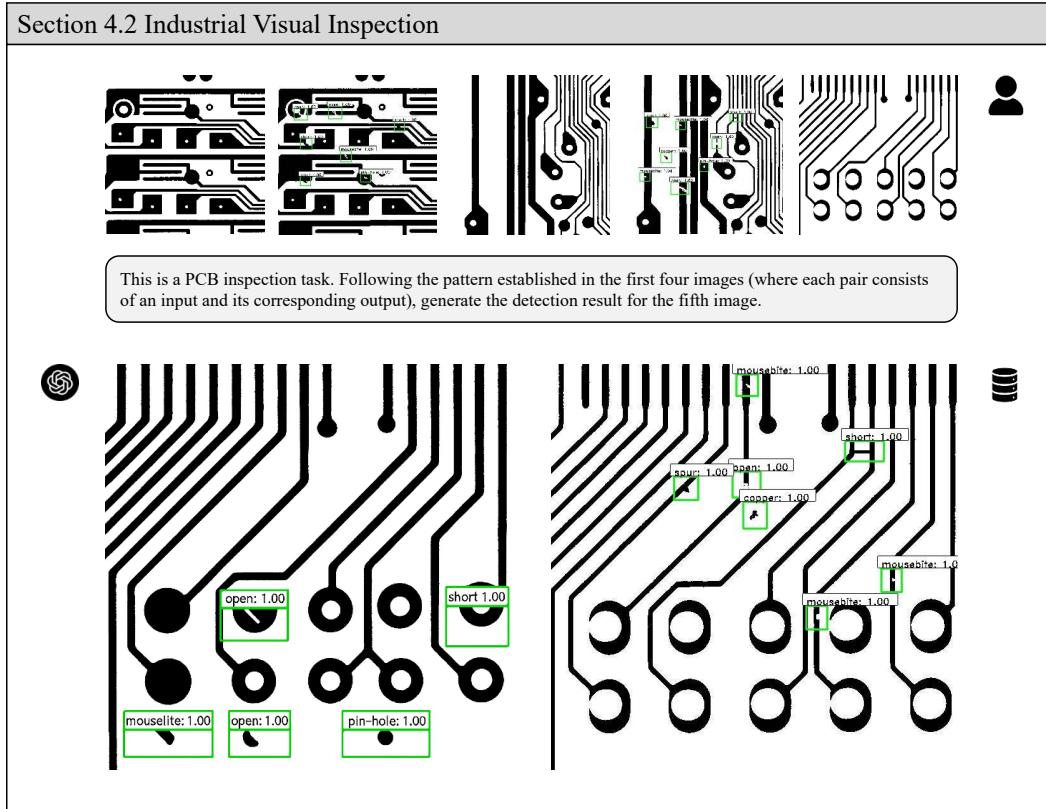


Figure 66: Examples of PCB defect detection results generated by GPT-4o on DeepDCB dataset[155]. The model detects various defects in PCB layouts, including open, short, mousebite, spur, pin hole and spurious copper. However, the detection accuracy is unsatisfactory, with missed detections and incorrect classifications.

4.2 Image Segmentation

Image segmentation tasks assess a model’s ability to recognize, delineate, and label visual entities at different levels of granularity[213, 214, 35, 140, 31, 32, 24]. In this section, we explore GPT-4o’s performance on four representative segmentation paradigms: semantic segmentation, instance segmentation, panoptic segmentation, and instruction-based or in-context segmentation. Each task provides a unique challenge in terms of understanding category definitions, spatial boundaries, and output format alignment.

Semantic Segmentation. As shown in Fig. 67, GPT-4o is able to perform basic region labeling and distinguish between different object categories. However, the model exhibits significant deviations from standard semantic segmentation conventions. First, the same semantic class is often rendered in inconsistent colors across different regions. Second, instead of grouping pixels solely by object class, the model sometimes performs part-level segmentation (e.g., dividing different window panes or tree parts). Additionally, generated masks are not always spatially accurate—the number of windows and shapes of bushes in the right image differ noticeably from the original input, suggesting semantic misalignment and geometric distortion.

Instance Segmentation. In instance segmentation (Fig. 68), the model’s output suffers from both visual and functional limitations. In the left example, some masks are rendered in colors too similar to the underlying image content (e.g., a black cat is segmented using a nearly black mask), making it difficult to distinguish object boundaries. In the right example, the model fails to produce instance-level masks and instead defaults to class-level segmentation, essentially reverting to a semantic segmentation output. These results highlight the model’s limited awareness of the distinction between class-level and instance-level segmentation.

Panoptic Segmentation. As shown in Fig. 69, the model generates panoptic segmentation outputs that are visually coherent and structurally reasonable. It manages to cover both foreground instances and background classes simultaneously. However, category labeling is occasionally incorrect, such as labeling the sky region with unrelated or mismatched class names, revealing a gap in taxonomy grounding and label accuracy.

Segmentation with Task Instruction and In-context Learning. To address the misalignment between prompts and task-specific outputs observed in the previous settings, we experiment with providing explicit task instructions (Fig. 70) or using in-context learning with visual exemplars (Fig. 71 and Fig. 72). These methods show partial improvement. The segmentation becomes more consistent with the task type, and the visual format aligns better with expected outputs. However, some inconsistencies still remain, especially when input images contain ambiguous or densely packed objects.

Our analysis reveals that GPT-4o is capable of identifying and segmenting major semantic entities in images. However, it lacks a precise understanding of the differences between segmentation task types and struggles to fully align outputs with specific task requirements. These limitations suggest that while GPT-4o has strong visual reasoning capabilities, its task grounding and format alignment can benefit from more explicit prompt tuning or modular control mechanisms.

Section 4.2 Image Segmentation

	
<p>Please generate the semantic segmentation of this image.</p> 	<p>Perform semantic segmentation on the provided image by analyzing and labeling each pixel with its corresponding object class. Generate a segmented output map where distinct colors represent different categories (e.g., blue for sky, green for vegetation). Ensure precise boundaries and avoid overlapping labels. Focus on clarity and accuracy while maintaining contextual coherence with the original image.</p>  <p>Legend: house, door, window, garage, vegetation</p>
	
<p>Please generate the semantic segmentation of this image.</p> 	

Figure 67: Examples of semantic segmentation results generated by GPT-4o.

Section 4.2 Image Segmentation



Please perform instance segmentation on the attached image, segmenting only cats and butterflies while setting all other regions to black. Instance segmentation is a computer vision task that precisely identifies and segments individual objects at the pixel level.

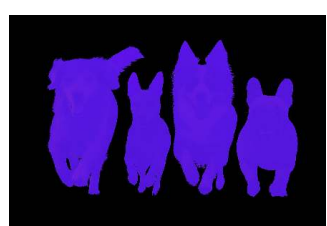


Figure 68: Examples of instance segmentation results generated by GPT-4o.

Section 4.2 Image Segmentation

Please perform panoptic segmentation on the attached image, assigning each pixel a semantic label along with an instance ID to comprehensively differentiate between foreground objects and background regions. Panoptic segmentation combines semantic and instance segmentation into one unified task.

Please perform panoptic segmentation on the attached image, assigning each pixel a semantic label along with an instance ID to comprehensively differentiate between foreground objects and background regions. Panoptic segmentation combines semantic and instance segmentation into one unified task.

Semantic Classes and Colors:

- Sky (Red)
- House (Yellow)
- Garage door (Blue)
- Driveway (Green)
- Shrub (Purple)
- Bush (Orange)
- Grass (Yellow)
- Tree (Green)

Figure 69: Examples of panoptic segmentation results generated by GPT-4o.

Section 4.2 Image Segmentation



Please perform instance segmentation on the attached image, segmenting only cats and butterflies while setting all other regions to black; ensure that each individual instance is represented by a solid color, with different instances assigned distinct colors. Instance segmentation is a computer vision task that identifies and segments individual objects at the pixel level.



Please perform instance segmentation on the attached image, segmenting only dogs while setting all other regions to black; ensure that each individual dog is represented by a uniform solid color with different dogs assigned distinct colors. Instance segmentation is a computer vision task that identifies and segments individual objects at the pixel level.

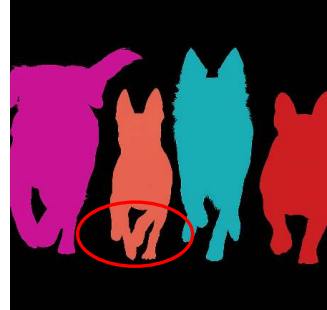


Figure 70: Examples of instance segmentation results with task instruction generated by GPT-4o.

Section 4.2 Image Segmentation



Using the first image (the real image) and the second image (its semantic segmentation) as references for style and labeling, generate the semantic segmentation of the third image using the same color scheme and segmentation approach.



Figure 71: Examples of semantic segmentation with in-context learning generated by GPT-4o.

Section 4.2 Image Segmentation



Using the first image (the real image) and the second image (its semantic segmentation) as references for style and labeling, generate the semantic segmentation of the third image using the same color scheme and segmentation approach.



Figure 72: Examples of semantic segmentation with in-context learning generated by GPT-4o.

4.3 Counting

Counting is a fundamental vision task that requires models to identify and enumerate all instances of specified objects within a scene[118, 88, 33]. It serves as a benchmark for both object detection and fine-grained visual reasoning.

Thanks to its strong visual understanding capabilities, GPT-4o can directly perform counting from natural language instructions alone. As shown in Fig. 73 (a), when prompted with “How many dogs are in this image?”, the model correctly outputs the numerical result in text format, without requiring any visual guidance or interactive interface.

To further examine whether visual reasoning could enhance counting accuracy, we explore an additional setup where the model is instructed to annotate the image by placing colored dots on each detected instance before providing the final count (see Fig. 73 b1 and b2). In these cases, the model is asked to mark each object (e.g., red dots for dogs, blue dots for butterflies), then return both the annotated image and the object count. However, our observations show that visual annotation does not lead to a significant improvement in final counting accuracy. Although the model successfully places visual markers on object instances in some cases, errors such as missed counts or incorrect object classification still occur.

GPT-4o demonstrates a competent ability to perform direct object counting via textual output, and is capable of localizing objects when prompted. However, integrating visual outputs (e.g., annotated dots) does not necessarily improve performance, suggesting that visual reasoning and numerical generation remain decoupled to some extent in the model’s architecture.

Section 4.3 Counting

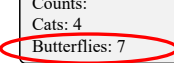
 <p>Please tell me how many dogs are in this image.</p> <p> There are four dogs in the image you provided.</p> <p>(a) Textual counting result</p>	 <p>Analyze the provided image to identify and count all instances of cats and butterflies. Then, annotate the image by overlaying red dots on each cat and blue dots on each butterfly. Finally, please output both the counts and the annotated image. Do not use any program tools.</p> <p> </p> <p> Counts: Cats: 4 Butterflies: 7</p> <p>  </p> <p>(b2) Visual and textual counting result</p>
 <p>Analyze the provided image to identify and count all visible dogs. Accurately mark the center point of each detected dog with a prominent red circular dot, ensuring clear visibility while maintaining the image's original context. Provide both the numerical count and the annotated image as output.</p> <p> </p> <p> </p> <p>There are 4 dogs in the image!</p> <p></p> <p>(b1) Visual and textual counting result</p>	

Figure 73: Examples of object counting results by GPT-4o.

4.4 Human-centric Understanding

4.4.1 Human Pose Estimation

Human Pose Estimation (HPE) aims to localize keypoints on the human body, such as joints and limbs, and is typically divided into 2D[6, 173, 37] and 3D[168, 192, 215] variants. This task evaluates a model’s spatial understanding of human anatomy, its ability to detect joint relationships, and alignment with pose estimation protocols.

We evaluate GPT-4o on both 2D and 3D human pose estimation tasks. As illustrated in Fig. 74, Fig. 75, and Fig. 76, GPT-4o is able to highlight approximate human body structures by generating pose lines or keypoint overlays. However, its performance varies significantly across instances and often fails to align with standard pose estimation requirements.

In the 2D setting, the model sometimes misplaces major joints (e.g., knees or shoulders), produces anatomically implausible connections, or detects an incorrect number of keypoints. In the 3D setting, while the model attempts to simulate spatial depth through shading or perspective cues, the resulting poses lack realistic depth continuity and spatial coherence. Moreover, the outputs are not consistent with any specific annotation format (e.g., COCO 17-keypoint), and the keypoint count often deviates from task specifications.

Overall, GPT-4o exhibits a rudimentary ability to infer body structure and perform coarse pose visualization. However, it lacks task-specific alignment, standardized output structure, and precise keypoint localization. This suggests that without explicit fine-tuning or structured pose templates, current multimodal models struggle with high-fidelity human pose estimation.

Section 4.4.1 Human Pose Estimation

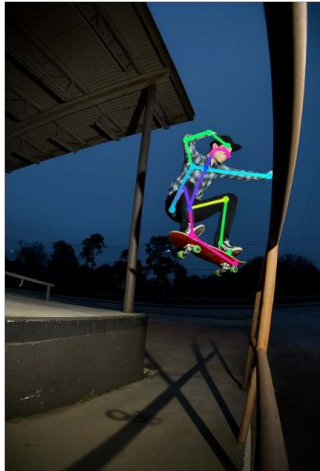
			
<p>Overlay 2D human pose skeletons onto the original image for all visible people, accurately estimating the 17 keypoints defined by the COCO dataset for each person: nose, left eye, right eye, left ear, right ear, left shoulder, right shoulder, left elbow, right elbow, left wrist, right wrist, left hip, right hip, left knee, right knee, left ankle, and right ankle. For each individual, draw a separate skeleton consisting of clear, minimalistic lines connecting these joints in a clean and anatomically correct style. Maintain the original image as the background and ensure skeletons are distinct and do not overlap confusingly.</p>			

Figure 74: Examples of human pose estimation results by GPT-4o.

Section 4.4.1 Human Pose Estimation



Overlay a 2D human pose skeleton onto the original image, accurately estimating the 17 keypoints defined by the COCO dataset: nose, left eye, right eye, left ear, right ear, left shoulder, right shoulder, left elbow, right elbow, left wrist, right wrist, left hip, right hip, left knee, right knee, left ankle, and right ankle. The skeleton should consist of clean lines connecting these joints, representing the pose in a minimalistic, clean, and anatomically correct style. Maintain the original image as the background.



Generate a 3D human pose skeleton from the input image. Represent the skeleton as a set of 3D keypoints connected by straight lines, forming a clean and simplified stick-figure structure. Use COCO-style keypoints including: nose, left eye, right eye, left ear, right ear, left shoulder, right shoulder, left elbow, right elbow, left wrist, right wrist, left hip, right hip, left knee, right knee, left ankle, and right ankle. Ensure proper anatomical proportions and perspective depth. Display the full-body pose clearly on a clean, neutral background. Avoid realistic bones or anatomical models—focus only on joint markers and lines, suitable for 3D pose estimation tasks and scientific visualization.

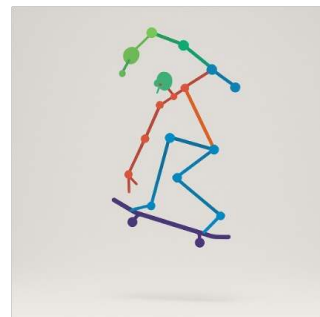


Figure 75: Additional Examples of human pose estimation results by GPT-4o.

Section 4.4.1 Human Pose Estimation



Overlay a 2D human pose skeleton onto the original image, accurately estimating the 17 keypoints defined by the COCO dataset: nose, left eye, right eye, left ear, right ear, left shoulder, right shoulder, left elbow, right elbow, left wrist, right wrist, left hip, right hip, left knee, right knee, left ankle, and right ankle. The skeleton should consist of clear lines connecting these joints, representing the pose in a minimalistic, clean, and anatomically correct style. Maintain the original image as the background.



Generate a 3D human pose skeleton from the input image. Represent the skeleton as a set of 3D keypoints connected by straight lines, forming a clean and simplified stick-figure structure. Use COCO-style keypoints including: nose, left eye, right eye, left ear, right ear, left shoulder, right shoulder, left elbow, right elbow, left wrist, right wrist, left hip, right hip, left knee, right knee, left ankle, and right ankle. Ensure proper anatomical proportions and perspective depth. Display the full-body pose clearly on a clean, neutral background. Avoid realistic bones or anatomical models—focus only on joint markers and lines, suitable for 3D pose estimation tasks and scientific visualization.

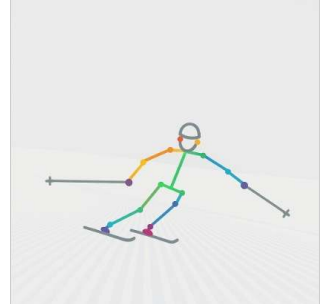


Figure 76: Additional examples of human pose estimation results by GPT-4o.

4.4.2 Human Parsing

Human parsing involves segmenting fine-grained parts of the human body, such as clothing, facial features, limbs, and accessories, into semantically meaningful regions[188, 191, 189, 142, 190]. It is a dense prediction task that requires precise spatial alignment and a detailed understanding of human anatomy and appearance.

As shown in Fig. 77 and Fig. 78, GPT-4o demonstrates the ability to perform semantic segmentation over image regions. However, its results often fail to meet the specific requirements of human parsing. For example, in Fig. 77 (right), the model incorrectly segments a bicycle as part of the human parsing output and fails to isolate facial accessories like eyeglasses. Additionally, it produces segmentation errors in crowded scenes, as can be seen in right part of Fig. 77.

In Fig. 78, these issues become more pronounced. The model produces parsing results that appear to be influenced more by the overall image style and composition than by the actual spatial structure of the individuals. For instance, in the leftmost person of the left image, the generated segments do not correspond to meaningful anatomical or clothing regions. This suggests a lack of fine-grained spatial alignment and insufficient grounding in the input image's local content.

While GPT-4o can distinguish broad semantic regions and generate plausible masks, it lacks task-specific understanding of human parsing. Its outputs fail to reflect detailed human part structures and often include irrelevant or inconsistent regions. This highlights the need for stronger spatial grounding and part-aware supervision to adapt GPT-4o to parsing tasks.

Section 4.4.2 Human Parsing

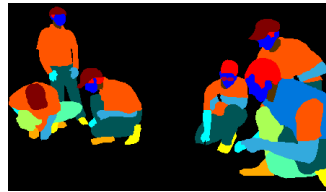
	
<p>Given the input image, generate a human parsing result image that segments the human figure into distinct parts. Use clear visual segmentation with color-coded regions for each of the following categories: head, hair, face, torso, left arm, right arm, left leg, right leg, upper clothing, lower clothing, shoes, and accessories. Ensure each part is clearly delineated with smooth edges and consistent labeling. The result should look like a human segmentation map suitable for pose analysis or clothing parsing.</p>	<p>Given the input image, generate a human parsing result image that segments the human figure into distinct parts. Use clear visual segmentation with color-coded regions for each of the following categories: head, hair, face, torso, left arm, right arm, left leg, right leg, upper clothing, lower clothing, shoes, and accessories. Ensure each part is clearly delineated with smooth edges and consistent labeling. The result should look like a human segmentation map suitable for pose analysis or clothing parsing.</p>
	
	

Figure 77: Examples of human parsing generated by GPT-4o.

Section 4.4.2 Human Parsing



Given the input image, generate a human parsing result image that segments the human figure into distinct parts. Use clear visual segmentation with color-coded regions for each of the following categories: head, hair, face, torso, left arm, right arm, left leg, right leg, upper clothing, lower clothing, shoes, and accessories. Ensure each part is clearly delineated with smooth edges and consistent labeling. The result should look like a human segmentation map suitable for pose analysis or clothing parsing.



Given the input image, generate a human parsing result image that segments the human figure into distinct parts. Use clear visual segmentation with color-coded regions for each of the following categories: head, hair, face, torso, left arm, right arm, left leg, right leg, upper clothing, lower clothing, shoes, and accessories. Ensure each part is clearly delineated with smooth edges and consistent labeling. The result should look like a human segmentation map suitable for pose analysis or clothing parsing.



Figure 78: Additional examples of human parsing generated by GPT-4o.

4.4.3 Human Mesh Recovery

Human mesh recovery aims to reconstruct a 3D mesh representation of the human body from a single image[75, 119, 146], capturing detailed attributes such as pose, shape, and orientation. The ideal output is a mesh overlay with visible contours and vertex structure, following formats like SMPL.

As illustrated in Fig. 79, we use this task to evaluate whether GPT-4o possesses spatial reasoning and 3D body structure perception capabilities. The results vary across different inputs. In the right example, the generated mesh demonstrates good alignment with the original body pose and proportions, reflecting a well-formed understanding of body orientation and shape. However, in the left example, we observe significant misalignment between the rendered mesh and the original person. The pose and limb configuration of the generated mesh deviate from the input, leading to unrealistic overlays.

These findings suggest that while GPT-4o shows some ability to infer 3D mesh structure from 2D visual input, its robustness and consistency remain limited. In challenging scenarios, it may struggle with precise geometric alignment and structural integrity.

Section 4.4.3 Human Mesh Recovery



Based on the input image, generate a 3D human mesh recovery result. The output should depict a realistic human mesh overlay on the body in the image, showing the underlying 3D structure with vertices and mesh lines. Include body pose, shape, and orientation. Use a clean, semi-transparent rendering style if overlaid on the original image, or a standalone 3D view if separate. Emulate mesh outputs like those from SMPL or similar human body models, with visible joints and contours.



Based on the input image, generate a 3D human mesh recovery result. The output should depict a realistic human mesh overlay on the body in the image, showing the underlying 3D structure with vertices and mesh lines. Include body pose, shape, and orientation. Use a clean, semi-transparent rendering style if overlaid on the original image, or a standalone 3D view if separate. Emulate mesh outputs like those from SMPL or similar human body models, with visible joints and contours.



Figure 79: Examples of human mesh recovery generated by GPT-4o.

4.5 Depth Estimation

Depth estimation aims to infer the relative or absolute distance of objects in a scene from a single 2D image[109, 11, 177], producing a depth map that captures geometric structure and spatial relationships. This task is fundamental to scene understanding and 3D reasoning.

As illustrated in Fig. 80–82, GPT-4o demonstrates a reasonable ability to estimate depth from monocular input. In general, the generated depth maps preserve the overall layout and object boundaries. However, we still observe some inconsistencies in fine details. For example, in Fig. 80, the bush on the right is inaccurately estimated, showing artifacts and depth discontinuities. Moreover, GPT-4o appears to be sensitive to lighting conditions and global appearance cues. In Fig. 82, the model misinterprets the depth due to lighting variations and shadows, leading to a less accurate estimation of surface geometry.

While GPT-4o performs moderately well in capturing general spatial layout, its depth predictions still lack robustness under complex lighting or detailed geometry. Future improvements could focus on enhancing geometry fidelity and reducing sensitivity to photometric factors.

Section 4.5 Depth Estimation

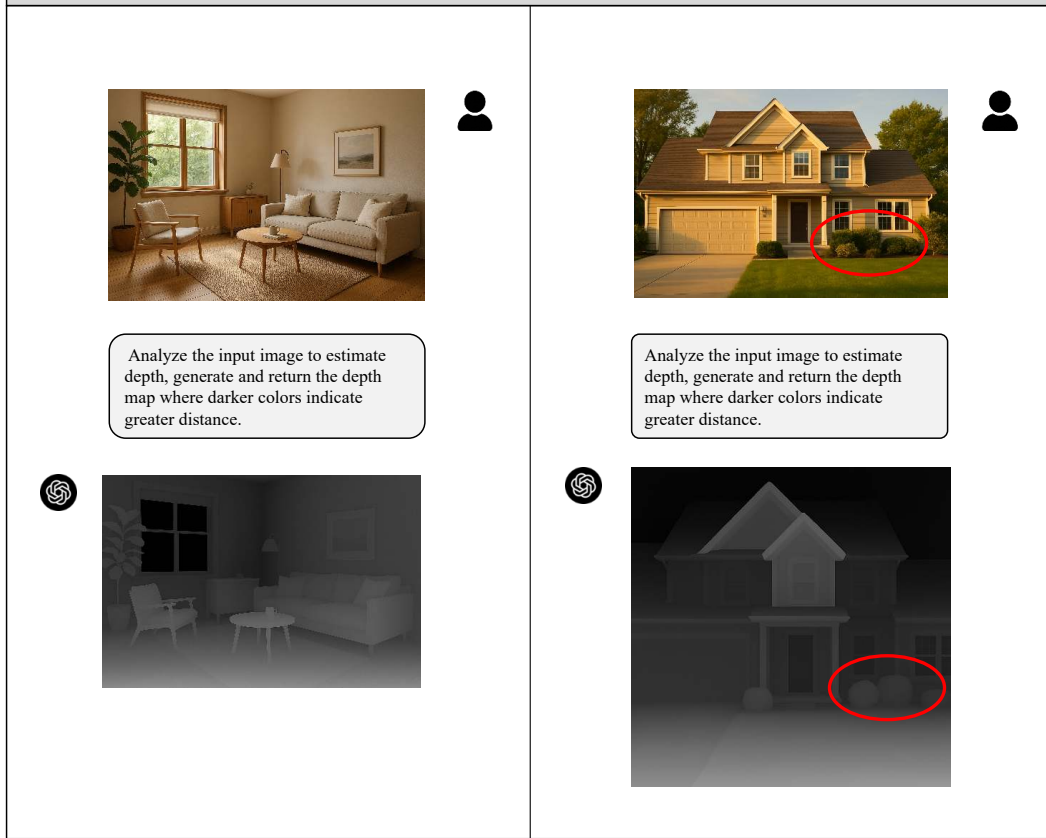
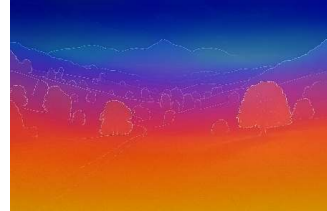


Figure 80

Section 4.5 Depth Estimation



Please perform monocular depth estimation on the attached image, generating an output that includes depth indicators; monocular depth estimation is a computer vision task that infers the distance of scene elements from a single image by predicting depth for each pixel.



Analyze the input image to estimate depth, generate and return the depth map where darker colors indicate greater distance.



Figure 81

Section 4.5 Depth Estimation



Analyze the input image to estimate depth, generate and return the depth map where darker colors indicate greater distance.



Analyze the input image to estimate depth, generate and return the depth map where darker colors indicate greater distance.



Figure 82

4.6 Surface Normal Estimation

Surface normal estimation aims to infer the per-pixel orientation of surfaces in a 3D scene[123, 170, 8], which is essential for understanding object geometry, shape, and spatial layout. In this experiment, we provide a single polarization image as input and ask GPT-4o to generate a dense surface normal map.

As shown in Fig. 83, GPT-4o is able to produce visually plausible surface normal maps that follow general structural cues. However, there are still noticeable issues in geometry consistency. For example, in the left column, the model incorrectly estimates the surface normal of the ground’s lane markings, despite them being part of the same plane. The vehicle’s angular surface orientation and the wall thickness are also misaligned with the input image. Similarly, while the right example appears convincing at first glance, it fails to preserve key structural details such as the correct number of windows. This suggests the model struggles with fine-grained spatial geometry and may hallucinate details that do not exist in the input.

Overall, the results indicate that while GPT-4o can generate surface normal estimations with a reasonable appearance, it lacks precise geometric fidelity and often deviates from the spatial layout of the original image.

Section 4.6 Surface Normal Estimation

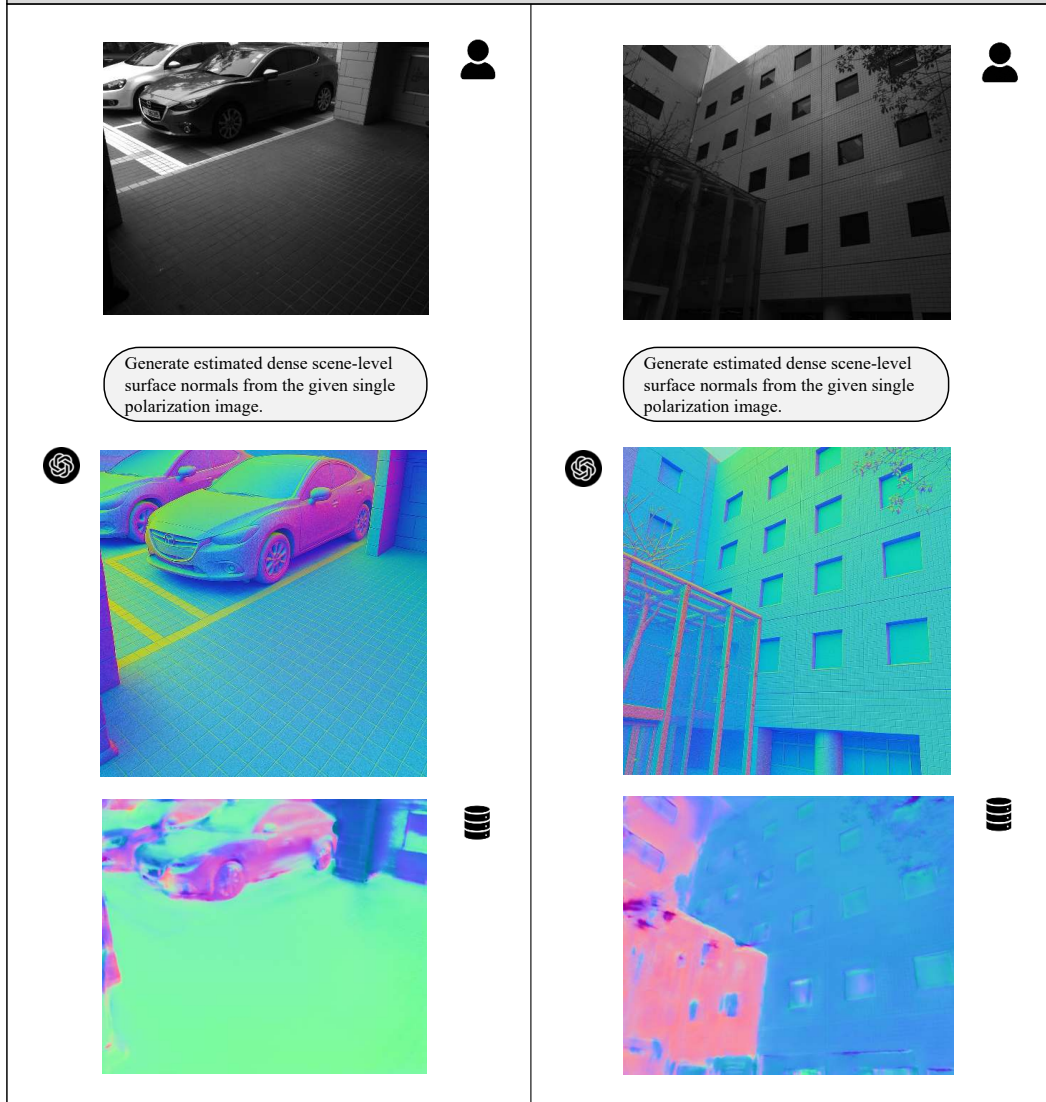


Figure 83

4.7 Optical Flow Estimation

Optical flow estimation aims to predict the per-pixel motion between consecutive frames in a video, often visualized as a dense vector field using hue and brightness to encode direction and magnitude[66, 199, 134, 64]. This task evaluates whether a model can perceive temporal continuity, understand object motion, and differentiate between static background and moving objects.

We test GPT-4o on this task using pairs of consecutive frames and evaluate its ability to produce dense, color-coded flow maps that conform to standard visualization conventions. As shown in Fig. 84, while the model captures the general direction of movement, it introduces hallucinated motion structures—in this case, generating an additional ramp flow not aligned with the ground truth displacement. In Fig. 85, the model demonstrates improved perception of human and animal motion. However, it also synthesizes a non-existent dog-like structure in the flow map, revealing a tendency to infer motion beyond the input evidence. This suggests a reliance on visual priors over strict frame-to-frame correlation.

Overall, GPT-4o shows potential in optical flow estimation but lacks precision in adhering to actual inter-frame motion, often introducing artifacts and inconsistencies in the predicted motion fields.

Section 4.7 Optical Flow Estimation



Generate an optical flow visualization from two consecutive RGB video frames, producing a single high-resolution image that illustrates pixel-wise motion between the inputs. The visualization should use color coding to represent both the direction and magnitude of movement: motion direction should be encoded through hue, reflecting the angle of displacement, while motion magnitude should be represented by brightness or saturation, with faster movements appearing brighter or more saturated. The flow map should be dense, capturing motion across all moving regions with fine detail, and should clearly differentiate areas of activity from static background, which should appear in neutral or dark tones. The visual style should follow the conventions of the Middlebury optical flow visualization standard, ensuring clarity and consistency. The output should provide an accurate, detailed, and aesthetically coherent representation of motion between the two frames.

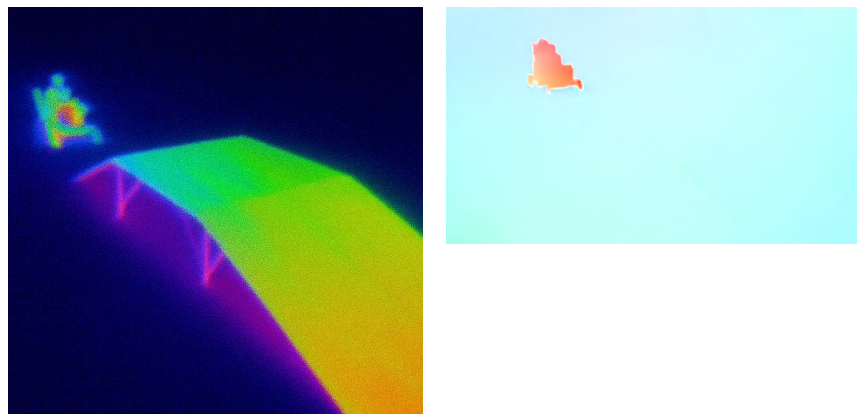


Figure 84

Section 4.7 Optical Flow Estimation



Generate an optical flow visualization from two consecutive RGB video frames, producing a single high-resolution image that illustrates pixel-wise motion between the inputs. The visualization should use color coding to represent both the direction and magnitude of movement: motion direction should be encoded through hue, reflecting the angle of displacement, while motion magnitude should be represented by brightness or saturation, with faster movements appearing brighter or more saturated. The flow map should be dense, capturing motion across all moving regions with fine detail, and should clearly differentiate areas of activity from static background, which should appear in neutral or dark tones. The visual style should follow the conventions of the Middlebury optical flow visualization standard, ensuring clarity and consistency. The output should provide an accurate, detailed, and aesthetically coherent representation of motion between the two frames.



Figure 85

4.8 Remote Sensing Change Detection

Remote sensing change detection is a specialized task that requires identifying and localizing changes between two satellite or aerial images captured at different times[7, 68]. This involves semantic understanding of man-made and natural structures, and distinguishing alterations such as new constructions, deforestation, flooding, or land-use transformation.

In our evaluation, we input two temporally distinct remote sensing images and prompt GPT-4o to generate a change map that highlights the differences. However, as illustrated in Fig. 86 and Fig. 87, the model fails to capture the essence of the task. Instead of identifying changes between the two images, the model merely segments out features like roads and buildings from one of the inputs.

This indicates that GPT-4o has not grasped the concept of temporal comparison or semantic difference analysis required for change detection. The results suggest that either the model lacks task-specific priors or is overly biased towards static semantic segmentation, treating the input more like a single-image understanding task than a comparative one.

Overall, GPT-4o currently exhibits limited capability in remote sensing change detection and requires further task-aware instruction alignment to generate meaningful temporal comparisons.

Section 4.8 Remote Sensing Change Detection



You are an AI model specialized in remote sensing and computer vision. You will be provided with two satellite or aerial images of the same geographic region taken at different times. Your task is to:
Analyze both images and detect any significant changes in land cover, vegetation, construction, water bodies, or other features.

Generate a binary change mask image where:
White (255) indicates regions where significant changes have occurred.
Black (0) indicates unchanged regions.

Requirements: – Ensure pixel-wise alignment between the input images and the change mask. – Apply appropriate pre-processing like normalization if needed. – Be robust to illumination and seasonal variations.

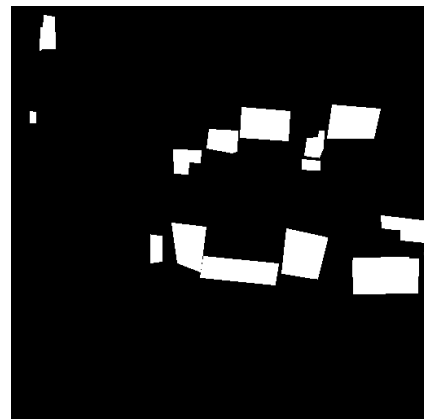
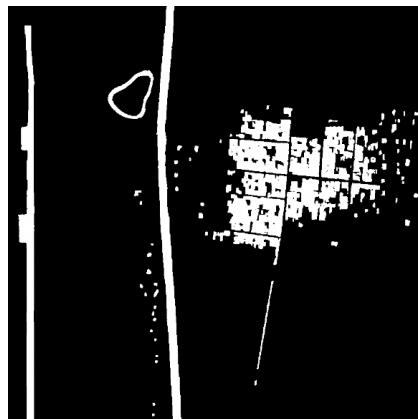


Figure 86

Section 4.8 Remote Sensing Change Detection



You are an AI model specialized in remote sensing and computer vision. You will be provided with two satellite or aerial images of the same geographic region taken at different times. Your task is to:

Analyze both images and detect any significant changes in land cover, vegetation, construction, water bodies, or other features.

Generate a binary change mask image where:

White (255) indicates regions where significant changes have occurred.

Black (0) indicates unchanged regions.

Requirements: – Ensure pixel-wise alignment between the input images and the change mask. – Apply appropriate pre-processing like normalization if needed. – Be robust to illumination and seasonal variations.

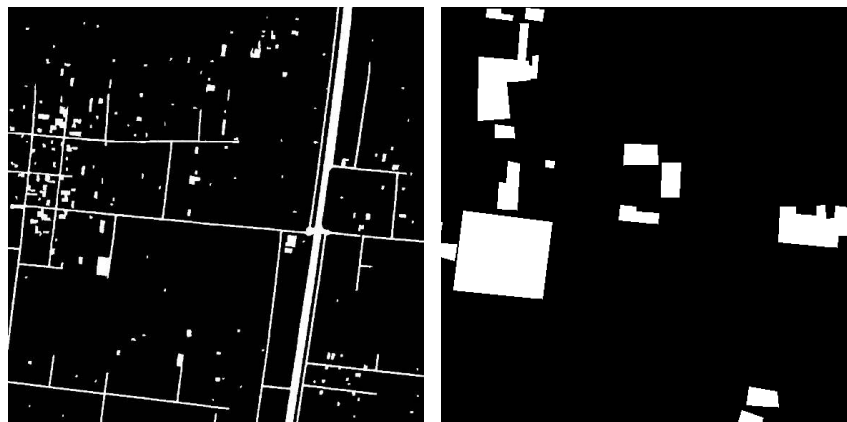


Figure 87

5 Knowledge-based Image Generation

5.1 Physics

Physics understanding in image generation evaluates the model’s ability to reflect fundamental physical laws and commonsense in visual content[108, 151, 99, 89, 92]. This capability is essential for generating plausible and scientifically reasonable scenes, especially in educational or simulation-related applications. In this section, we follow the taxonomy defined in PhyBench[108], which categorizes physical knowledge into several sub-fields, including force, optics, thermodynamics, and material properties.

As shown in Fig. 88-96, we evaluate GPT-4o across these categories. Overall, we find that GPT-4o demonstrates good performance in most physical commonsense scenarios, generating results that align well with real-world physics. However, we also observe some failure cases. In particular, the model fails to correctly handle light refraction in Fig. 92, and the thermodynamics-related generation in Fig. 94 exhibits incorrect visual patterns inconsistent with physical laws.

This highlights the potential and limitations of current multi-modal models in understanding and applying physical knowledge through image generation.

Section 5.1 Physics

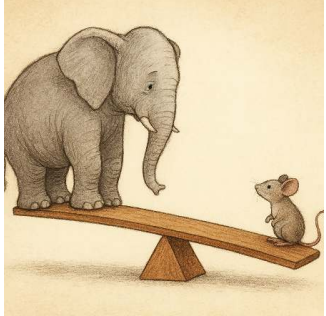
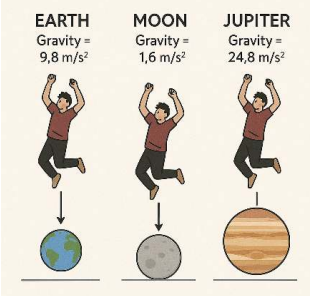
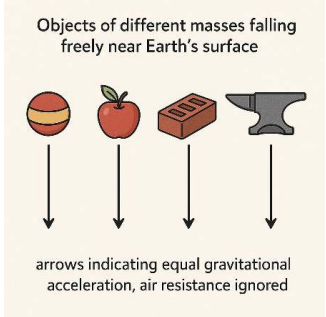
<p>An elephant and a mouse stand on either side of a seesaw.</p>  <p>The balance is unrealistic: the mouse is lower than the elephant on the seesaw.</p>	<p>Generate a side-by-side comparison image showing a person jumping on Earth, the Moon, and Jupiter, illustrating the effect of gravity on jump height with labeled gravity values.</p> <p>EARTH Gravity = $9,8 \text{ m/s}^2$</p> <p>MOON Gravity = $1,6 \text{ m/s}^2$</p> <p>JUPITER Gravity = $24,8 \text{ m/s}^2$</p> 
<p>Generate a realistic diagram showing objects of different masses falling freely near Earth's surface, with arrows indicating equal gravitational acceleration and air resistance ignored.</p>  <p>Objects of different masses falling freely near Earth's surface</p> <p>arrows indicating equal gravitational acceleration, air resistance ignored</p>	<p>Generate an interior scene of astronauts floating inside the International Space Station, illustrating microgravity conditions and free-fall motion.</p> 

Figure 88: Examples of force effect results generated by GPT-4o.

Section 5.1 Physics

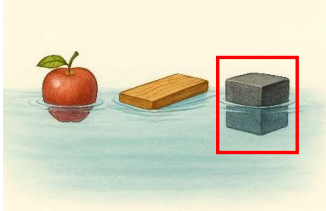
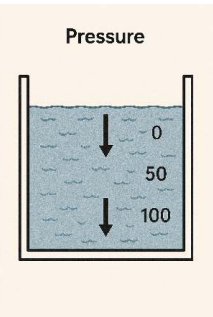
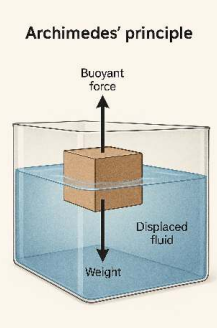
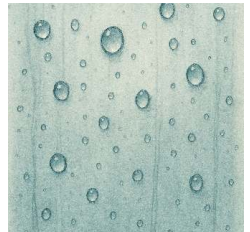
<p>An apple, a piece of wood, and an iron block in water.</p>  <p>The iron block should sink in the water.</p>	<p>Generate a cross-sectional diagram of a container filled with water, using arrows and pressure values to illustrate the distribution of pressure at different depths.</p>  <p>Pressure</p> <p>0 50 100</p>
<p>Generate a realistic diagram illustrating Archimedes' principle: an object partially submerged in water experiences an upward buoyant force equal to the weight of the displaced fluid.</p> <p>Archimedes' principle</p> 	<p>A hat hanging on a hook on the wall.</p> 
<p>An empty plastic bottle at the bottom of the sea.</p> 	<p>A few drops of water on the glass.</p> 

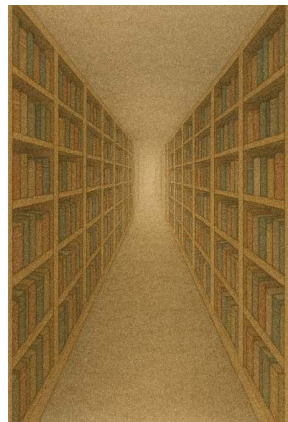
Figure 89: Examples of force effect results generated by GPT-4o.

Section 5.1 Physics

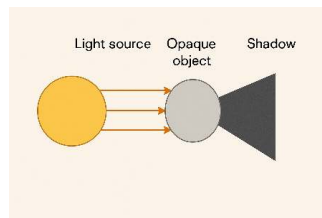
Generate an image of a narrow beam of sunlight entering a dark room through a small hole in the window, with the beam clearly visible through the dust in the air.



A corridor with bookshelves stretches into the distance.



Generate an illustration showing the formation of a sharp shadow behind an opaque object placed in front of a light source.



Generate a realistic 3D illustration showing the formation of a sharp-edged shadow cast by an opaque object placed in front of a point light source in a dark environment.



Figure 90: Examples of optical results generation by GPT-4o.

Section 5.1 Physics

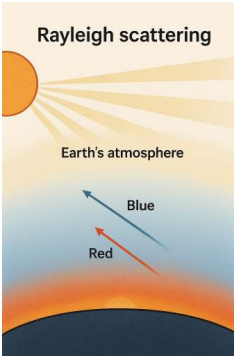
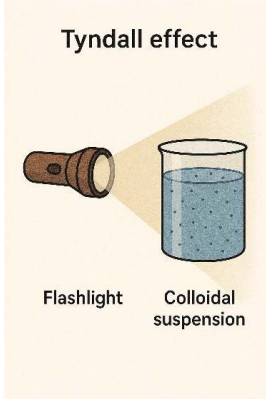
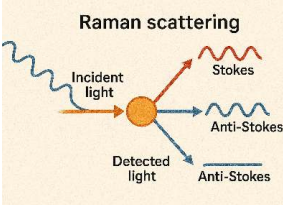
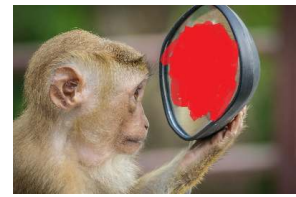
<p>A ray of light passing through dust-filled air.</p> 	<p>Generate an atmospheric diagram showing Rayleigh scattering of sunlight in Earth's atmosphere, illustrating why the sky appears blue and the sunset red.</p> 
<p>Generate a diagram illustrating the Tyndall effect.</p> <p>Tyndall effect</p> 	<p>Generate a scientific diagram illustrating Raman scattering.</p> <p>Raman scattering</p> 

Figure 91: Examples of optical results generation by GPT-4o.

Section 5.1 Physics

A cylindrical block of wood placed in front of a mirror.



Restore the redacted area in the image to show a realistic reflection of the monkey's face in the mirror, consistent with the angle and lighting of the original photo.



Add a realistic mirror to the right side of the uploaded portrait. The mirror should reflect the person's face from the correct angle, with accurate lighting and perspective based on the original image.

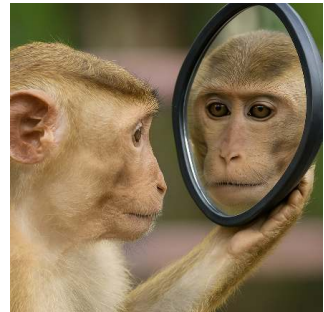


Figure 92: Examples of optical results generated by GPT-4o.

Section 5.1 Physics

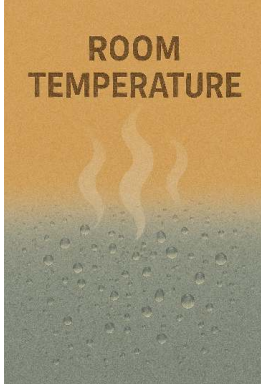
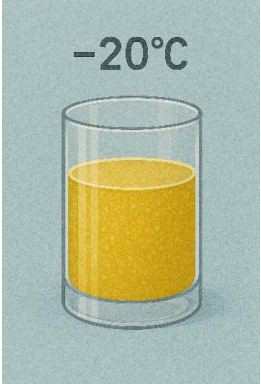
<p>Water vapor hits glass at room temperature.</p> 	<p>A glass of oil at minus twenty degrees Celsius.</p> 
<p>Generate a realistic image of a cold drink bottle placed outdoors on a hot day.</p> 	<p>Generate a close-up image of a partially burned candle that is still lit, with molten wax dripping down the side. The image should be physically accurate.</p> 

Figure 93: Examples of thermodynamic effect generated by GPT-4o.

Section 5.1 Physics

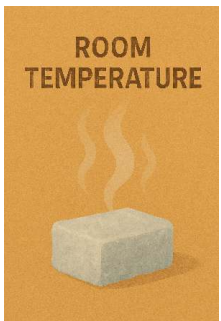
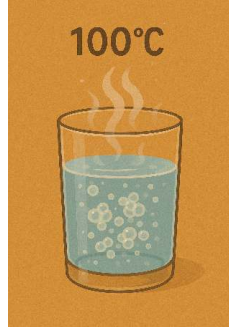
<p>A dry ice at room temperature.</p>  <p>The sublimation of dry ice will produce a large amount of mist, which is not well represented in the picture.</p>	<p>Generate a close-up image of a piece of chocolate slowly melting on a warm plate.</p>  <p>A glass of ice cubes at fifty degrees Celsius.</p>
<p>A glass of water at above one hundred degrees Celsius.</p>  <p>Ice will melt at 50 degrees Celsius, and there should be water in the cup. The grammatical errors in the prompt words are the original errors in the reference documents.</p>	

Figure 94: Examples of thermodynamic effect generated by GPT-4o.

Section 5.1 Physics

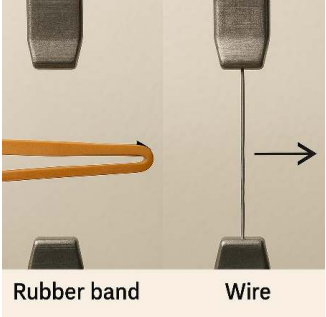
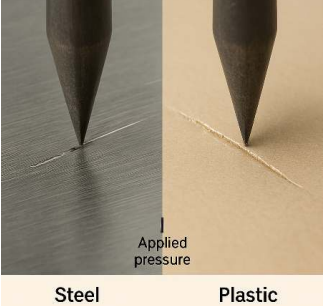
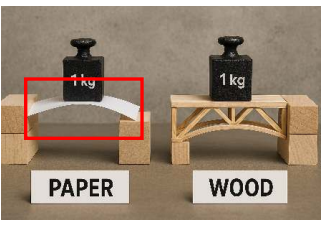
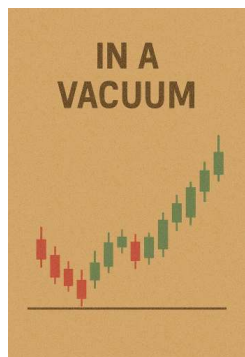
<p>Generate a realistic side-by-side image of a rubber band and a piece of wire being stretched by equal forces, both clamped at one end and pulled at the other, under identical conditions.</p>  <p>Rubber band Wire</p>	<p>Generate a realistic image comparing a steel surface and a plastic surface being scratched with a sharp metal tip under the same applied pressure.</p>  <p>Steel Plastic</p>
<p>Generate a realistic image comparing a piece of clay and a piece of glass being struck with identical force from a falling steel ball in a controlled setup.</p>  <p>CLAY GLASS</p>	<p>Generate a realistic comparison image of two small-scale bridge models, one made of paper and one of wood, both placed between blocks and loaded with identical weights in the center. The image should clearly show the structural deformation of each bridge under the load.</p>  <p>PAPER WOOD</p>

Figure 95: Examples of material properties generated by GPT-4o.

Section 5.1 Physics

A candlestick chart in a vacuum.

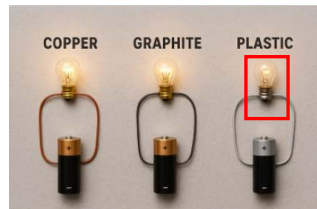


An irrelevant picture has been generated.

Generate a realistic side-by-side comparison image of three identical candles placed in different environments: one in open air, one in a sealed container filled with oxygen, and one in a sealed vacuum chamber.



Generate a realistic comparison image showing a simple circuit with a battery, a light bulb, and different connecting wires made of copper, graphite, and plastic. The image should clearly show the setup and how each material affects the brightness of the bulb.



Generate a realistic comparison image showing rods made of different materials—metal, glass, and plastic—placed on a uniformly heated surface. The image should depict their thermal expansion, with each material labeled clearly.

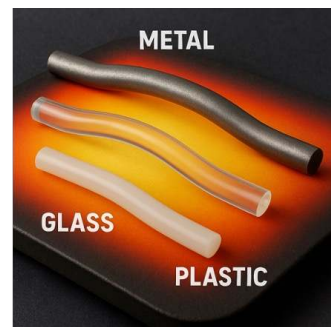


Figure 96: Examples of material properties generated by GPT-4o.

5.2 Chemistry

Chemistry understanding in image generation evaluates the model’s ability to correctly reflect chemical knowledge, molecular structures, laboratory scenes, and reaction processes in visual content[96, 125].

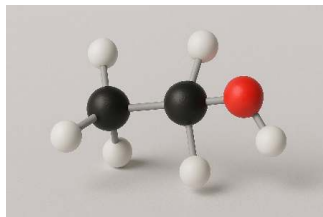
As shown in Fig. 97 to Fig. 99, we test GPT-4o across various chemistry-related tasks, including molecular structure generation, laboratory experiment scene generation, and chemical reaction diagram generation.

We find that while GPT-4o is capable of generating chemistry-related images with reasonable visual style and layout, there are significantly more errors compared to physics generation tasks. These errors mainly include incorrect labeling of chemical substances (e.g., wrong label for copper sulfate in Fig. 98), inaccurate experimental phenomena (e.g., wrong color reaction for litmus test in Fig. 98), and mistakes in structural molecular diagrams (e.g., missing or misconnected atoms in Fig. 99).

These results indicate that GPT-4o still lacks reliable domain-specific knowledge in the chemistry field, especially for tasks requiring accurate scientific details and strict visual correctness.

Section 5.2 Chemistry

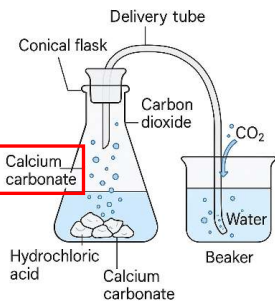
Generate a ball-and-stick model image of an ethanol molecule, accurately depicting the bonding between atoms and its three-dimensional spatial structure.



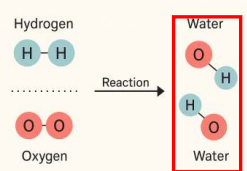
Generate a realistic image of the Elephant Toothpaste experiment in action.



Generate the device diagram for preparing carbon dioxide in the laboratory, label the names of all the instruments and the chemicals, and also show the process of carbon dioxide generation in the reaction device.



Generate a microscopic schematic diagram of the chemical reaction in which hydrogen burns in oxygen to produce water, clearly showing the changes of molecules before and after the reaction.



A water molecule is composed of two hydrogen atoms and one oxygen atom.

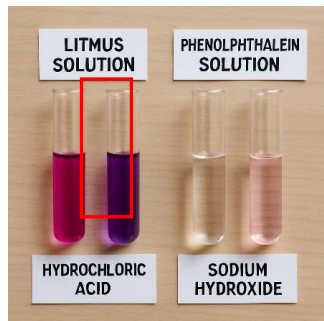
Figure 97: Examples of chemistry-related generation results, including molecule models, reaction diagrams, and experiment phenomena.

Section 5.2 Chemistry

Generate a laboratory scene showcasing the acid-base test using purple litmus and colorless phenolphthalein on hydrochloric acid and sodium hydroxide. The image should clearly depict the experimental phenomena.



Generate a realistic image showing two acid-base tests side by side: one using purple litmus solution and the other using colorless phenolphthalein solution, on samples of hydrochloric acid and sodium hydroxide. The image should clearly display the expected color changes for each reagent in their respective tests.



Clearly, the first generated image had significant flaws. Therefore, we provided a more detailed prompt and obtained a higher quality image. However, when litmus solution is added to sodium hydroxide, it is supposed to turn blue.

Generate an image of the thermite reaction experiment being carried out in a laboratory environment.



Generate an image of a flame color reaction experiment in a chemistry laboratory, showing multiple distinct flames produced by dipping different labeled solutions of metal salts, so it's clear which flame corresponds to which solution.

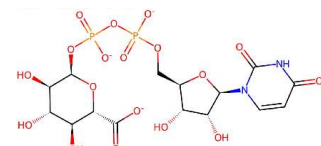
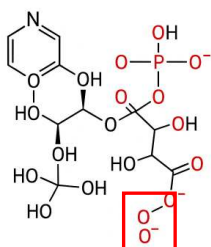


The flame produced the correct color; however, the label might be inaccurate. It is commonly copper(II) sulfate, with copper ions in the +2 oxidation state.

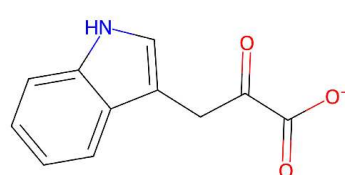
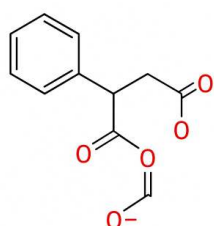
Figure 98: Examples of laboratory scene generation for chemistry experiments, with several incorrect labels and inaccurate experiment phenomena.

Section 5.2 Chemistry

The molecule is a nucleotide-sugar oxoanion that is a trianion arising from deprotonation of the carboxy and diphosphate OH groups of UDP-alpha-D-glucuronic acid; major species at pH 7.3. It has a role as a human metabolite. It is a nucleotide-sugar oxoanion and a carbohydrate acid derivative anion. It is a conjugate base of an UDP-alpha-D-glucuronic acid.



The molecule is an indol-3-yl carboxylic acid anion that is the conjugate base of 3-(indol-3-yl)pyruvic acid. It has a role as a *Saccharomyces cerevisiae* metabolite and a plant metabolite. It is an indol-3-yl carboxylic acid anion and a 2-oxo monocarboxylic acid anion. It is a conjugate base of a 3-(indol-3-yl)pyruvic acid.



(2R)-trihomocitric acid is a chiral tricarboxylic acid in which a central carbon carries hydroxy, carboxy, carboxymethyl and 4-carboxybutyl substituents with R-configuration at the chiral centre. It is a conjugate acid of a (2R)-trihomocitrate(3-).

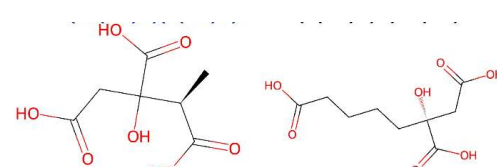
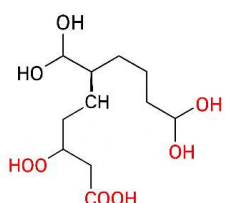


Figure 99: Examples of chemical structure generation results, with some structural errors and misconnected molecular diagrams.

5.3 Biology

Biology-related image generation tasks evaluate the model’s ability to understand biological knowledge and visually represent biological phenomena, structures, and experimental processes[195, 184, 141, 41]. These tasks cover a wide range of biological concepts, including microbiology, botany, genetics, ecology, and cell biology.

As shown in Fig. 100 and Fig. 101, we test GPT-4o in various biology scenarios, such as generating labeled bacterial colony images, genetic experiment diagrams, ecological cycle illustrations, cellular structure generation, and biological image analysis tasks (e.g., cell segmentation, immunofluorescent image synthesis).

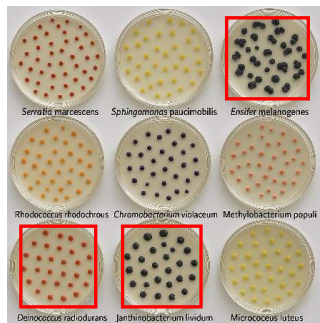
We observe that compared to physics generation, biology generation tasks are even more challenging for GPT-4o. Although the model shows a certain level of understanding in visual style and scene layout, many errors exist in the scientific details. These errors include incorrect colony color representation for specific bacterial species (Fig. 100), misunderstanding of ecological knowledge (e.g., carbon cycle generation in Fig. 100), and mistakes in experimental labeling or biological structures.

In addition, when facing professional biomedical image analysis tasks, such as cell segmentation and fluorescence image synthesis, GPT-4o still struggles to achieve accurate pixel-level generation, showing a clear performance gap compared to traditional domain-specific models.

These results indicate that while GPT-4o has basic biological commonsense understanding, there is still a large room for improvement in generating scientifically accurate biology-related images, especially for tasks requiring strict domain knowledge and precision.

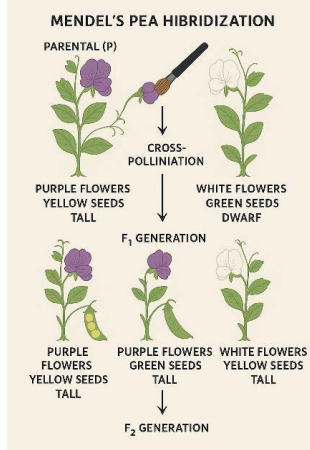
Section 5.3 Biology

Generate an image of multiple agar plates featuring pigmented bacterial colonies, each labeled with the specific bacterial species.

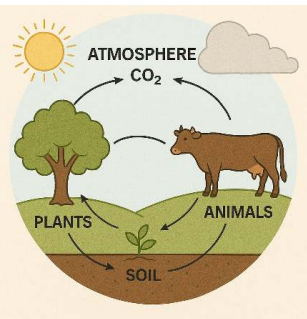


Deinococcus radiodurans generally forms pink colonies under normal conditions. Janthinobacterium lividum typically appears blue to purple in color on culture dishes.

Generate an experimental diagram of Mendel's pea hybridization, depicting the parental (P) generation, the cross-pollination process, and the resulting F1 and F2 offspring, with annotations indicating the inherited traits.



Generate a clear diagram of the carbon cycle, illustrating the movement of carbon among the atmosphere, plants, animals, and soil.



There are some problems. For example, plants can not only release carbon dioxide but also absorb it.

Generate a high-power micro-sco-pic image of a spinach leaf, clearly revealing the cellular structure, with annotations labeling the key features.

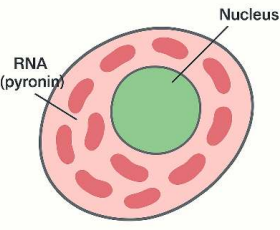
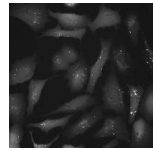
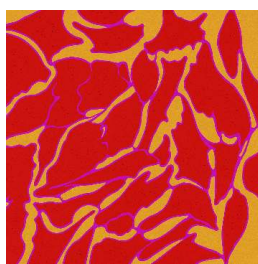


Figure 100: Examples of biology-related image generation, including bacterial colonies, genetic diagrams, ecological cycles, and cellular structures.

Section 5.3 Biology



Please perform precise cell segmentation on the cell image I provide to you, and generate an image that clearly demonstrates the segmentation effect.



Please generate the immunofluorescent (IF) image corresponding to the cell nucleus (DNA) channel based on the provided bright - field (BF) image.

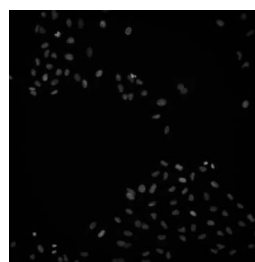
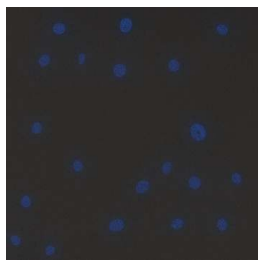


Figure 101: Examples of biology image analysis tasks, including cell segmentation and immunofluorescence image generation.

5.4 Mathematics

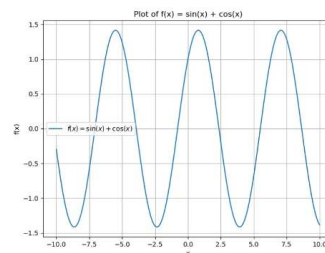
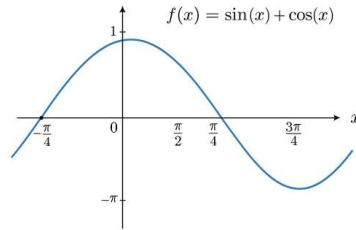
Mathematics-related image generation evaluates the model's capability to visualize mathematical concepts, including function plots, geometric diagrams, and mathematical annotations[79, 169, 62]. Compared with other domains, mathematical image generation requires precise understanding of mathematical semantics, accurate spatial layout, and strict labeling of axes, points, and annotations.

As shown in Fig. 102 and Fig. 103, we test GPT-4o on two typical categories of mathematical generation tasks: function plotting and geometry diagram generation[169]. For function plotting, although GPT-4o is able to generate visually reasonable curve shapes, the coordinate axes and labels are often incorrect or missing. For geometry diagram generation, the results are even less satisfactory. The model often fails to correctly understand geometric relationships, resulting in structurally incorrect diagrams, such as point positions inconsistent with the given conditions or lines violating the specified constraints.

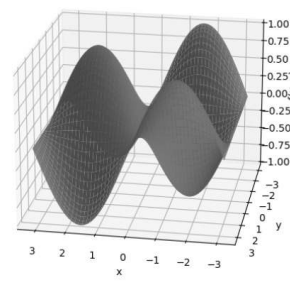
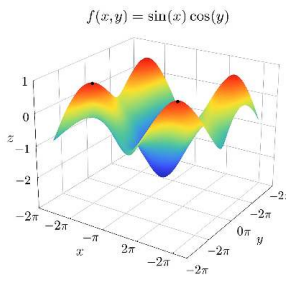
These findings reveal that while GPT-4o shows a certain level of visual generation ability, its understanding of mathematical logic and precise graphical representation is still far from practical applications, especially in educational or scientific scenarios that require high accuracy.

Section 5.4 Mathematics

Generate the graph of the function $f(x) = \sin(x) + \cos(x)$, and it is required to accurately label the coordinate axes and key points.



Generate the graph of the function $f(x, y) = \sin(3x + 4\cos(2y)) + \cos(5y + 3\sin(3x))$, and it is required to accurately label the x-axis, y-axis, z-axis (representing the value of the function $f(x, y)$), in the three-dimensional coordinate system, as well as the key points such as the maximum points.

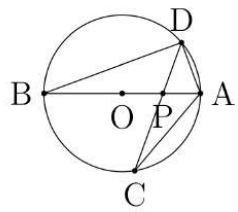
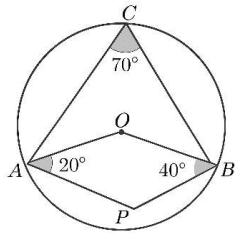


The generated graph of the function exhibits significant errors, especially regarding the labeling of the coordinate axes.

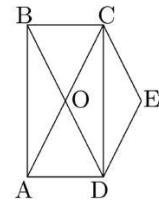
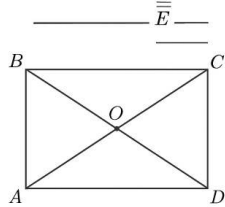
Figure 102: Examples of function plotting generation, with common mistakes in axis labeling and key point annotations.

Section 5.4 Mathematics

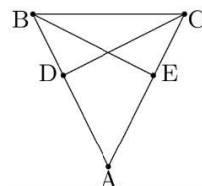
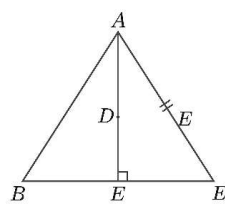
In circle $\odot O$, the diameter AB intersects the chord CD at point P. Connect AC, AD, and BD. Given that $\angle ACD = 20^\circ$, $\angle BPC = 70^\circ$, and $\angle ADC = 40^\circ$.



In rectangle ABCD, point O lies on AC and BD. Point E is outside the rectangle, with $DE \parallel AC$ and $CE \parallel BD$.



In $\triangle ABC$, point D is on AB, and point E is on AC. Given that $AB = AC$, $CD \perp AB$, and $BE \perp AC$.



The generated geometric image contains significant errors, and GPT-4O has difficulty accurately understanding the geometric relationships.

Figure 103: Examples of geometry diagram generation, with incorrect geometric relationships and inconsistent structures.

5.5 Agriculture

Agriculture-related image generation tasks evaluate the model’s capability to understand basic agricultural knowledge and generate realistic agricultural scenes[145, 34, 58, 111, 112]. This section is divided into two parts: the first part (Fig. 104) focuses on testing the model’s basic agricultural knowledge, such as pest identification, crop growth stages, soil profiles, and agricultural cycles. The second part (Fig. 104) explores the model’s ability to generate realistic synthetic agricultural images, which are commonly used in agricultural vision tasks and dataset construction.

From Fig. 104, we observe that GPT-4o shows a reasonable understanding of general agricultural concepts and can generate diagrams with clear visual structures. However, the generated images still suffer from obvious errors, such as incorrect labels (e.g., spelling mistakes in pest names) and inaccurate scientific details (*i.e.*, failing to correctly associate pests). In Fig. 105, we evaluate the model’s capability of generating synthetic agricultural scenes. While the model demonstrates some ability in generating farmland environments, there are noticeable failures in prompt comprehension, such as generating wrong fruit categories or failing to synthesize fine-grained details like crop textures and growth characteristics.

Overall, these results suggest that GPT-4o possesses basic agricultural knowledge but still lacks domain-specific expertise required for generating high-quality agricultural images, especially when applied to data synthesis tasks for agricultural computer vision.

Section 5.5 Agriculture

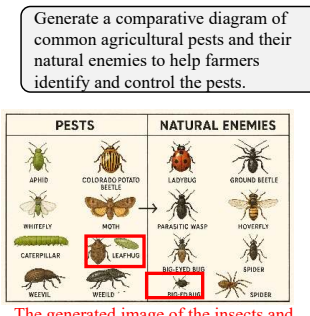
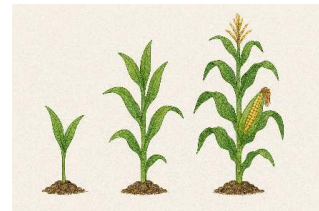
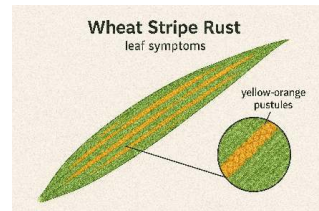
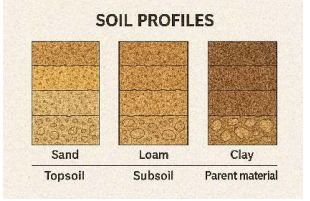
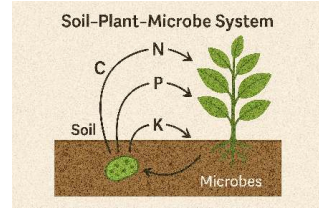
<p>Generate a comparative diagram of common agricultural pests and their natural enemies to help farmers identify and control the pests.</p> <p></p> <p>The generated image of the insects and their labels is generally correct, but there are spelling errors and it fails to clearly identify the pests and their corresponding natural enemies.</p>	<p>Generate a series of images showing maize at its different growth stages.</p> <p></p>
<p>Generate an illustrative diagram showcasing crops suitable for cultivation in Northern China, highlighting their key characteristics and planting requirements.</p> <p></p>	<p>Generate an image showing the leaf symptoms of wheat stripe rust, with close-ups of pustules and annotated labels for diagnosis.</p> <p></p>
<p>Generate a comparative diagram of soil profiles, illustrating the topsoil, subsoil, and parent material layers alongside representations of different soil textures—sand, loam, and clay—with clear labels for each layer and texture.</p> <p></p>	<p>Generate a schematic diagram illustrating the flow of carbon, nitrogen, phosphorus, and potassium within the soil–plant–microbe system, with arrows and labels indicating each element's pathways and transformations.</p> <p></p>

Figure 104: Examples of agriculture knowledge-based generation, including pest identification, crop growth stages, soil profiles, and agricultural cycles.

Section 5.5 Agriculture

<p>Generate realistic images of three different fruit crops—strawberries, mangoes, and apples—at their harvesting stage in outdoor agricultural fields, showing natural textures, colors, and background vegetation.</p>  <p>It doesn't match the prompt and fails to fully comprehend the meaning of the prompt.</p>	<p>Generate a realistic synthetic image of soybean plants at different growth stages in a farmland setting, including diverse leaf shapes, stem structures, and soil textures. The image should be suitable for training computer vision models in agriculture.</p> 
<p>Generate a realistic landscape image of an environment suitable for growing rice.</p>  <p>It doesn't match the prompt and fails to fully comprehend the meaning of the prompt.</p>	<p>Generate a realistic synthetic image of various weed species growing in an open field, with natural distribution across the soil and variation in plant appearance. The image should be suitable for training computer vision models in agriculture.</p> 

Figure 105: Examples of synthetic agricultural image generation, covering fruit crops, farmland environments, and various plant species in agricultural scenes.

6 Commonsense-based Image Generation

Commonsense-based image generation aims to evaluate the model’s ability to understand general knowledge and cultural concepts in the real world. This task is essential for testing the model’s capability to generate images that align with human common sense, cultural backgrounds, and general knowledge from different domains.

We design a comprehensive set of categories, including landmark, festival, food, clothing, painting, architecture, literature, logo, and health & safety. These tasks cover a wide range of cultural and commonsense scenarios, as investigated in previous works [72, 69, 82, 174, 10, 91, 77, 152, 39, 57, 147, 207, 122].

Experimental results show that GPT-4o performs well in most commonsense tasks, especially in landmark, food, clothing, and building generation, demonstrating its impressive cultural awareness and real-world knowledge. However, in the logo generation task, the model exhibits frequent factual errors, generating wrong characters or incorrect brand elements. In addition, we observe several unreasonable generations in the health and safety-related tasks, which deviate from common sense.

These results indicate that while GPT-4o shows strong commonsense and cultural understanding abilities, there is still room for improvement in precise factual generation and safety-critical scenarios.

Section 6 Commonsense-based Image Generation

<p>Generate an image of a famous scenic spot in China, with a clear label indicating its name.</p>  	<p>Generate an image of a famous scenic spot in Italy, with a clear label indicating its name.</p>  
<p>Generate an image of a famous landmark in Egypt, with a clear label indicating its name.</p>  	<p>Generate an image of a famous tourist attraction in Japan, with a clear label indicating its name.</p>  

Figure 106: Examples of landmark image generation, showcasing different iconic cultural and geographic locations.

Section 6 Commonsense-based Image Generation

<p>Generate an image of a traditional Chinese New Year celebration scene.</p> 	<p>Generate a realistic image of Brazil's Carnival parade.</p> 
<p>Generate an image of Diwali festivities in India.</p> 	<p>Generate a realistic image of Mexico's Day of the Dead altar setup.</p> 

Figure 107: Examples of festival image generation, showing traditional customs and cultural celebrations.

Section 6 Commonsense-based Image Generation

<p>Generate a realistic image of Peking duck served with pancakes and condiments.</p>  <p>Peking</p>	<p>Generate a realistic image of a Japanese sushi platter featuring nigiri and maki rolls.</p> 
<p>Generate a realistic image of a traditional Filipino dish called Balut.</p> 	<p>Generate a realistic image of a Mexican street-style taco with salsa and lime wedges.</p> 
<p>Generate a step-by-step visual recipe for making Chinese dumplings, showing dough preparation, meat and vegetable filling, folding technique, and steaming or boiling process, with each step illustrated clearly.</p> 	<p>Generate a step-by-step visual recipe for baking a classic French quiche, including ingredients layout, mixing of eggs and cream, filling the pastry shell, baking in the oven, and the final sliced serving.</p> 

Figure 108: Examples of food generation conditioned on different cultural recipes and cooking styles.

Section 6 Commonsense-based Image Generation

<p>Generate a realistic image of a person wearing traditional Chinese attire (e.g., Hanfu) with intricate embroidery and flowing silk, standing against a neutral backdrop, labeled "Hanfu."</p>  <p>HANFU</p>	<p>Generate a realistic image of a traditional Indian saree draped on a mannequin, showcasing intricate embroidery and rich colors, with a clear label "Saree."</p>  <p>SAREE</p>
<p>Generate a realistic image of a woman in a traditional Russian sarafan dress with kokoshnik headdress, labeled "Sarafan."</p>  <p>SARAFAN</p>	<p>Generate a realistic image of a person in Scottish Highland dress, featuring a tartan kilt, sporran, and ghillie brogues, labeled "Kilt."</p>  <p>KILT</p>

Figure 109: Examples of clothing generation guided by regional fashion styles and garment design.

Section 6 Commonsense-based Image Generation

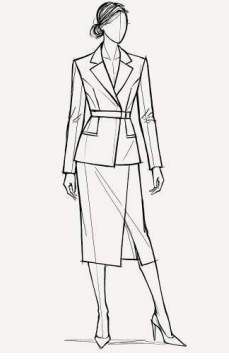
<p>Generate a black-and-white fashion design sketch of a modern outfit, focusing on silhouette, lines, and construction details without color or texture.</p> 	<p>Generate a complete fashion design illustration of a modern outfit, including clear garment structure, silhouette, fabric texture, and color scheme. The image should reflect both design concept and finished appearance.</p> 
<p>Using the previously generated fashion sketch, create a fully colored and textured version of the outfit, adding appropriate fabric materials, color schemes, and realistic shading while preserving the original design lines.</p> 	<p>Design a complete fashion illustration of a children's outfit based on the following elements: Age group: 5–7 years old Style: playful and practical Fabric: soft cotton with breathable mesh panels Colors: pastel blue, yellow, and white Details: elastic waistband, animal-themed front print, short sleeves with rounded edges.</p> 

Figure 110: More examples of clothing image generation with style control and appearance variation.

Section 6 Commonsense-based Image Generation

<p>Generate a realistic image in the style of a traditional Chinese ink wash landscape painting, featuring misty mountains, flowing water, and pine trees.</p> 	<p>Generate a realistic image in the style of a Dutch Golden Age still life, featuring flowers, fruit, and glassware on a table.</p> 
<p>Generate a digital art piece in the style of Japanese ukiyo-e, showing a traditional theater performance.</p> 	<p>Generate an abstract expressionist painting with bold colors and dynamic forms conveying emotion.</p> 

Figure 111: Examples of painting generation with various art styles and cultural elements.

Section 6 Commonsense-based Image Generation

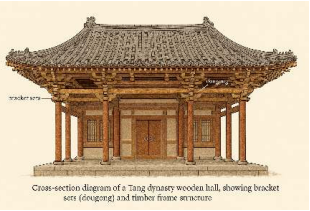
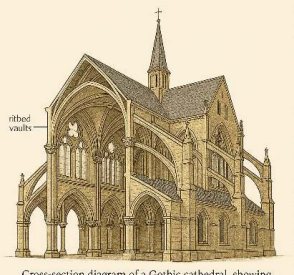
<p>Generate a detailed cross-section diagram of a Tang dynasty wooden hall, showing bracket sets (dougong) and timber frame structure.</p>  <p>Cross-section diagram of a Tang dynasty wooden hall, showing bracket sets (dougong) and timber frame structure.</p>	<p>Generate a detailed cross-section diagram of a Gothic cathedral, showing flying buttresses and ribbed vaults.</p>  <p>Cross-section diagram of a Gothic cathedral, showing flying buttresses and ribbed vaults.</p>
<p>Generate a photorealistic rendering of a traditional Japanese teahouse set in a zen garden.</p> 	<p>Generate a realistic image of a Brutalist civic center made of raw concrete blocks, showcasing heavy massing and minimal windows.</p> 

Figure 112: Examples of building generation based on architectural styles and cultural background.

Section 6 Commonsense-based Image Generation

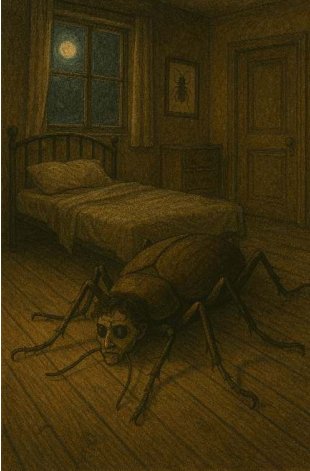
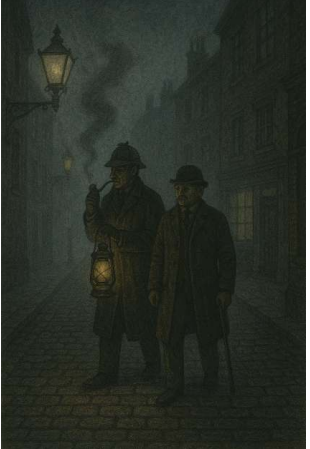
<p>Generate an illustration of the Monkey King (Sun Wukong) battling the Bull Demon King atop Flower-Fruit Mountain.</p> 	<p>Generate a dramatic scene of Romeo and Juliet on the balcony under moonlight, capturing their emotional expressions.</p> 
<p>Generate a surreal, symbolic illustration of Kafka's Metamorphosis, showing Gregor Samsa as an insect in his bedroom.</p> 	<p>Generate an atmospheric scene of Sherlock Holmes and Dr. Watson investigating a foggy London street at night.</p> 

Figure 113: Examples of literature-related generation, including book covers and literary visual elements.

Section 6 Commonsense-based Image Generation

<p>Generate a realistic image of the Harvard University emblem.</p>  The image shows the Harvard University crest, which is a red shield with a gold border. Inside the shield, there are two gold books at the top and a gold book at the bottom. The letters 'VE' and 'RI' are on the top book, and 'TAS' is on the bottom book. The word 'HARVARD' is written in gold letters along the bottom of the shield. A gold laurel wreath surrounds the shield. <p>Generate a realistic image of the Beijing University of Posts and Telecommunications emblem.</p>  The image shows the Beijing University of Posts and Telecommunications emblem, which is a circular seal. The outer ring contains the text '北京邮电大学' in Chinese and 'BEIJING UNIVERSITY OF POSTS AND TELECOMMUNICATIONS' in English, with the year '1955' in the center. Inside the ring is a stylized torch or flame. <p>An incorrect image was generated</p>	<p>Generate a realistic image of the logo of Blue Bottle Coffee.</p>  The image shows the logo for Blue Bottle Coffee, which consists of a blue bottle shape with a red cap. Below the bottle, the words 'BLUE BOTTLE COFFEE' are written in a serif font. <p>Generate a realistic image of the Nike Swoosh logo on a clean white background, emphasizing its simple yet iconic design.</p>  The image shows the Nike Swoosh logo, which is a black, swooping line forming a checkmark shape, set against a plain white background.
--	--

Figure 114: Examples of logo generation. GPT-4o tends to generate factual errors, such as wrong text or symbols.

Section 6 Commonsense-based Image Generation

<p>Generate a realistic image of someone performing CPR on a training mannequin, showing correct hand placement and posture.</p> 	<p>Generate a realistic illustration of proper fire extinguisher usage steps (P.A.S.S.: Pull, Aim, Squeeze, Sweep) next to an extinguisher.</p> 
<p>Generate a realistic illustration of a workplace emergency exit plan posted on a wall, showing arrows, exit routes, and assembly point.</p> 	<p>Generate a realistic diagram of a home first-aid kit layout, with bandages, antiseptic wipes, scissors, and medications neatly arranged.</p> 

Figure 115: Examples of health and safety-related generation.

7 Spatially-aware Image Generation

7.1 Multi-view Image Generation

Our evaluation begins with assessing the model’s target-level reconstruction capability, which involves generating novel-view images conditioned on a single input view of the target.

Normal Novel-view Synthesis. As shown in Fig. 121–123, we test GPT-4o’s ability to synthesize novel views for common objects with regular geometric structures. The model successfully produces visually plausible outputs from multiple viewpoints, capturing the overall shape and semantics of the targets. Especially for cartoon-style and simplified furniture objects, the outputs demonstrate strong viewpoint control and global structural consistency. However, we still observe subtle 3D misalignments in details such as window geometry and edge connections, indicating the absence of true volumetric reasoning.

Human-centric Novel-view Synthesis. We further evaluate GPT-4o’s ability to synthesize new views for human portraits and full-body figures. As illustrated in Fig. 124–126, the model generates front, side, and back views that maintain identity and pose coherence to a surprising degree. In portrait-level tasks, GPT-4o preserves key facial features under varying perspectives. For full-body generation, while the general body layout remains intact, issues such as inconsistent limb placement are still visible, reflecting the challenge of maintaining fine-grained spatial correspondence for articulated objects like the human body.

Scene-centric Novel-view Synthesis. Finally, we evaluate GPT-4o’s capability in synthesizing novel views of complex outdoor scenes (Fig. 127–128). While the model is capable of switching to plausible overhead or oblique viewpoints and preserves large-scale structure and style, its performance degrades significantly under large camera transformations. Inaccurate alignment of roofs, inconsistent vanishing points, and mislocated objects are frequent, suggesting that GPT-4o lacks sufficient 3D scene understanding to handle complex geometries and deep spatial layouts.

Section 7.1 Multi-view Image Generation

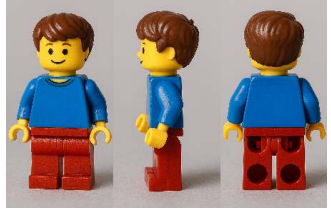
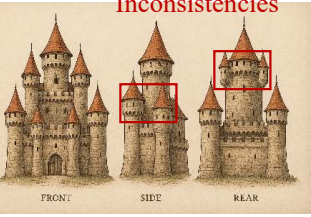
<p>Generate front, side and back view images of the Audi s5 vehicle in one figure</p> <p>Inaccurate viewpoint</p> 	<p>Generate front, side and back view images of a backpack in one figure</p> 
<p>Generate front, side and back view images of a lego-style boy in one figure</p> 	<p>Generate front, side and back view images of a castle in one figure</p> <p>Inconsistencies</p> 

Figure 116: Examples of multi-view image generation results produced by GPT-4o. The model is capable of generating coherent front, side, and back views for a variety of objects, such as backpacks and toy figures, maintaining consistent shapes and structures. However, challenges remain in handling complex geometries and rigid objects. For instance, the vehicle example exhibits inaccurate viewpoint alignment (top left), while the castle generation shows structural inconsistencies across views (bottom right).

Section 7.1 Multi-view Image Generation

<p>Generate front, side and back view images of a fish tank with several fishes in it in one figure</p>  <p>Inconsistencies</p>	<p>Generate 30 degree side and 60 degree side view images of a cup of coffee in one figure, photorealistic</p>  <p>Inaccurate viewpoint</p>
<p>Generate 30 degree side and 60 degree side view images of a toy car in one figure, photorealistic</p> 	<p>Generate front, 30 degree side and 60 degree side view images of a lego-style cowboy in one figure, photorealistic</p> 

Figure 117: Examples of angle-specific multi-view image generation results by GPT-4o. The model successfully renders photorealistic side-view transitions at specified angles (30° and 60°) for structured objects like toy cars and lego-style figures, maintaining high fidelity across views. However, it struggles with consistency in complex or cluttered scenes (e.g., the fish tank) and precise viewpoint transitions for symmetric objects (e.g., the coffee cup), where angular alignment is inaccurate or content appears altered, highlighting limitations under fine-grained view control.

Section 7.1 Multi-view Image Generation

<p>Generate front, side and back view images of a smiling woman in one figure</p>  	<p>Generate front, side and back view images of Abraham Lincoln making a speech in one figure</p>  
<p>Generate front, side and back view images of Abraham Lincoln in one figure</p>  	<p>Generate front, side and back view images of a woman singing a song in one figure</p>  

Figure 118: Examples of multi-view human image generation results by GPT-4o. The model accurately synthesizes front, side, and back views of human subjects in both static and dynamic scenarios, such as standing poses and singing actions. Viewpoint transitions are smooth and identity preservation is consistent across views, even under varied body orientations and clothing details, demonstrating the model's strong grasp of human 3D geometry and pose-aware rendering.

Section 7.1 Multi-view Image Generation

<p>Generate front, 30 degree side and 60 degree side view images of a cute girl singing in one figure, photorealistic</p> 	<p>Generate front, 30 degree side and 60 degree side view images of a man reading in one figure, photorealistic</p> 
<p>Generate front, side and back view images of Abraham Lincoln in one figure</p> 	<p>Generate front, 30 degree side and 60 degree side view images of a man smoking in one figure, photorealistic</p>  <p>Inconsistencies</p>

Figure 119: Examples of photorealistic multi-view human image generation by GPT-4o. The model generally produces consistent front and angled views of human subjects. However, certain cases still exhibit noticeable inconsistencies, particularly in hand-object interactions and facial details, indicating room for improvement in fine-grained coherence across views.

Section 7.1 Multi-view Image Generation

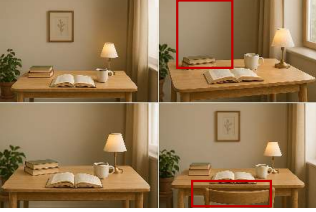
<p>Generate front, side and back view images of a wooden bench in a quiet park, green grass around, sunny day in one figure</p> 	<p>Generate front, side and back view images of a clean desk in a cozy room, books, a cup of coffee, soft window light in one figure</p> 
<p>Inconsistencies</p> 	<p>Generate front, side and back view images of a convenience store on a quiet street, glowing signboard at night in one figure</p>  <p>Inaccurate viewpoint</p>

Figure 120: Examples of multi-view scene generation results by GPT-4o. The model attempts to produce front, side, and back views of complex indoor and outdoor scenes. However, the outputs frequently suffer from object placement inconsistencies and inaccurate viewpoint transformations, particularly in structured environments like desks and storefronts. These issues reveal GPT-4o's current limitations in holistic scene understanding and spatial consistency across views.

7.2 Novel-view Synthesis

The novel-view synthesis task [176, 18, 160, 196] is a fundamental problem in the field of 3D vision, closely aligned with the goals of 3D reconstruction [110, 73] and image-to-3D [156, 98, 95, 153, 38, 158] generation. In this task, the model is required to generate images of a given object or scene from unseen viewpoints based on a single input image, effectively making it a form of **single-image reconstruction** [175, 185]. This setup allows us to assess GPT-4o’s spatial awareness capability from a reconstruction perspective. Similar to the previous section, we design a set of logically structured tasks with varying levels of difficulty to systematically evaluate the model’s performance.

7.2.1 Traditional View Synthesis

Our evaluation begins with assessing the model’s target-level reconstruction capability, which involves generating novel-view images conditioned on a single input view of the target.

Normal Novel-view Synthesis. As shown in Fig 121, 122, 123, GPT-4o demonstrates reasonable viewpoint control in novel view synthesis of common and simple targets. However, the generated results still lack perfect 3D consistency.

Human-centric Novel-view Synthesis. Next, we evaluate GPT-4o’s ability to generate novel views of humans, including both full-body figures and facial portraits. Surprisingly, despite some remaining inconsistencies, GPT-4o demonstrates an impressive level of 3D understanding when it comes to human subjects, as shown in Fig 124, 125, 126.

Scene-centric Novel-view Synthesis. We assess GPT-4o’s novel-view synthesis capabilities on complex outdoor scenes, as illustrated in Fig 127, 128. The results show that, while the model maintains a relatively strong degree of 3D consistency, GPT-4o fails to handle significant viewpoint shifts effectively, highlighting its limited capacity for 3D understanding in complex scene settings.

Section 7.2.1 Traditional Novel View Synthesis

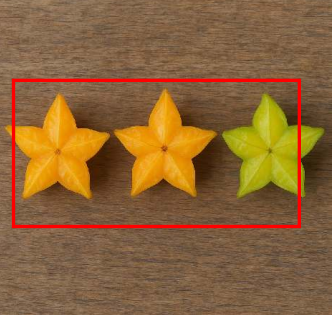
 <p>Based on the input image, generate a new image from a front view perspective.</p> 	 <p>Based on the input image, generate a new image from an overhead view perspective.</p> 
 <p>Generate a picture when viewed from the left side, without the need for high resolution</p> 	 <p>This is a picture of fruit on a table, please generate a picture when viewed from a top-down view,</p> 

Figure 121: Examples of novel-view synthesis on normal targets by GPT-4o. The model generates visually plausible images from new viewpoints given a single input view, showing reasonable spatial understanding for both objects and scenes. However, subtle 3D inconsistencies remain—such as misalignment in geometry or structure—indicating that perfect reconstruction fidelity has not yet been achieved.

Section 7.2.1 Traditional Novel View Synthesis

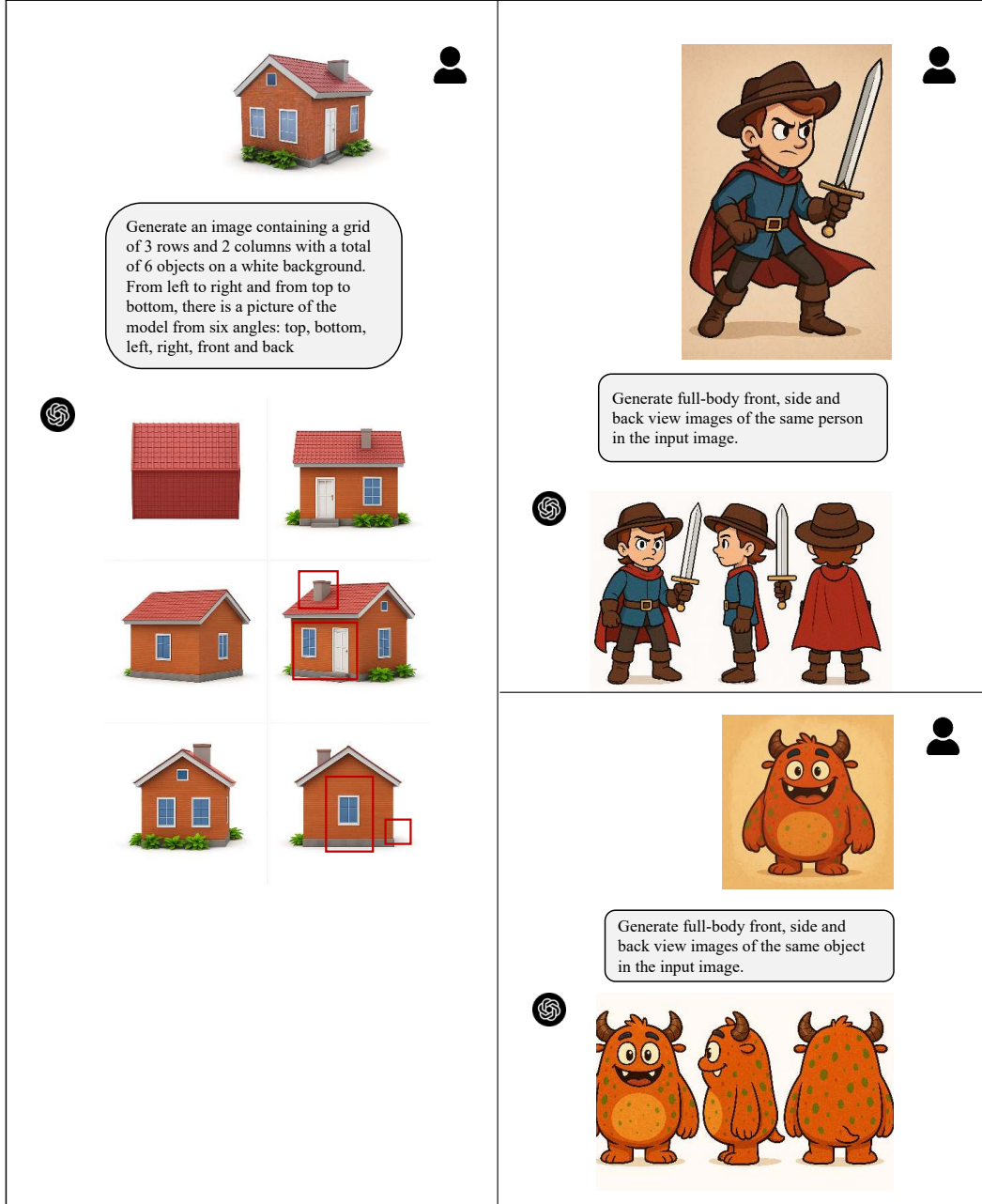


Figure 122: Examples of novel-view synthesis on cartoon-style normal targets by GPT-4o. The model generates coherent and visually consistent images from multiple new viewpoints, capturing the overall structure and appearance of stylized characters and objects. Despite minor geometric inaccuracies in complex shapes (e.g., roof or window details), the outputs demonstrate strong spatial reasoning and effective viewpoint control in simplified, non-photorealistic domains.

Section 7.2.1 Traditional Novel View Synthesis

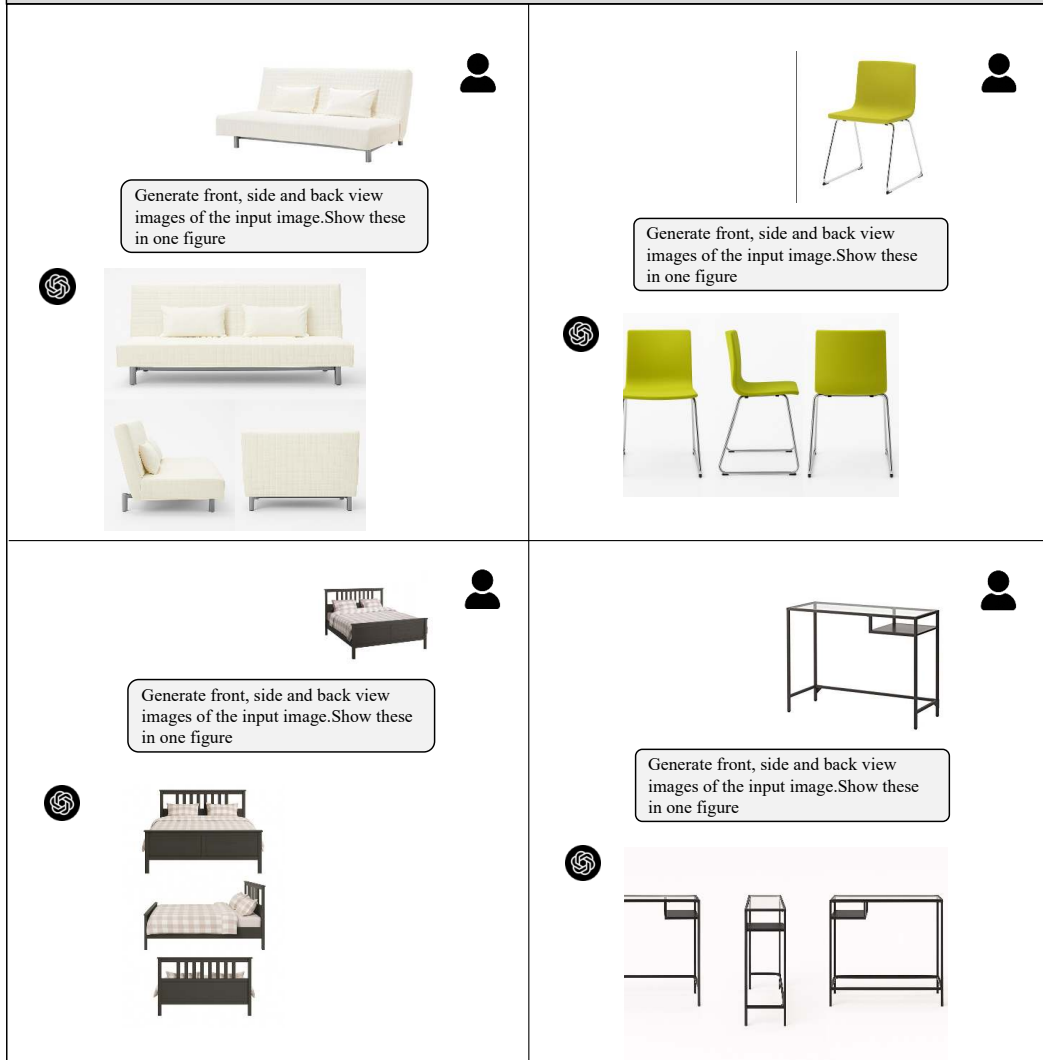


Figure 123: Examples of novel-view synthesis on structurally simple normal targets by GPT-4o. Given a single input image, the model accurately reconstructs front, side, and back views of furniture items with clean lines and regular shapes. The outputs exhibit strong geometric consistency and precise viewpoint transitions, demonstrating GPT-4o's capability to handle objects with simple, well-defined structures in controlled settings.

Section 7.2.1 Traditional Novel View Synthesis

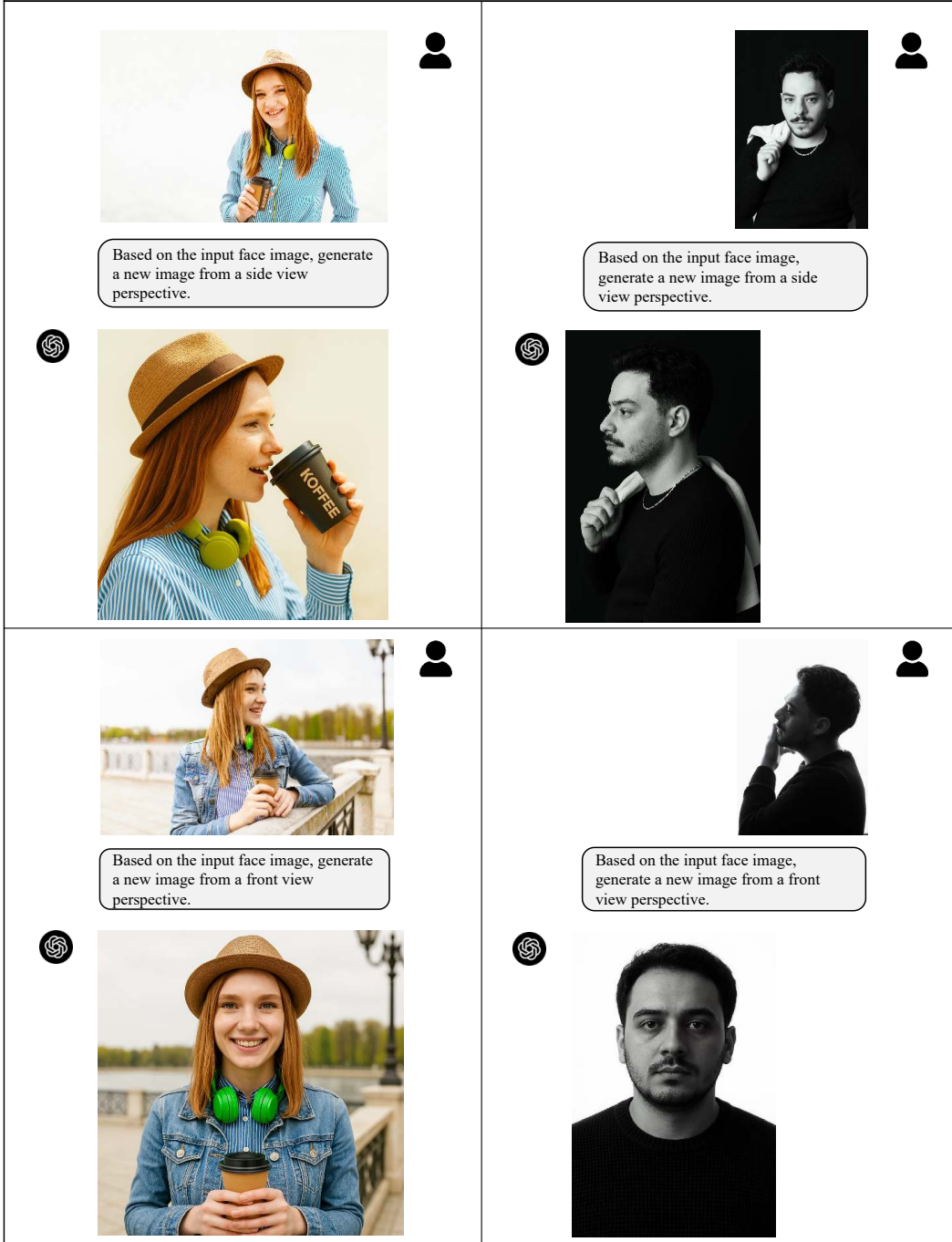


Figure 124: Examples of novel-view synthesis on face portrait (ID-style) images by GPT-4o. The model generates realistic and identity-consistent views from both front and side perspectives based on a single input image. Despite occasional artifacts in facial features or accessories, the overall viewpoint transformations demonstrate GPT-4o's strong 3D understanding of human faces.

Section 7.2.1 Traditional Novel View Synthesis

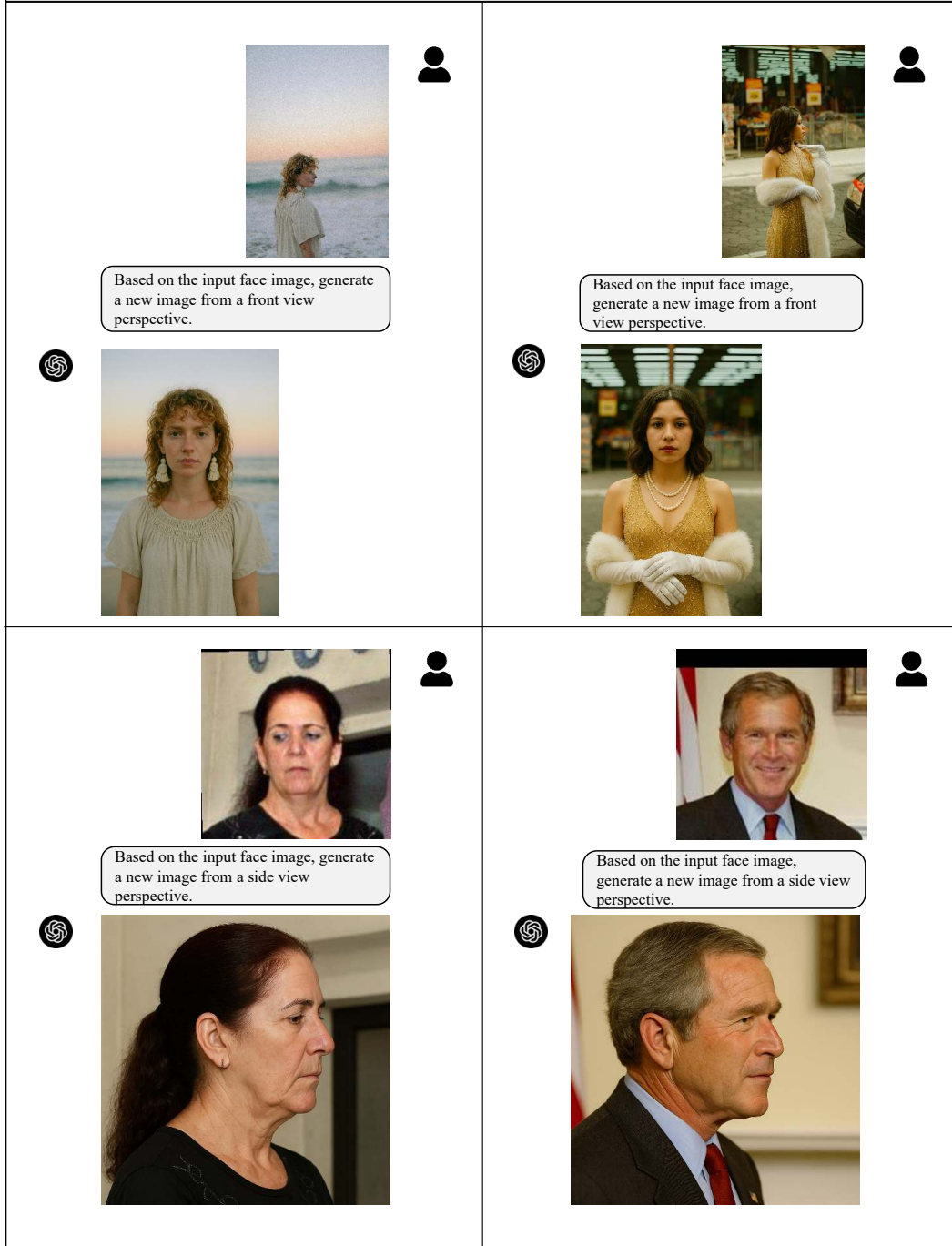


Figure 125: Additional examples of novel-view synthesis on face portrait (ID-style) images by GPT-4o. The model produces front and side views that are generally consistent with the input identity, showing a solid grasp of 3D facial structure with only minor variations.

Section 7.2.1 Traditional Novel View Synthesis

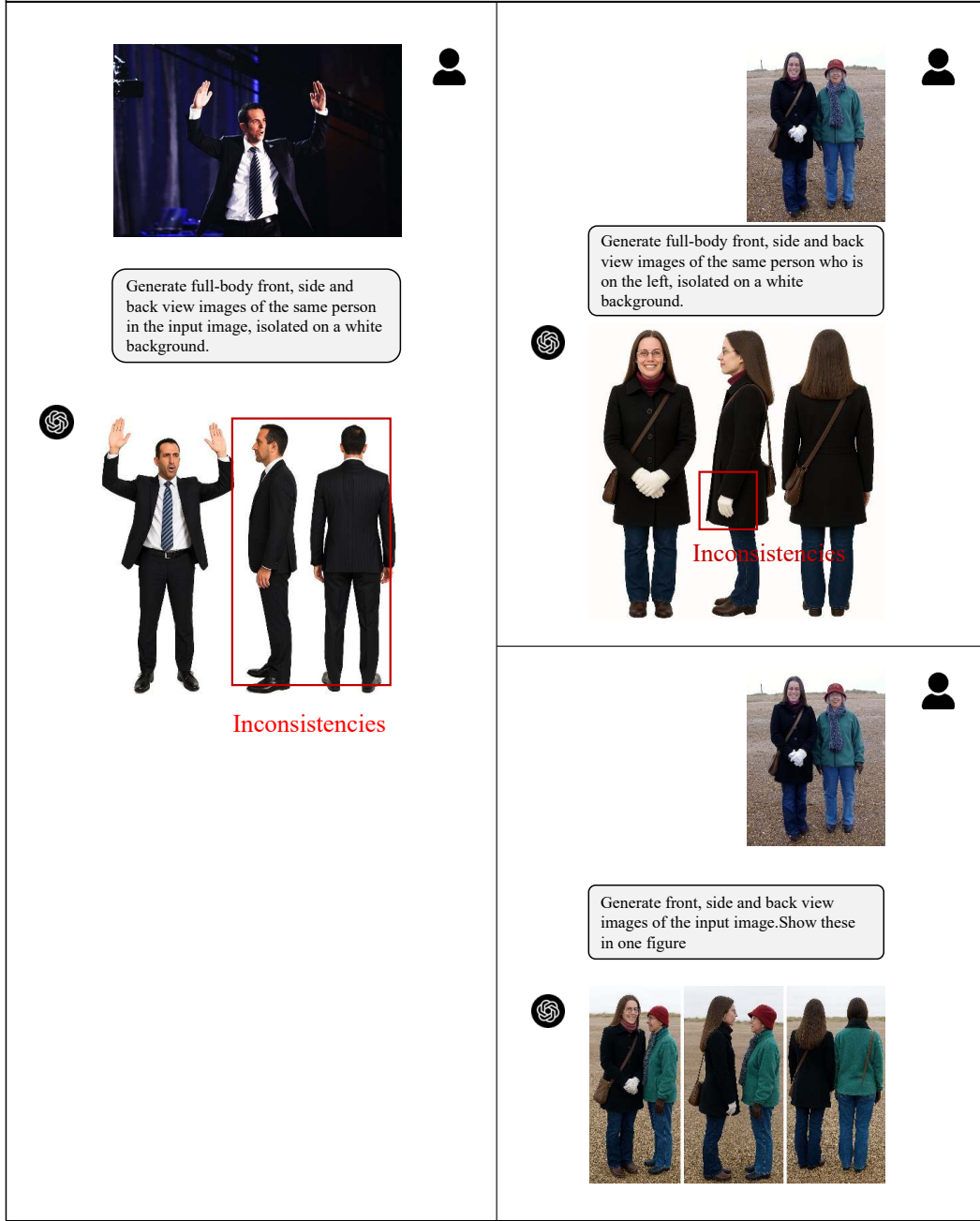


Figure 126: Examples of novel-view synthesis on full-body human images by GPT-4o. The model is able to generate front, side, and back views that broadly preserve body posture and clothing details. However, inconsistencies in limb position, accessories, and clothing geometry are still common, highlighting the challenge of achieving precise spatial alignment in full-body reconstructions.

Section 7.2.1 Traditional Novel View Synthesis

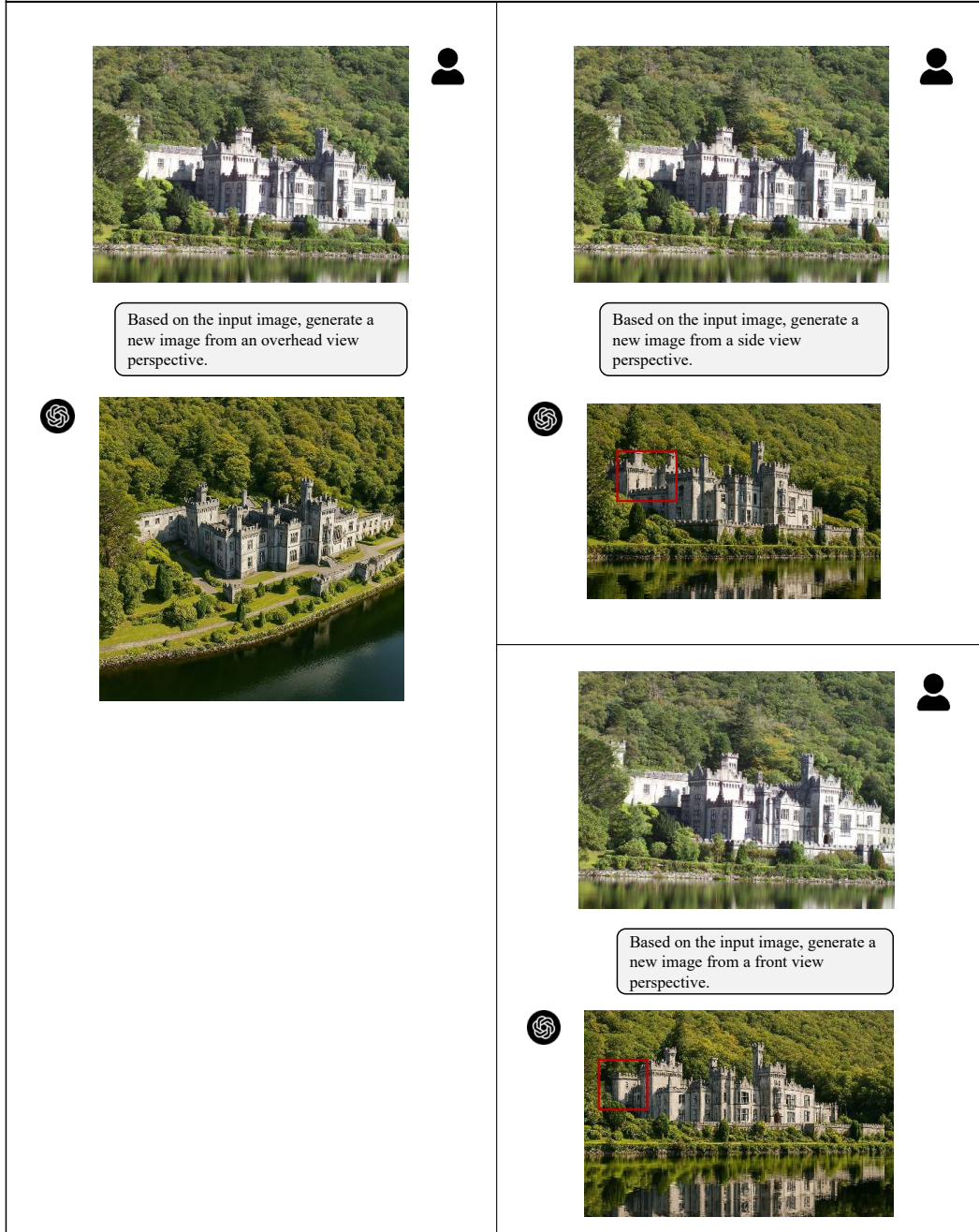


Figure 127: Examples of novel-view synthesis on complex outdoor scenes by GPT-4o. The model produces plausible overhead, side, and front views from a single input image, preserving the overall structure of the scene. However, structural inaccuracies emerge under large viewpoint shifts, revealing the model's limited ability to maintain full 3D consistency in complex environments.

Section 7.2.1 Traditional Novel View Synthesis

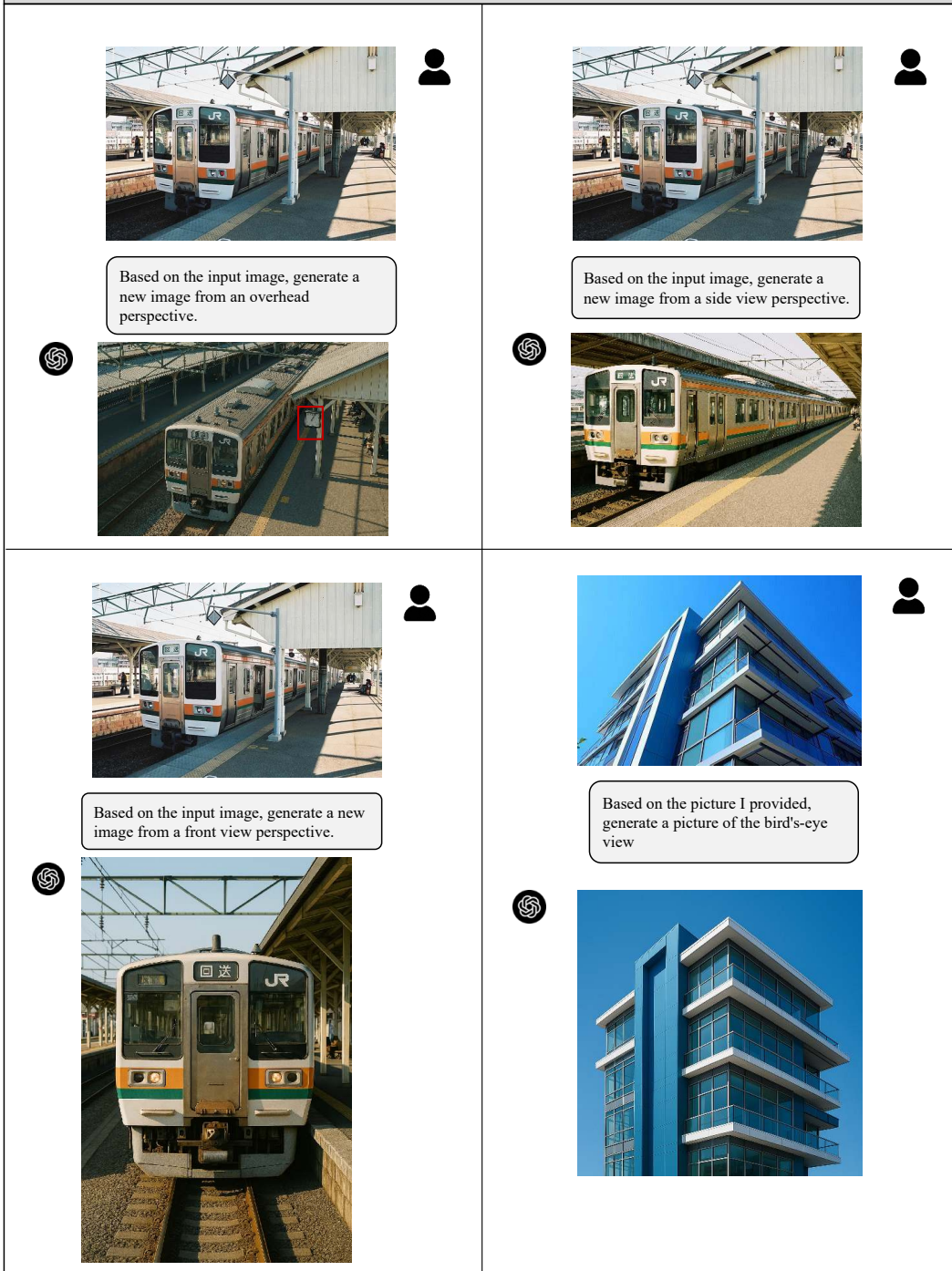


Figure 128: More examples of novel-view synthesis on complex scenes by GPT-4o. The model is able to preserve overall structure and visual fidelity across different viewpoints. However, the generated outputs often suffer from inaccurate viewpoint alignment, suggesting that GPT-4o still faces challenges in precisely controlling camera angles in complex real-world scenes.

7.2.2 View Synthesis under Embodied Scene

Viewpoint transformation in embodied or indoor environments is particularly critical for embodied intelligence research. Therefore, we specifically evaluate GPT-4o’s spatial understanding based on indoor scene images and layouts. Through our test, GPT-4o demonstrates strong viewpoint control but relatively weak consistency across views.

Image-based View Synthesis. As shown in Fig. 129, we evaluate GPT-4o on a set of tasks where the model is asked to generate images from new viewpoints based on a single input photograph of an indoor scene. The model shows promising performance in generating visually plausible results from new perspectives, demonstrating a reasonable grasp of camera positioning and viewpoint shift. However, the generated outputs still exhibit noticeable inconsistencies in spatial alignment. In particular, some objects undergo geometric distortion, positional shifts, or changes in appearance. For instance, the same lamp or keyboard may appear altered or misplaced between the original and generated view, indicating that while GPT-4o is capable of inferring approximate scene layouts, it lacks fine-grained 3D scene understanding and consistency-preserving mechanisms.

Layout-based View Synthesis. As shown in Fig. 130, we further evaluate GPT-4o using top-down scene layouts or stylized 3D room schematics as input conditions. The goal is to synthesize a plausible first-person perspective from a described location (e.g., “standing at the kitchen door looking at the living room”). GPT-4o successfully generates semantically reasonable images and often captures the high-level spatial arrangement outlined in the layout. Nonetheless, there are notable issues at the object level, including furniture discrepancies, missing elements, and incorrect room proportions. These problems highlight the difficulty in faithfully grounding generation based on abstract scene layouts and converting spatial instructions into accurate visual reconstructions.

Overall, these experiments demonstrate that while GPT-4o possesses a strong ability for global viewpoint control, its internal scene representations remain limited. The model often fails to maintain object permanence and spatial consistency across views, revealing a lack of true 3D reasoning capabilities. Improving these aspects is crucial for tasks such as embodied AI, navigation, and robotic perception, where viewpoint fidelity and spatial grounding are essential.

Section 7.2.2 View Synthesis under Embodied Scene

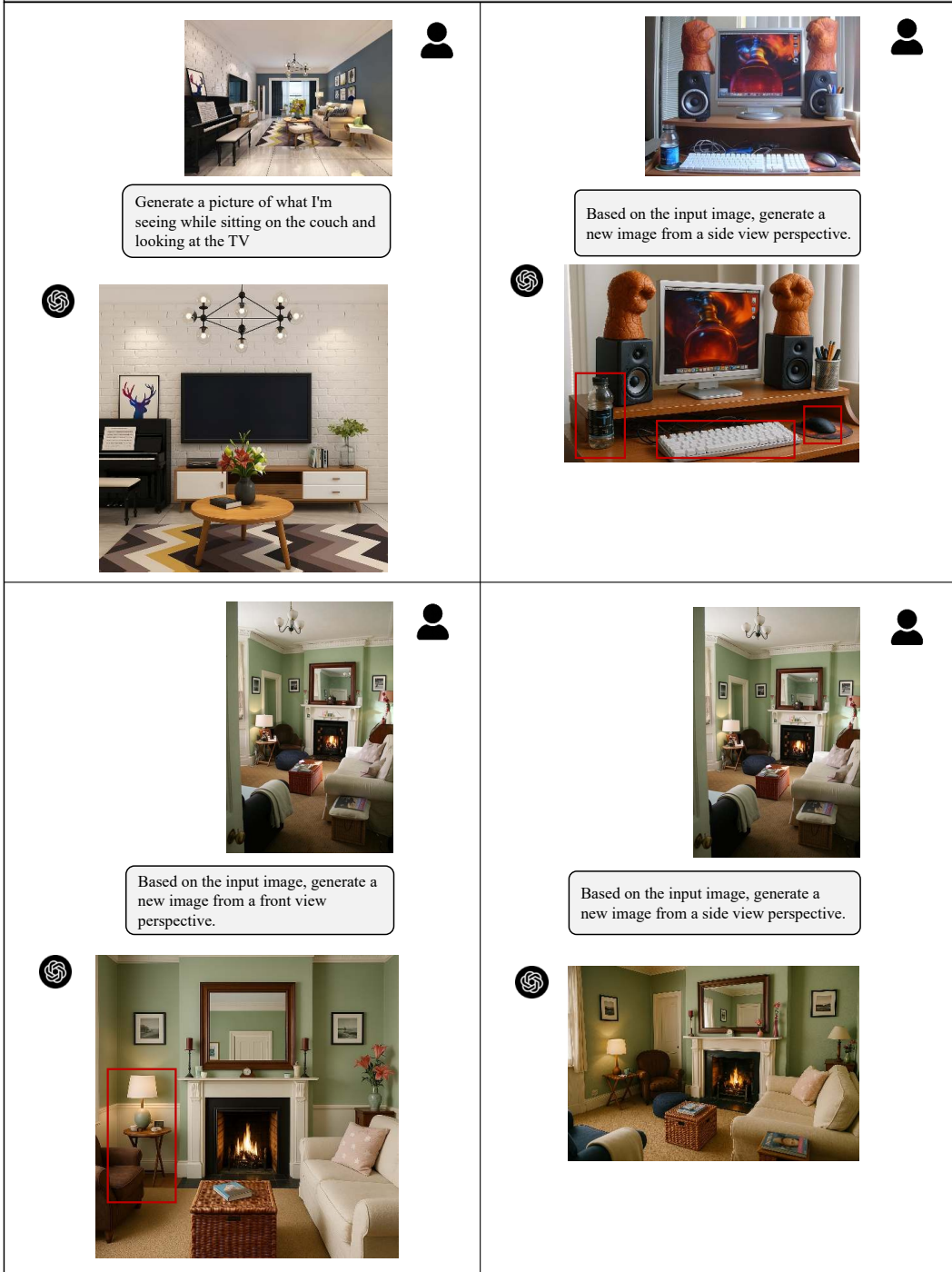


Figure 129: Examples of novel-view synthesis on indoor (embodied) scenes by GPT-4o. The model shows strong viewpoint control and can generate plausible views from new perspectives based on a single input. However, inconsistencies in object placement and appearance—such as furniture, lighting, and layout—are still noticeable, indicating limited spatial consistency in complex embodied environments.

Section 7.2.2 View Synthesis under Embodied Scene

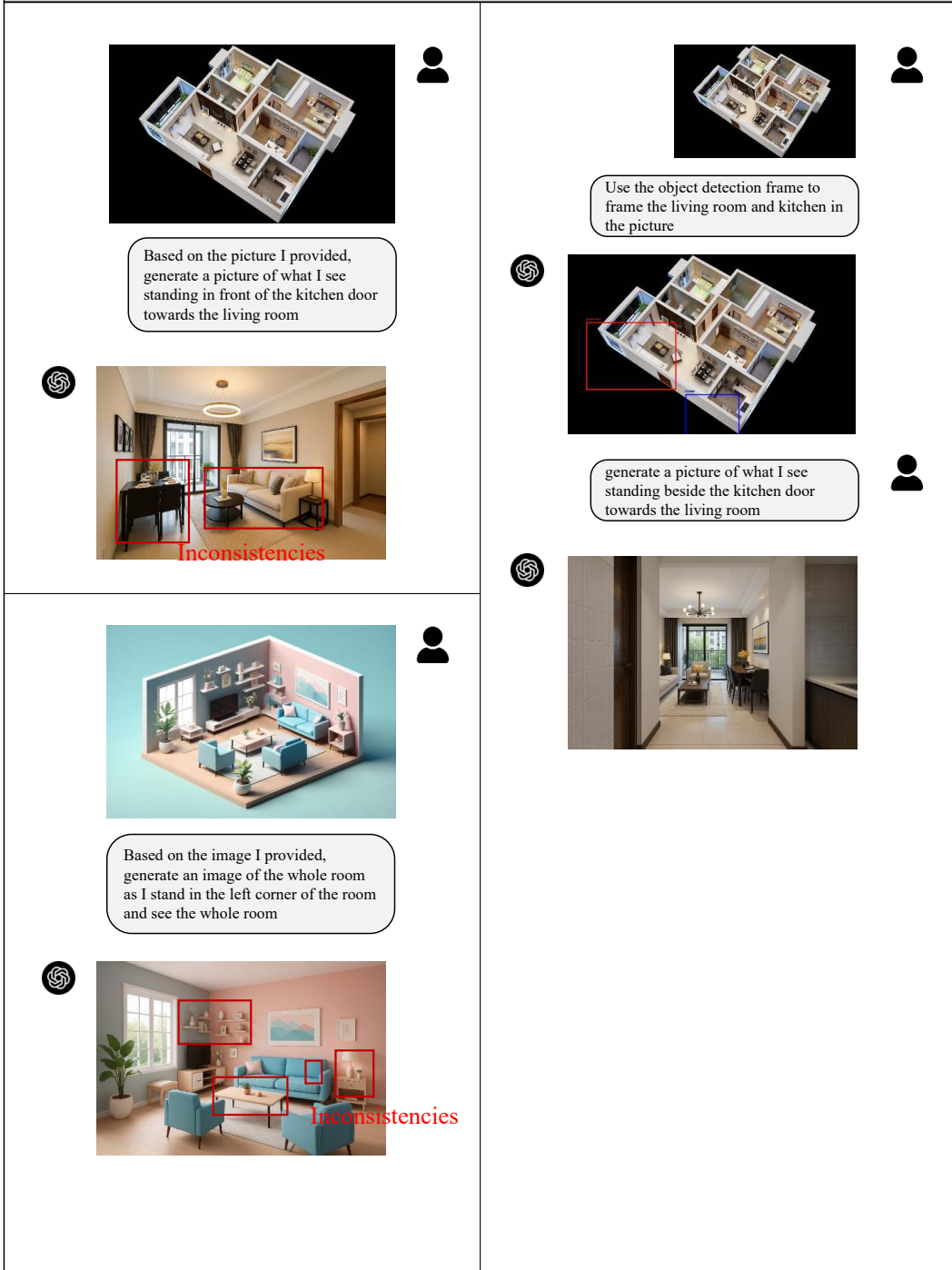


Figure 130: Examples of novel-view synthesis based on layout images by GPT-4o. The model can generate plausible first-person perspectives from specific locations in the scene, conditioned on 3D floor plans or stylized layouts. While the overall spatial arrangement is preserved, the generated views often contain object-level inaccuracies, indicating challenges in fine-grained grounding and geometric precision from abstract layout inputs.

7.3 Spatial Reasoning

The spatial reasoning task [19, 29, 166] evaluates a model’s ability to interpret and visually realize spatial relationships described in a textual prompt. In this task, the model is asked to generate images that accurately reflect specific object placements or relative spatial configurations—for example, “a person standing behind a tree” or “a cat sitting between two chairs.” Successfully completing this task requires not only semantic understanding of the involved entities, but also the ability to reason about depth, occlusion, and relative positioning in a physically coherent manner. As such, this task serves as a critical benchmark for assessing GPT-4o’s spatial awareness, particularly in terms of scene composition and depth-based reasoning.

Prompt-based Reasoning. As shown in Fig. 131, we evaluate the model’s ability to control spatial relationships through textual prompts. GPT-4o demonstrates a certain level of spatial understanding, particularly in interpreting depth-related relationships.

Image-based Reasoning. As shown in Fig. 132, 133, 134, 135, we test GPT-4o’s ability to arrange multiple objects in space based on a given prompt. The model demonstrates promising capabilities in composing multiple targets within a scene, but still exhibits inconsistencies with the specified spatial instructions.

Section 7.3 Spatial Reasoning

Generate a picture: In the foreground, a person is standing in front of a large tree. Behind the tree, partially hidden, another person is standing. Further in the background, a car is parked behind that second person.



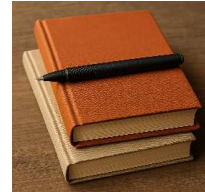
Correct

Generate a top-down view of a white badminton shuttlecock lying on fresh green grass, partially or fully covered by two crossed badminton rackets placed directly on top of it. The rackets are arranged in a crisscross pattern and rest firmly over the shuttlecock.



Correct

Generate a picture: A top-down view of a realistic table scene with layered objects. A closed book lies flat on the table. On top of the book, a pen is placed horizontally. Another closed book is resting directly on top of the pen, pressing it down. The pen is slightly squeezed between the two books, with its tip and cap visible on opposite sides.



Incorrect

Figure 131: Examples of spatial reasoning through textual prompts by GPT-4o. The model demonstrates a strong grasp of relative spatial relationships and occlusion in certain scenarios—such as depth-based person placement and object layering (top). However, in more complex configurations involving subtle interactions (e.g., multiple levels of layering and pressure), failures occur, suggesting limitations in fine-grained spatial composition and physical plausibility.

Section 7.3 Spatial Reasoning



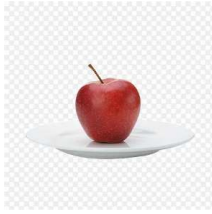
Place the items in pictures 2, 3, and 4 in the first picture, with the table against the wall on the right, the bookcase against the middle wall, and place the chair in front of the table so that when sitting on it we can face the table



Take the fruit platter from the second image and place it on the right side of the cutting board in the first image

Figure 132: Examples of image-based spatial reasoning by GPT-4o. The model successfully integrates multiple objects into a coherent scene according to visual and textual instructions, demonstrating an ability to handle basic spatial placement and alignment. While overall composition is reasonable, some positional inaccuracies remain, indicating room for improvement in precise spatial grounding and instruction following.

Section 7.3 Spatial Reasoning



Place the apple in Figure 2 in the fruit platter in Figure 1 and place the apple on top of the kiwifruit



Replace the sofa in the scene with the sofa from the second image, ensuring that the pillows on the sofa remain unchanged and all other elements in the background stay intact.

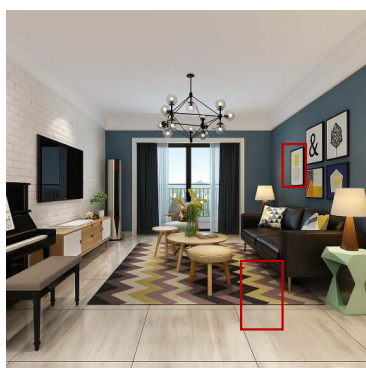


Figure 133: More examples of image-based spatial reasoning by GPT-4o. The model is able to follow compositional instructions such as object placement and substitution with reasonable success. While the apple is correctly added with appropriate layering, the sofa replacement introduces minor inconsistencies in lighting and background alignment, indicating limitations in fine-grained control and global scene consistency.

Section 7.3 Spatial Reasoning



Figure 134: Examples of spatial reasoning through 2D-to-3D reassembly by GPT-4o. Given flat box layouts, the model is able to generate plausible 3D box renderings, capturing overall structure, folding logic, and surface continuity. While most reassembled results are visually coherent, minor inconsistencies in texture alignment and panel orientation still occur, reflecting the challenge of precise spatial reconstruction from UV-like input maps.

Section 7.3 Spatial Reasoning

	
<p>Stack the item circled in red on top of the item circled in yellow</p>	<p>let the shuttlecock be placed underneath two badminton rackets lying on grass</p>
	
<p>place the bag above the pen</p>	<p>Let the soft grey pouch partially cover the light grey pen, with part of the pen sticking out from underneath the pouch</p>
 <p>Incorrect</p>	 <p>Correct</p>

Figure 135: Examples of spatial reasoning through localized object editing by GPT-4o. The model shows partial success in interpreting fine-grained spatial instructions involving occlusion, stacking, and partial covering. While some generations correctly reflect the intended relationships (e.g., partial occlusion), others misinterpret layering or spatial order, indicating ongoing challenges in precise object-level spatial manipulation.

8 Temporally-aware Image Generation

Temporally-aware image generation [83, 104] is a critical task for assessing a model’s ability to maintain coherence over time and understand dynamic visual processes. In this task, the model is required to generate a sequence of images that depict consistent temporal evolution—such as motion, transformation, or progression—based on a given series of frame images. This setup enables the evaluation of GPT-4o’s understanding of causality, temporal continuity, and object permanence, all of which are essential for applications involving video generation, animation, and real-world scene understanding. We evaluate GPT-4o’s capability across three representative tasks: future frame prediction, intermediate frame prediction, and past frame prediction. Each task provides distinct challenges in terms of temporal reasoning and spatial consistency.

Future Frame Prediction. This task involves generating the next plausible frame in a visual sequence, given the initial few frames. The model is expected to predict a visually consistent and temporally reasonable continuation of scene dynamics, object motion, and structural transitions. As shown in Fig. 136 to Fig. 140, GPT-4o demonstrates the ability to maintain global scene layouts and preserve image fidelity. However, it consistently struggles to model precise object motion and directionality. For instance, in Fig. 136, although the spatial structure under the bridge is roughly preserved, the bridge’s predicted continuation fails to match the previous trajectory. In Fig. 137, the model generates a plausible car scene, but completely ignores the expected motion of the vehicle, indicating weak motion extrapolation. Similarly, in Fig. 138, the drifting clouds fail to align with the observed trajectory, suggesting difficulties in modeling natural dynamics. While Fig. 139 and Fig. 140 show correct semantic context (e.g., scoring a goal), the details of the ball and goalkeeper’s motion are inaccurate. These examples highlight that GPT-4o primarily prioritizes static scene generation over temporal causality.

Intermediate Frame Prediction. This task requires the model to generate a plausible intermediate frame, given both the starting and ending frames. The model must infer continuous motion trajectories and interpolate realistic transitions between visual states. As shown in Fig. 141 to Fig. 145, the results are mixed. In Fig. 141, the model produces a semantically coherent intermediate frame with reasonable alignment and motion. However, in Fig. 142, the car’s orientation is reversed, indicating poor spatial continuity. While Fig. 143 shows strong temporal alignment between hand and film roll, Fig. 144 and Fig. 145 reveal serious failures in understanding player position, motion trajectory, and semantic relationships in soccer scenes. These examples demonstrate the challenge of fine-grained motion interpolation, where GPT-4o often falls short in preserving both local interactions and global structure.

Past Frame Prediction. This task evaluates the model’s ability to hallucinate plausible earlier frames given subsequent ones. It requires temporal inversion, causal reasoning, and backward consistency of object positions and motion. As shown in Fig. 146 to Fig. 150, the model tends to focus on generating semantically valid but temporally inconsistent scenes. In Fig. 146, the predicted past frame omits critical structural elements like the bridge, revealing flaws in memory-based reconstruction. In Fig. 147, the car’s position does not reflect reverse movement, and in Fig. 148, the hand-action interaction is misaligned with the temporal flow. While Fig. 149 shows some temporal consistency, interactions remain physically implausible. Fig. 150 captures the kicking motion effectively, but inconsistencies in surrounding players highlight the model’s limited understanding of spatial continuity in dynamic group interactions.

Across all tasks, GPT-4o demonstrates a general capability to reconstruct coherent individual frames with high visual fidelity. However, its understanding of temporal consistency, motion dynamics, and causality remains limited. The model often focuses on plausible scene completion rather than faithfully continuing motion or reasoning over time. Failures are especially apparent in sports scenes and scenes involving complex interactions or occlusions, where precise alignment across frames is critical.

Section 8 Future Frame Prediction



Given frame 1 , frame 2 and frame 3 , generate the most plausible future frame (frame 4).
Generate it as a image.



Figure 136: Example of future frame prediction by GPT-4o. Given three input frames showing a gradual camera movement under a bridge, the model attempts to generate the next plausible frame. While the general scene layout is preserved, the predicted frame fails to accurately continue the motion trajectory of the bridge, indicating limited temporal understanding of the scene's main structure.

Section 8 Future Frame Prediction



Given frame 1 , frame 2 and frame 3 , generate the most plausible future frame (frame 4).Generate it as a image

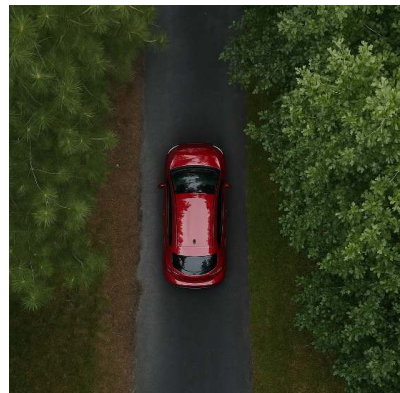


Figure 137: Example of future frame prediction by GPT-4o. Although the model produces a visually plausible image, the predicted frame does not reflect the expected temporal progression of the moving vehicle. Instead, it appears to focus solely on reconstructing a static scene, lacking awareness of motion cues present in the input sequence.

Section 8 Future Frame Prediction



Given frame 1 , frame 2 and frame 3 , generate the most plausible future frame (frame 4).Generate it as a image

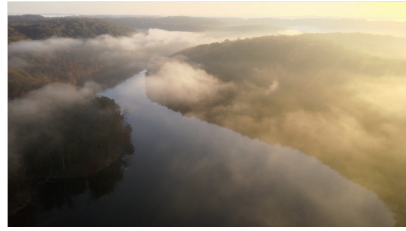
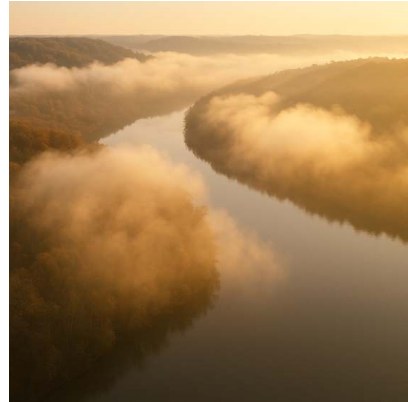


Figure 138: Example of future frame prediction by GPT-4o. While the generated image maintains overall scene appearance and lighting, it fails to accurately capture the motion trajectory of the drifting clouds observed in the input frames. This suggests limited capability in modeling dynamic elements within temporally evolving natural scenes.

Section 8 Future Frame Prediction

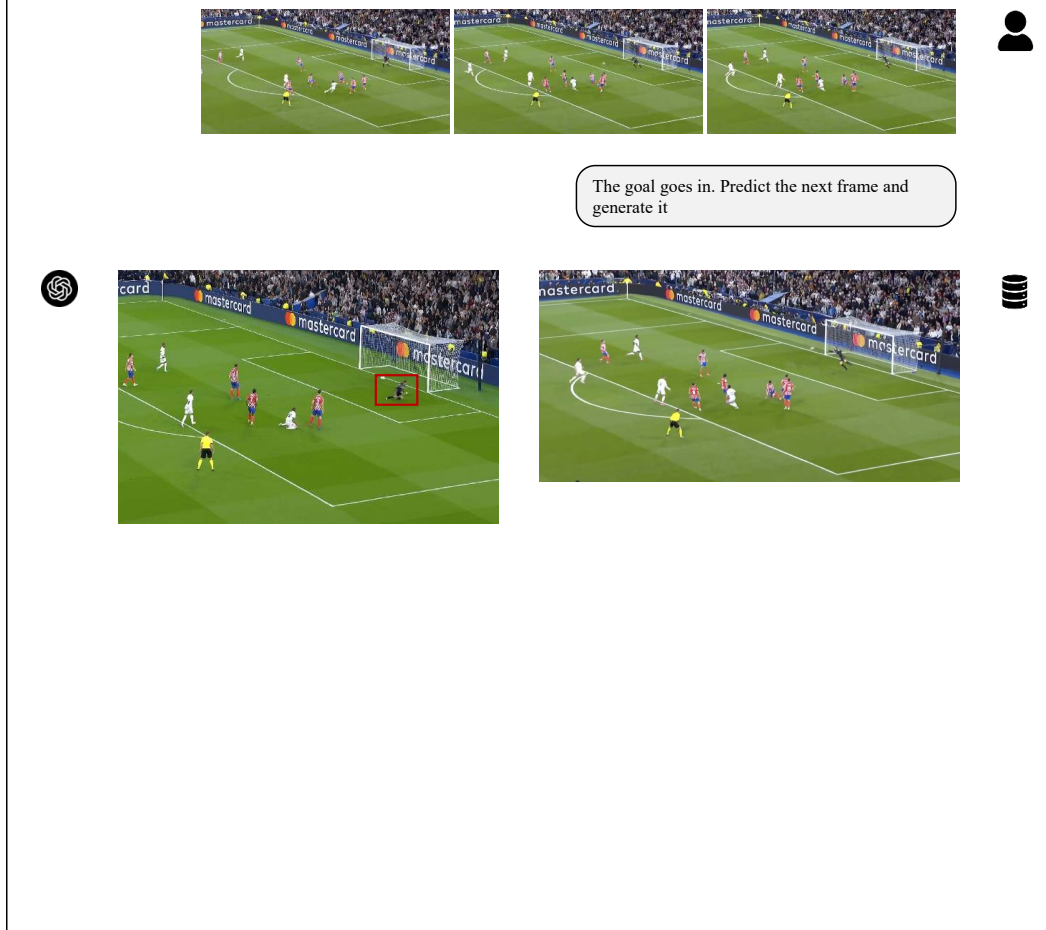


Figure 139: Example of future frame prediction by GPT-4o. Although the overall scene and context of a goal being scored are maintained, the predicted frame fails to capture the dynamic motion of the goalkeeper accurately.

Section 8 Future Frame Prediction



Given the sequence of images (Frame 1, Frame 2, Frame 3), please predict and generate the next frame that maintains temporal continuity, spatial coherence, and consistent lighting. Pay special attention to the movement trends of objects within the scene



Figure 140: Example of future frame prediction by GPT-4o. The generated frame maintains strong spatial coherence and visual quality, accurately reconstructing the scene layout. However, it fails to capture the correct motion trajectory of key elements—such as the player and the ball—indicating limited understanding of action dynamics despite solid scene rendering.

Section 8 Intermediate Frame Prediction

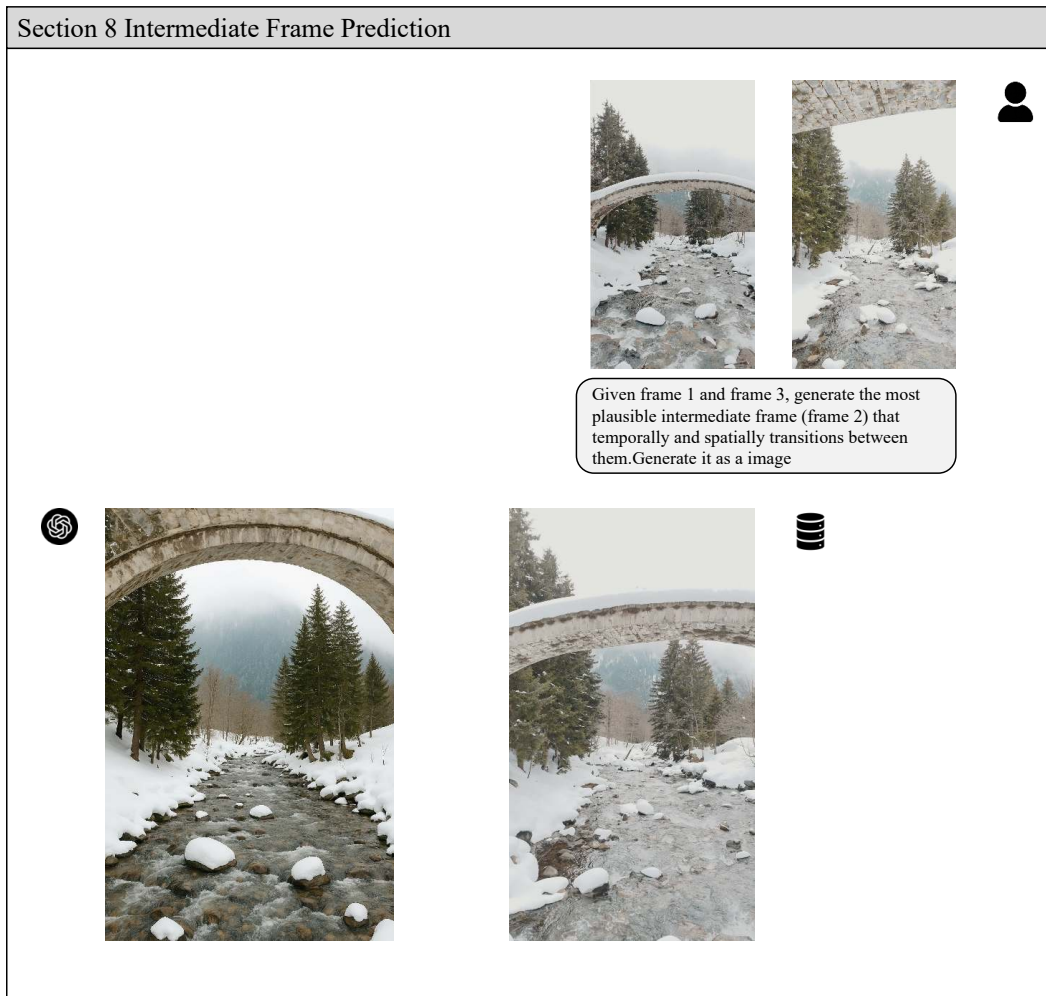


Figure 141: Example of intermediate frame prediction by GPT-4o. Given the first and third frames, the model successfully generates a visually coherent intermediate frame that preserves spatial layout and motion continuity. Aside from slight color tone discrepancies, the reconstruction and temporal prediction are handled effectively.

Section 8 Intermediate Frame Prediction



Given frame 1 , frame 2 and frame 4, generate the most plausible intermediate frame (frame 3) that temporally and spatially transitions between them. Generate it as an image

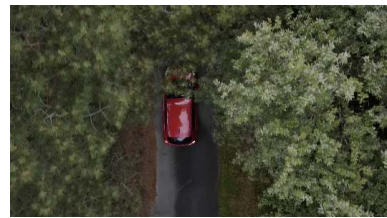
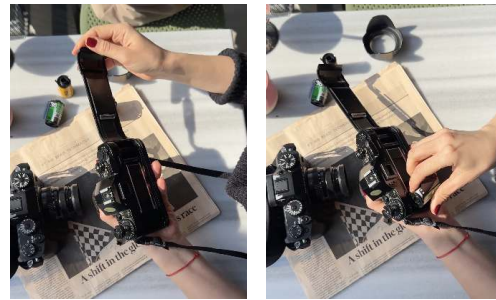


Figure 142: Example of intermediate frame prediction by GPT-4o. The generated frame fails to align with the spatial and temporal patterns observed in the input sequence. In particular, the car's orientation is incorrectly reconstructed, and the overall scene lacks visual coherence, indicating poor understanding of motion continuity and spatial consistency.

Section 8 Intermediate Frame Prediction



Given frame 1 and frame 3, generate the most plausible intermediate frame (frame 2) that temporally and spatially transitions between them. Generate it as an image



Figure 143: Example of intermediate frame prediction by GPT-4o. The generated frame demonstrates accurate spatial understanding and smooth temporal transition, effectively bridging the motion and object positions between the two input frames. Both the hand pose and film placement are well reconstructed, showcasing strong reasoning and visual consistency.

Section 8 Intermediate Frame Prediction

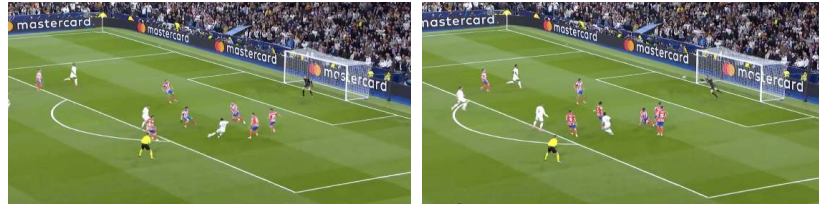


Given frame 1 , frame 2 and frame 4, generate the most plausible intermediate frame (frame 3) that temporally and spatially transitions between them. Generate it as a image



Figure 144: Example of intermediate frame prediction by GPT-4o. The generated frame fails to preserve the spatial and temporal coherence of the input sequence. The positions and interactions between the player, ball, and goalkeeper are inconsistent with the surrounding frames, indicating a breakdown in understanding the underlying motion dynamics and object relationships.

Section 8 Intermediate Frame Prediction



Given frame 1 and frame 3, generate the most plausible intermediate frame (frame 2) that temporally and spatially transitions between them. Generate it as an image



Figure 145: Example of intermediate frame prediction by GPT-4o. The generated frame exhibits major inconsistencies in the spatial arrangement of players and the shooting action. The kicker's pose and position, as well as the placement of surrounding players, deviate significantly from the temporal flow established in the input frames, revealing poor motion understanding and scene continuity.

Section 8 Past Frame Prediction



Given frame 2 and frame 3, generate the most plausible past frame (frame 1). Generate it as a image



Figure 146: Example of past frame prediction by GPT-4o. Although the model attempts to infer a plausible earlier frame from the given sequence, it fails to preserve key structural elements—most notably the bridge, which is entirely missing. This highlights significant limitations in scene reconstruction under backward temporal reasoning.

Section 8 Past Frame Prediction

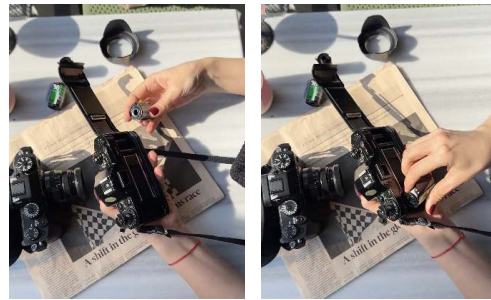


Given frame 2 , frame 3 and frame 4 , generate the most plausible past frame (frame 1).Generate it as a image



Figure 147: Example of past frame prediction by GPT-4o. The generated image appears to prioritize scene reconstruction, producing a visually coherent frame. However, it fails to reflect the expected temporal regression of the car's position, indicating that the model neglects backward motion reasoning in favor of static visual fidelity.

Section 8 Past Frame Prediction



Given frame 1 and frame 3, generate the most plausible intermediate frame (frame 2) that temporally and spatially transitions between them. Generate it as an image



Figure 148: Example of past frame prediction by GPT-4o. Although the generated image visually resembles the surrounding frames, it fails to capture the correct temporal progression of the action—specifically, the interaction between the hand and the film roll. This suggests limited capability in reasoning about the sequence of physical actions over time.

Section 8 Past Frame Prediction



Given frame 1 and frame 3, generate the most plausible intermediate frame (frame 2) that temporally and spatially transitions between them. Generate it as an image



Figure 149: Example of past frame prediction by GPT-4o. The model demonstrates a reasonable understanding of the overall temporal progression in the scene. However, the interaction between the goalkeeper and the goal structure is physically inconsistent, revealing challenges in accurately modeling fine-grained spatial relationships.

Section 8 Past Frame Prediction



Given frame 2 , frame 3 and frame 4 , generate the most plausible past frame (frame 1).Generate it as a image



Figure 150: Example of past frame prediction by GPT-4o. The model successfully captures the temporal dynamics of the ball-kicking action, demonstrating decent motion reasoning. However, the reconstruction of the surrounding players is inaccurate, with noticeable inconsistencies in their positions and postures, revealing challenges in maintaining global scene consistency.

9 Limitations

9.1 GPT-4o is Not Yet a World Model

The ability to imitate and reason about the real world is a foundational requirement for a model to be considered a *world model*. In principle, a world model should be able to understand physical structure, causality, common sense, and the temporal evolution of events, allowing it to reason about how the world behaves under various conditions.

However, our experiments reveal that GPT-4o falls short of reliably generating knowledge-grounded visual content across multiple scientific domains. In physics-related generation (Sec. 5.1), while the model succeeds in many commonsense cases, it fails to capture key physical principles in scenarios involving light refraction and thermodynamics. In chemistry tasks (Sec. 5.2), the model often produces scientifically inaccurate results, such as mislabeled substances, incorrect reaction phenomena, or structurally flawed molecular diagrams. Biology-related tasks (Sec. 5.3) further expose limitations in domain-specific understanding, with frequent errors in microbial coloring, ecosystem modeling, and biomedical segmentation. Similarly, in mathematics (Sec. 5.4), GPT-4o struggles with representing precise spatial and logical relationships, often misplacing annotations or violating geometric constraints. Even in agriculture (Sec. 5.5), where the visual domain is more natural, the model still fails to associate correct visual semantics with textual prompts, generating wrong crop types, incorrect labels, or hallucinated scene details. These findings indicate that despite its strong general vision-language capabilities, GPT-4o lacks the structured scientific grounding and symbolic reasoning needed to serve as a reliable knowledge-driven visual generator.

In spatially-aware generation tasks (Sec. 7), the model fails to consistently preserve structural layouts and spatial constraints. It often disregards reference layouts, misrepresents pose orientations, or alters semantic regions during inpainting or segmentation. These errors imply that GPT-4o does not maintain a coherent internal representation of space, which is essential for reasoning about object positions, geometry, and physical feasibility.

In temporally-aware generation (Sec. 8), GPT-4o shows limited understanding of motion continuity and causality. It struggles to infer plausible future or past frames in dynamic scenes and often produces temporally inconsistent actions or object trajectories. Such behavior highlights the absence of robust temporal modeling mechanisms within the generation process.

Taken together, these observations indicate that GPT-4o, despite its impressive multimodal generation ability, cannot yet be regarded as a world model. It lacks grounded representations of physics, commonsense, and time—key attributes necessary for coherent and causally consistent world understanding. Closing this gap will likely require new inductive biases, structured world knowledge integration, and training objectives beyond pattern learning.

9.2 Limitations in Generation Process Control

Despite its strong generative capabilities, GPT-4o exhibits clear limitations in controlling low-level visual properties, such as image resolution, aspect ratio, and pixel-wise numerical constraints.

As observed in Sec. 2.1 and Sec. 2.2, the model cannot accurately follow user-specified resolutions or aspect ratios. It is restricted to producing images in only three predefined resolutions, making it impossible to generate outputs at arbitrary sizes or layouts. Even when different resolutions are explicitly requested, the model defaults to the closest fixed resolution, which restricts its usability in applications requiring strict layout or scaling control.

Furthermore, as shown in Sec. 2.3, GPT-4o struggles to handle precise numerical conditions. It fails to produce exact RGB values when asked to generate black or grayscale images, and introduces unexpected noise or variability in what should be pixel-accurate segmentation outputs. This behavior indicates that the model optimizes for perceptual plausibility rather than low-level numerical accuracy.

These findings highlight a fundamental limitation: GPT-4o lacks mechanisms for fine-grained control over structural and quantitative properties in image generation. This restricts its effectiveness in scientific, industrial, or graphics applications where pixel-level consistency, spatial accuracy, or numerical fidelity are critical.

9.3 Limitations in Spatial Alignment

One of the critical limitations observed in GPT-4o is its difficulty in handling tasks that require precise spatial alignment between visual inputs and outputs. While the model demonstrates strong semantic understanding and plausible image generation capabilities, it often struggles with faithfully preserving spatial structures, positional constraints, and layout consistency across various tasks.

This limitation becomes evident in tasks such as spatial control (Sec. 3.2.3), low-level synthesis (Sec. 3.3), and segmentation (Sec. 4.2). For example, in layout-to-image generation, the model frequently ignores object positions or produces misaligned placements even when the layout is explicitly defined. In sketch-based and pose-based generation, although the model captures high-level semantics, it often fails to strictly follow spatial cues—such as body orientation or object alignment—resulting in images that are semantically correct but spatially inconsistent.

Similarly, in segmentation tasks, GPT-4o often misinterprets the visual instruction. It may assign inconsistent colors to the same class in semantic segmentation or fail to preserve instance boundaries in instance segmentation. The generated outputs tend to resemble stylized interpretations rather than precise spatial mappings, suggesting that the model prioritizes visual plausibility over pixel-level accuracy.

These findings suggest that GPT-4o lacks strong inductive bias for spatial alignment, which is essential for tasks that require precise spatial grounding. In contrast, many recent vision-language models designed for unified multimodal perception [71, 181, 204], such as those trained with spatially-aligned outputs like segmentation masks or bounding boxes, tend to incorporate architectural components (e.g., spatial token decoders, vision backbones with explicit positional encoding) that enforce spatial consistency. Similarly, models like ControlNet [202] integrate conditional control branches that directly guide the spatial generation process, leading to improved alignment in tasks such as edge-to-image or pose-to-image generation. The general-purpose architecture of GPT-4o, while effective for high-level visual understanding and instruction following, may lack such spatial priors at the structural level. As a result, it may require either significantly more aligned training data, or architectural augmentation (e.g., external control modules or auxiliary spatial heads) to improve its ability to faithfully align outputs with spatial inputs in generation tasks.

9.4 Limitations in Instruction Alignment

Another key limitation observed in GPT-4o is its inconsistent alignment with provided instructions, particularly when simultaneously conditioned on both text and image prompts. While the model demonstrates strong multimodal comprehension in general, it often fails to accurately reflect all details or constraints from the input instructions in the generated outputs.

This misalignment appears across a variety of tasks. For instance, in image editing (Sec. 3.2.1) and personalization (Sec. 3.2.2) scenarios, specific attributes described in the prompt may be ignored or altered (e.g., missing accessories, color mismatches). Similarly, in temporal generation (Sec. 8) and story visualization (Sec. 3.2.5), the model sometimes drops key narrative elements or misrepresents the intended progression. Furthermore, in discriminative tasks (Sec. 4), GPT-4o often fails to follow task-level instructions defined by either task names or natural language prompts. Despite efforts to specify the expected task type, such as “semantic segmentation,” “object detection,” or “pose estimation”, the model frequently produces mismatched outputs or ignores the instruction altogether. This behavior also persists when in-context learning is applied, indicating that the model lacks robust task disambiguation and flexible prompt conditioning (Sec. 4.2).

These inconsistencies suggest that while GPT-4o can interpret rich instructions, it lacks a robust grounding mechanism to ensure strict adherence. This may be due to limited alignment supervision during training or the model’s tendency to prioritize global plausibility over fine-grained control. Improving instruction alignment will likely require more structured data or enhanced training objectives.

10 Conclusion

In this paper, we conducted a comprehensive qualitative evaluation of GPT-4o’s image generation capabilities, covering a wide spectrum of tasks from traditional synthesis to advanced multimodal reasoning. Our evaluation framework is structured around six key dimensions, and we summarize the model’s performance as follows:

- **Overall Characteristics.** As discussed in Sec. 2, GPT-4o exhibits clear limitations in generation process control. It fails to generate images at arbitrary resolutions, cannot flexibly adjust aspect ratios, and struggles to produce numerically accurate visual outputs such as precise RGB values or segmentation masks.
- **Visual Synthesis and Conditional Alignment.** As shown in Sec. 3, GPT-4o performs strongly across a wide range of traditional image generation tasks. It shows solid capabilities in text-conditioned and multimodal-conditioned generation, stylization, and even low-level image processing tasks such as colorization and relighting.
- **Visual Understanding.** In Sec. 4, GPT-4o is evaluated on discriminative tasks with both visual and textual outputs. Although it can align outputs with general task goals, it often relies on global semantics rather than precise reasoning, leading to frequent hallucinations, spatial misalignments, and misunderstanding of task definitions.
- **Knowledge and Commonsense-based Generation.** Sec. 5 and Sec. 6 evaluate the model’s ability to encode domain-specific knowledge and commonsense reasoning. While GPT-4o shows surface-level competence, it frequently fails to follow scientific principles and factual accuracy, particularly in fields such as physics, chemistry, biology, and mathematics. This suggests that the model lacks the foundational grounding to act as a true world model (Sec. 9.1).
- **Spatial Reasoning.** In Sec. 7, the model is tested on spatially-conditioned tasks such as layout-to-image, pose-to-image, and segmentation. Although GPT-4o captures high-level semantics, it struggles to maintain pixel-level spatial alignment. These issues likely stem from a lack of architectural inductive biases for structured spatial reasoning (Sec. 9.3).
- **Temporal Reasoning.** In Sec. 8, the model is evaluated on temporally-aware generation tasks. The results indicate emerging abilities in handling sequence dynamics, but a lack of consistent scene continuity, causality modeling, and temporal memory remains a significant bottleneck.

Despite its remarkable performance in general synthesis and instruction following, GPT-4o still faces key limitations in four major aspects: (1) its inability to model real-world knowledge across scientific domains and temporal processes (Sec. 9.1), (2) its lack of fine-grained generation control (Sec. 9.2), (3) insufficient spatial alignment in structure-aware tasks (Sec. 9.3), and (4) difficulty in strictly following task instructions and prompts (Sec. 9.4). We hope our findings not only provide insights into the current limitations of GPT-4o but also inspire future research directions toward more controllable, grounded, and structured multimodal generation systems.

References

- [1] Abdullah Abuolaim and Michael S Brown. Defocus deblurring using dual-pixel data. In *Computer Vision–ECCV 2020: 16th European Conference, Glasgow, UK, August 23–28, 2020, Proceedings, Part X 16*, pages 111–126. Springer, 2020.
- [2] Abdullah Abuolaim, Mauricio Delbracio, Damien Kelly, Michael S Brown, and Peyman Milanfar. Learning to reduce defocus blur by realistically modeling dual-pixel data. In *Proceedings of the IEEE/CVF International Conference on Computer Vision*, pages 2289–2298, 2021.
- [3] Eirikur Agustsson and Radu Timofte. Ntire 2017 challenge on single image super-resolution: Dataset and study. In *Proceedings of the IEEE conference on computer vision and pattern recognition workshops*, pages 126–135, 2017.
- [4] Hao Ai, Zidong Cao, Haonan Lu, Chen Chen, Jian Ma, Pengyuan Zhou, Tae-Kyun Kim, Pan Hui, and Lin Wang. Dream360: Diverse and immersive outdoor virtual scene creation via transformer-based 360 image outpainting. *IEEE transactions on visualization and computer graphics*, 2024.
- [5] Ali Amanlou, Amir Abolfazl Suratgar, Jafar Tavoosi, Ardashir Mohammadzadeh, and Amir Mosavi. Single-image reflection removal using deep learning: a systematic review. *IEEE Access*, 10:29937–29953, 2022.
- [6] Mykhaylo Andriluka, Leonid Pishchulin, Peter Gehler, and Bernt Schiele. 2d human pose estimation: New benchmark and state of the art analysis. In *Proceedings of the IEEE Conference on computer Vision and Pattern Recognition*, pages 3686–3693, 2014.
- [7] Anju Asokan and JGESI Anitha. Change detection techniques for remote sensing applications: A survey. *Earth Science Informatics*, 12:143–160, 2019.
- [8] Gwangbin Bae and Andrew J Davison. Rethinking inductive biases for surface normal estimation. In *Proceedings of the IEEE/CVF Conference on Computer Vision and Pattern Recognition*, pages 9535–9545, 2024.
- [9] Yogesh Balaji, Seungjun Nah, Xun Huang, Arash Vahdat, Jiaming Song, Karsten Kreis, Miika Aittala, Timo Aila, Samuli Laine, Bryan Catanzaro, et al. ediffi: Text-to-image diffusion models with an ensemble of expert denoisers. *arXiv preprint arXiv:2211.01324*, 2022.
- [10] Zahra Bayramli, Ayhan Suleymanzade, Na Min An, Huzama Ahmad, Eunsu Kim, Junyeong Park, James Thorne, and Alice Oh. Diffusion models through a global lens: Are they culturally inclusive? *arXiv preprint arXiv:2502.08914*, 2025.
- [11] Shariq Farooq Bhat, Ibraheem Alhashim, and Peter Wonka. Adabins: Depth estimation using adaptive bins. In *Proceedings of the IEEE/CVF conference on computer vision and pattern recognition*, pages 4009–4018, 2021.
- [12] Manuel Brack, Felix Friedrich, Katharia Kornmeier, Linoy Tsaban, Patrick Schramowski, Kristian Kersting, and Apolinário Passos. Ledits++: Limitless image editing using text-to-image models. pages 8861–8870, 2024.
- [13] Tim Brooks, Aleksander Holynski, and Alexei A Efros. Instructpix2pix: Learning to follow image editing instructions. In *Proceedings of the IEEE/CVF conference on computer vision and pattern recognition*, pages 18392–18402, 2023.
- [14] Yuanhao Cai, Xiaowan Hu, Haoqian Wang, Yulun Zhang, Hanspeter Pfister, and Donglai Wei. Learning to generate realistic noisy images via pixel-level noise-aware adversarial training. *Advances in Neural Information Processing Systems*, 34:3259–3270, 2021.
- [15] Yufei Cai, Yuxiang Wei, Zhilong Ji, Jinfeng Bai, Hu Han, and Wangmeng Zuo. Decoupled textual embeddings for customized image generation. *arXiv preprint arXiv:2312.11826*, 2023.
- [16] Pu Cao, Feng Zhou, Qing Song, and Lu Yang. Controllable generation with text-to-image diffusion models: A survey. *arXiv preprint arXiv:2403.04279*, 2024.

- [17] Nicolas Carion, Francisco Massa, Gabriel Synnaeve, Nicolas Usunier, Alexander Kirillov, and Sergey Zagoruyko. End-to-end object detection with transformers. In *European conference on computer vision*, pages 213–229. Springer, 2020.
- [18] Eric R Chan, Koki Nagano, Matthew A Chan, Alexander W Bergman, Jeong Joon Park, Axel Levy, Miika Aittala, Shalini De Mello, Tero Karras, and Gordon Wetzstein. Generative novel view synthesis with 3d-aware diffusion models. In *Proceedings of the IEEE/CVF International Conference on Computer Vision*, pages 4217–4229, 2023.
- [19] Boyuan Chen, Zhuo Xu, Sean Kirmani, Brain Ichter, Dorsa Sadigh, Leonidas Guibas, and Fei Xia. Spatialvlm: Endowing vision-language models with spatial reasoning capabilities. In *Proceedings of the IEEE/CVF Conference on Computer Vision and Pattern Recognition*, pages 14455–14465, 2024.
- [20] Dar-Yen Chen, Hamish Tennent, and Ching-Wen Hsu. Artadapter: Text-to-image style transfer using multi-level style encoder and explicit adaptation. *arXiv preprint arXiv:2312.02109*, 2023.
- [21] Hong Chen, Yipeng Zhang, Xin Wang, Xuguang Duan, Yuwei Zhou, and Wenwu Zhu. Disen-booth: Disentangled parameter-efficient tuning for subject-driven text-to-image generation. *arXiv preprint arXiv:2305.03374*, 2023.
- [22] Jingye Chen, Yupan Huang, Tengchao Lv, Lei Cui, Qifeng Chen, and Furu Wei. Textdiffuser-2: Unleashing the power of language models for text rendering. *arXiv preprint arXiv:2311.16465*, 2023.
- [23] Jingye Chen, Yupan Huang, Tengchao Lv, Lei Cui, Qifeng Chen, and Furu Wei. Textdiffuser: Diffusion models as text painters. *arXiv preprint arXiv:2305.10855*, 2023.
- [24] Liang-Chieh Chen, George Papandreou, Iasonas Kokkinos, Kevin Murphy, and Alan L Yuille. Semantic image segmentation with deep convolutional nets and fully connected crfs. *arXiv preprint arXiv:1412.7062*, 2014.
- [25] Sixiang Chen, Jinbin Bai, Zhuoran Zhao, Tian Ye, Qingyu Shi, Donghao Zhou, Wenhao Chai, Xin Lin, Jianzong Wu, Chao Tang, et al. An empirical study of gpt-4o image generation capabilities. *arXiv preprint arXiv:2504.05979*, 2025.
- [26] Siyu Chen, Dengjie Li, Zenghao Bao, Yao Zhou, Lingfeng Tan, Yujie Zhong, and Zheng Zhao. Manga generation via layout-controllable diffusion. In *arXiv preprint arXiv:2412.19303*, 2024.
- [27] Wei-Ting Chen, Hao-Yu Fang, Cheng-Lin Hsieh, Cheng-Che Tsai, I Chen, Jian-Jiun Ding, Sy-Yen Kuo, et al. All snow removed: Single image desnowing algorithm using hierarchical dual-tree complex wavelet representation and contradict channel loss. In *Proceedings of the IEEE/CVF international conference on computer vision*, pages 4196–4205, 2021.
- [28] Zhuowei Chen, Shancheng Fang, Wei Liu, Qian He, Mengqi Huang, Yongdong Zhang, and Zhendong Mao. Dreamidentity: Improved editability for efficient face-identity preserved image generation. *arXiv preprint arXiv:2307.00300*, 2023.
- [29] An-Chieh Cheng, Hongxu Yin, Yang Fu, Qiushan Guo, Ruihan Yang, Jan Kautz, Xiaolong Wang, and Sifei Liu. Spatialrgpt: Grounded spatial reasoning in vision language models. *arXiv preprint arXiv:2406.01584*, 2024.
- [30] Bodong Cheng, Juncheng Li, Ying Chen, and Tieyong Zeng. Snow mask guided adaptive residual network for image snow removal. *Computer Vision and Image Understanding*, 236:103819, 2023.
- [31] Bowen Cheng, Ishan Misra, Alexander G Schwing, Alexander Kirillov, and Rohit Girdhar. Masked-attention mask transformer for universal image segmentation. In *Proceedings of the IEEE/CVF conference on computer vision and pattern recognition*, pages 1290–1299, 2022.
- [32] Bowen Cheng, Alex Schwing, and Alexander Kirillov. Per-pixel classification is not all you need for semantic segmentation. *Advances in neural information processing systems*, 34:17864–17875, 2021.

- [33] Hisham Cholakkal, Guolei Sun, Fahad Shahbaz Khan, and Ling Shao. Object counting and instance segmentation with image-level supervision. In *Proceedings of the IEEE/CVF Conference on Computer Vision and Pattern Recognition*, pages 12397–12405, 2019.
- [34] Mikolaj Cieslak, Umabharathi Govindarajan, Alejandro Garcia, Anuradha Chandrashekhar, Torsten Hadrich, Aleksander Mendoza-Drosik, Dominik L Michels, Soren Pirk, Chia-Chun Fu, and Wojciech Palubicki. Generating diverse agricultural data for vision-based farming applications. In *Proceedings of the IEEE/CVF Conference on Computer Vision and Pattern Recognition*, pages 5422–5431, 2024.
- [35] Marius Cordts, Mohamed Omran, Sebastian Ramos, Timo Rehfeld, Markus Enzweiler, Rodrigo Benenson, Uwe Franke, Stefan Roth, and Bernt Schiele. The cityscapes dataset for semantic urban scene understanding. In *Proc. of the IEEE Conference on Computer Vision and Pattern Recognition (CVPR)*, 2016.
- [36] Ciprian Corneanu, Raghudeep Gadde, and Aleix M Martinez. Latentpaint: Image inpainting in latent space with diffusion models. pages 4334–4343, 2024.
- [37] Qi Dang, Jianqin Yin, Bin Wang, and Wenqing Zheng. Deep learning based 2d human pose estimation: A survey. *Tsinghua Science and Technology*, 24(6):663–676, 2019.
- [38] Kangle Deng, Gengshan Yang, Deva Ramanan, and Jun-Yan Zhu. 3d-aware conditional image synthesis. In *Proceedings of the IEEE/CVF Conference on Computer Vision and Pattern Recognition*, pages 4434–4445, 2023.
- [39] Minglong Dong, Dongliang Zhou, Jianghong Ma, and Haijun Zhang. Towards intelligent design: A self-driven framework for collocated clothing synthesis leveraging fashion styles and textures. In *ICASSP 2024-2024 IEEE International Conference on Acoustics, Speech and Signal Processing (ICASSP)*, pages 3725–3729. IEEE, 2024.
- [40] Ziyi Dong, Pengxu Wei, and Liang Lin. Dreamartist: Towards controllable one-shot text-to-image generation via contrastive prompt-tuning. *arXiv preprint arXiv:2211.11337*, 2022.
- [41] Mohannad Elhamod, Mridul Khurana, Harish Babu Manogaran, Josef C Uyeda, Meghan A Balk, Wasila Dahdul, Yasin Bakis, Henry L Bart Jr, Paula M Mabee, Hilmar Lapp, et al. Discovering novel biological traits from images using phylogeny-guided neural networks. In *Proceedings of the 29th ACM SIGKDD Conference on Knowledge Discovery and Data Mining*, pages 3966–3978, 2023.
- [42] M. Everingham, L. Van Gool, C. K. I. Williams, J. Winn, and A. Zisserman. The PASCAL Visual Object Classes Challenge 2007 (VOC2007) Results. <http://www.pascal-network.org/challenges/VOC/voc2007/workshop/index.html>.
- [43] M. Everingham, L. Van Gool, C. K. I. Williams, J. Winn, and A. Zisserman. The PASCAL Visual Object Classes Challenge 2012 (VOC2012) Results. <http://www.pascal-network.org/challenges/VOC/voc2012/workshop/index.html>.
- [44] Tsu-Jui Fu, Wenze Hu, Xianzhi Du, William Yang Wang, Yinfei Yang, and Zhe Gan. Guiding instruction-based image editing via multimodal large language models. *arXiv preprint arXiv:2309.17102*, 2023.
- [45] Rinon Gal, Yuval Alaluf, Yuval Atzmon, Or Patashnik, Amit H Bermano, Gal Chechik, and Daniel Cohen-Or. An image is worth one word: Personalizing text-to-image generation using textual inversion. *arXiv preprint arXiv:2208.01618*, 2022.
- [46] Amirhosein Ghasemabadi, Muhammad Kamran Janjua, Mohammad Salameh, Chunhua Zhou, Fengyu Sun, and Di Niu. Cascadedgaze: Efficiency in global context extraction for image restoration. *arXiv preprint arXiv:2401.15235*, 2024.
- [47] Ross Girshick. Fast r-cnn. In *Proceedings of the IEEE international conference on computer vision*, pages 1440–1448, 2015.

- [48] Ross Girshick, Jeff Donahue, Trevor Darrell, and Jitendra Malik. Rich feature hierarchies for accurate object detection and semantic segmentation. In *Proceedings of the IEEE conference on computer vision and pattern recognition*, pages 580–587, 2014.
- [49] Yuan Gong, Youxin Pang, Xiaodong Cun, Menghan Xia, Yingqing He, Haoxin Chen, Longyue Wang, Yong Zhang, Xintao Wang, Ying Shan, and Yujiu Yang. Talecrafter: Interactive story visualization with multiple characters, 2023.
- [50] Jiatao Gu, Yuyang Wang, Yizhe Zhang, Qihang Zhang, Dinghuai Zhang, Navdeep Jaitly, Josh Susskind, and Shuangfei Zhai. Dart: Denoising autoregressive transformer for scalable text-to-image generation. *arXiv preprint arXiv:2410.08159*, 2024.
- [51] Cusuh Ham, James Hays, Jingwan Lu, Krishna Kumar Singh, Zhifei Zhang, and Tobias Hinz. Modulating pretrained diffusion models for multimodal image synthesis. *arXiv preprint arXiv:2302.12764*, 2023.
- [52] Jian Han, Jinlai Liu, Yi Jiang, Bin Yan, Yuqi Zhang, Zehuan Yuan, Bingyue Peng, and Xiaobing Liu. Infinity: Scaling bitwise autoregressive modeling for high-resolution image synthesis. *arXiv preprint arXiv:2412.04431*, 2024.
- [53] Xintong Han, Ying Jin, Jing Zhang, Qiulei Dong, and Larry S. Davis. Viton-hd: High-resolution virtual try-on via misalignment-aware normalization. In *Proceedings of the IEEE/CVF Conference on Computer Vision and Pattern Recognition (CVPR)*, pages 14131–14140, 2021.
- [54] Xintong Han, Zuxuan Wu, Zhe Wu, Ruichi Yu, and Larry S. Davis. Viton: An image-based virtual try-on network. In *Proceedings of the IEEE Conference on Computer Vision and Pattern Recognition (CVPR)*, pages 7543–7552, 2018.
- [55] Huiguo He, Huan Yang, Zixi Tuo, Yuan Zhou, Qiuyue Wang, Yuhang Zhang, Zeyu Liu, Wenhao Huang, Hongyang Chao, and Jian Yin. Dreamstory: Open-domain story visualization by llm-guided multi-subject consistent diffusion, 2025.
- [56] Jiawei He, Yunchao Wei, and Yi Yang. Styleposegan: Pose-consistent virtual try-on via pose-guided style transfer. *IEEE Transactions on Pattern Analysis and Machine Intelligence (TPAMI)*, 44(11):8110–8124, 2022.
- [57] Kai He, Kaixin Yao, Qixuan Zhang, Jingyi Yu, Lingjie Liu, and Lan Xu. Dresscode: Autoregressively sewing and generating garments from text guidance. *ACM Transactions on Graphics (TOG)*, 43(4):1–13, 2024.
- [58] Andrew Heschl, Mauricio Murillo, Keyhan Najafian, and Farhad Maleki. Synthset: Generative diffusion model for semantic segmentation in precision agriculture. *arXiv preprint arXiv:2411.03505*, 2024.
- [59] Minghui Hu, Jianbin Zheng, Daqing Liu, Chuanxia Zheng, Chaoyue Wang, Dacheng Tao, and Tat-Jen Cham. Cocktail: Mixing multi-modality controls for text-conditional image generation. *arXiv preprint arXiv:2306.00964*, 2023.
- [60] Lianghua Huang, Di Chen, Yu Liu, Yujun Shen, Deli Zhao, and Jingren Zhou. Composer: Creative and controllable image synthesis with composable conditions. *arXiv preprint arXiv:2302.09778*, 2023.
- [61] Siteng Huang, Biao Gong, Yutong Feng, Xi Chen, Yuqian Fu, Yu Liu, and Donglin Wang. Learning disentangled identifiers for action-customized text-to-image generation. *arXiv preprint arXiv:2311.15841*, 2023.
- [62] Zihan Huang, Tao Wu, Wang Lin, Shengyu Zhang, Jingyuan Chen, and Fei Wu. Autoge: Automating geometric image dataset creation for enhanced geometry understanding. *arXiv preprint arXiv:2409.09039*, 2024.
- [63] Ziqi Huang, Tianxing Wu, Yuming Jiang, Kelvin CK Chan, and Ziwei Liu. Reversion: Diffusion-based relation inversion from images. *arXiv preprint arXiv:2303.13495*, 2023.

- [64] Tak-Wai Hui, Xiaoou Tang, and Chen Change Loy. Liteflownet: A lightweight convolutional neural network for optical flow estimation. In *Proceedings of the IEEE conference on computer vision and pattern recognition*, pages 8981–8989, 2018.
- [65] Nils Hütten, Richard Meyes, and Tobias Meisen. Vision transformer in industrial visual inspection. *Applied Sciences*, 12(23):11981, 2022.
- [66] Eddy Ilg, Nikolaus Mayer, Tonmoy Saikia, Margret Keuper, Alexey Dosovitskiy, and Thomas Brox. Flownet 2.0: Evolution of optical flow estimation with deep networks. In *Proceedings of the IEEE conference on computer vision and pattern recognition*, pages 2462–2470, 2017.
- [67] Da-Wei Jaw, Shih-Chia Huang, and Sy-Yen Kuo. Desnowgan: An efficient single image snow removal framework using cross-resolution lateral connection and gans. *IEEE Transactions on Circuits and Systems for Video Technology*, 31(4):1342–1350, 2020.
- [68] John R Jensen and Jungho Im. Remote sensing change detection in urban environments. *Geo-spatial Technologies in Urban Environments: Policy, Practice, and Pixels*, pages 7–31, 2007.
- [69] Suchae Jeong, Inseong Choi, Youngsik Yun, and Jihie Kim. Culture-trip: Culturally-aware text-to-image generation with iterative prompt refinement. *arXiv preprint arXiv:2502.16902*, 2025.
- [70] Chengyou Jia, Minnan Luo, Zhuohang Dang, Guang Dai, Xiaojun Chang, Mengmeng Wang, and Jingdong Wang. Ssmg: Spatial-semantic map guided diffusion model for free-form layout-to-image generation. *arXiv preprint arXiv:2308.10156*, 2023.
- [71] Yang Jiao, Shaoxiang Chen, Zequn Jie, Jingjing Chen, Lin Ma, and Yu-Gang Jiang. Lumen: Unleashing versatile vision-centric capabilities of large multimodal models. *arXiv preprint arXiv:2403.07304*, 2024.
- [72] Nithish Kannen, Arif Ahmad, Marco Andreetto, Vinodkumar Prabhakaran, Utsav Prabhu, Adji Bousso Dieng, Pushpak Bhattacharyya, and Shachi Dave. Beyond aesthetics: Cultural competence in text-to-image models. *arXiv preprint arXiv:2407.06863*, 2024.
- [73] Bernhard Kerbl, Georgios Kopanas, Thomas Leimkühler, and George Drettakis. 3d gaussian splatting for real-time radiance field rendering. *ACM Trans. Graph.*, 42(4):139–1, 2023.
- [74] Sungnyun Kim, Junsoo Lee, Kibeam Hong, Daesik Kim, and Namhyuk Ahn. Diff-blender: Scalable and composable multimodal text-to-image diffusion models. *arXiv preprint arXiv:2305.15194*, 2023.
- [75] Nikos Kolotouros, Georgios Pavlakos, Dinesh Jayaraman, and Kostas Daniilidis. Probabilistic modeling for human mesh recovery. In *Proceedings of the IEEE/CVF international conference on computer vision*, pages 11605–11614, 2021.
- [76] Hyuk-Ju Kwon and Sung-Hak Lee. Raindrop-removal image translation using target-mask network with attention module. *Mathematics*, 11(15):3318, 2023.
- [77] Ajda Lampe, Julija Stopar, Deepak K Jain, Shinichiro Omachi, Peter Peer, and Vitomir Štruc. Dicti: Diffusion-based clothing designer via text-guided input. In *2024 IEEE 18th International Conference on Automatic Face and Gesture Recognition (FG)*, pages 1–9. IEEE, 2024.
- [78] Hieu Le and Dimitris Samaras. Physics-based shadow image decomposition for shadow removal. *IEEE Transactions on Pattern Analysis and Machine Intelligence*, 44(12):9088–9101, 2021.
- [79] Jaewook Lee, Jeongah Lee, Wanyong Feng, and Andrew Lan. From text to visuals: Using llms to generate math diagrams with vector graphics. *arXiv preprint arXiv:2503.07429*, 2025.
- [80] Chongyi Li, Chunle Guo, Wenqi Ren, Runmin Cong, Junhui Hou, Sam Kwong, and Dacheng Tao. An underwater image enhancement benchmark dataset and beyond. *IEEE transactions on image processing*, 29:4376–4389, 2019.

- [81] Haoying Li, Ziran Zhang, Tingting Jiang, Peng Luo, Huajun Feng, and Zhihai Xu. Real-world deep local motion deblurring. In *proceedings of the AAAI conference on artificial intelligence*, volume 37, pages 1314–1322, 2023.
- [82] Peiyu Li, Xiaobao Huang, Yijun Tian, and Nitesh V Chawla. Cheffusion: Multimodal foundation model integrating recipe and food image generation. In *Proceedings of the 33rd ACM International Conference on Information and Knowledge Management*, pages 3872–3876, 2024.
- [83] Xiaochuan Li, Baoyu Fan, Runze Zhang, Liang Jin, Di Wang, Zhenhua Guo, Yaqian Zhao, and Rengang Li. Image content generation with causal reasoning. In *Proceedings of the AAAI Conference on Artificial Intelligence*, volume 38, pages 13646–13654, 2024.
- [84] Yu Li and Michael S Brown. Exploiting reflection change for automatic reflection removal. In *Proceedings of the IEEE international conference on computer vision*, pages 2432–2439, 2013.
- [85] Yuheng Li, Haotian Liu, Yangming Wen, and Yong Jae Lee. Generate anything anywhere in any scene. *arXiv preprint arXiv:2306.17154*, 2023.
- [86] Yuheng Li, Haotian Liu, Qingyang Wu, Fangzhou Mu, Jianwei Yang, Jianfeng Gao, Chunyuan Li, and Yong Jae Lee. Gligen: Open-set grounded text-to-image generation. In *Proceedings of the IEEE/CVF Conference on Computer Vision and Pattern Recognition*, pages 22511–22521, 2023.
- [87] Jingyun Liang, Jiezheng Cao, Guolei Sun, Kai Zhang, Luc Van Gool, and Radu Timofte. Swinir: Image restoration using swin transformer. In *Proceedings of the IEEE/CVF international conference on computer vision*, pages 1833–1844, 2021.
- [88] Hui Lin, Xiaopeng Hong, and Yabin Wang. Object counting: You only need to look at one. *arXiv preprint arXiv:2112.05993*, 2021.
- [89] Jiajing Lin, Zhenzhong Wang, Shu Jiang, Yongjie Hou, and Min Jiang. Phys4dgen: A physics-driven framework for controllable and efficient 4d content generation from a single image. *arXiv preprint arXiv:2411.16800*, 2024.
- [90] Tsung-Yi Lin, Michael Maire, Serge Belongie, James Hays, Pietro Perona, Deva Ramanan, Piotr Dollár, and C Lawrence Zitnick. Microsoft coco: Common objects in context. In *Computer vision–ECCV 2014: 13th European conference, zurich, Switzerland, September 6-12, 2014, proceedings, part v 13*, pages 740–755. Springer, 2014.
- [91] Bingshuai Liu, Longyue Wang, Chenyang Lyu, Yong Zhang, Jinsong Su, Shuming Shi, and Zhaopeng Tu. On the cultural gap in text-to-image generation. In *ECAI 2024*, pages 930–937. IOS Press, 2024.
- [92] Daochang Liu, Junyu Zhang, Anh-Dung Dinh, Eunbyung Park, Shichao Zhang, and Chang Xu. Generative physical ai in vision: A survey. *arXiv preprint arXiv:2501.10928*, 2025.
- [93] Gongye Liu, Menghan Xia, Yong Zhang, Haoxin Chen, Jinbo Xing, Xintao Wang, Yujiu Yang, and Ying Shan. Stylecrafter: Enhancing stylized text-to-video generation with style adapter. *arXiv preprint arXiv:2312.00330*, 2023.
- [94] Haipeng Liu, Yang Wang, Biao Qian, Meng Wang, and Yong Rui. Structure matters: Tackling the semantic discrepancy in diffusion models for image inpainting. pages 8038–8047, 2024.
- [95] Minghua Liu, Chao Xu, Haian Jin, Linghao Chen, Mukund Varma T, Zexiang Xu, and Hao Su. One-2-3-45: Any single image to 3d mesh in 45 seconds without per-shape optimization. *Advances in Neural Information Processing Systems*, 36:22226–22246, 2023.
- [96] Pengfei Liu, Yiming Ren, Jun Tao, and Zhixiang Ren. Git-mol: A multi-modal large language model for molecular science with graph, image, and text. *Computers in biology and medicine*, 171:108073, 2024.

- [97] Rosanne Liu, Dan Garrette, Chitwan Saharia, William Chan, Adam Roberts, Sharan Narang, Irina Blok, RJ Mical, Mohammad Norouzi, and Noah Constant. Character-aware models improve visual text rendering. *arXiv preprint arXiv:2212.10562*, 2022.
- [98] Ruoshi Liu, Rundi Wu, Basile Van Hoorick, Pavel Tokmakov, Sergey Zakharov, and Carl Vondrick. Zero-1-to-3: Zero-shot one image to 3d object. In *Proceedings of the IEEE/CVF international conference on computer vision*, pages 9298–9309, 2023.
- [99] Shaowei Liu, Zhongzheng Ren, Saurabh Gupta, and Shenlong Wang. Physgen: Rigid-body physics-grounded image-to-video generation. In *European Conference on Computer Vision*, pages 360–378. Springer, 2024.
- [100] Wei Liu, Dragomir Anguelov, Dumitru Erhan, Christian Szegedy, Scott Reed, Cheng-Yang Fu, and Alexander C Berg. Ssd: Single shot multibox detector. In *Computer Vision–ECCV 2016: 14th European Conference, Amsterdam, The Netherlands, October 11–14, 2016, Proceedings, Part I* 14, pages 21–37. Springer, 2016.
- [101] Ye Liu, Lei Zhu, Shunda Pei, Huazhu Fu, Jing Qin, Qing Zhang, Liang Wan, and Wei Feng. From synthetic to real: Image dehazing collaborating with unlabeled real data. In *Proceedings of the 29th ACM international conference on multimedia*, pages 50–58, 2021.
- [102] Yibo Liu, Amaldev Haridevan, Hunter Schofield, and Jinjun Shan. Application of ghost-deblurgan to fiducial marker detection. In *2022 IEEE/RSJ International Conference on Intelligent Robots and Systems (IROS)*, pages 6827–6832. IEEE, 2022.
- [103] Zhiheng Liu, Ruili Feng, Kai Zhu, Yifei Zhang, Kecheng Zheng, Yu Liu, Deli Zhao, Jingren Zhou, and Yang Cao. Cones: Concept neurons in diffusion models for customized generation. *arXiv preprint arXiv:2303.05125*, 2023.
- [104] Yuanhuiyi Lyu, Xu Zheng, and Lin Wang. Image anything: Towards reasoning-coherent and training-free multi-modal image generation. *arXiv preprint arXiv:2401.17664*, 2024.
- [105] Jian Ma, Mingjun Zhao, Chen Chen, Ruichen Wang, Di Niu, Haonan Lu, and Xiaodong Lin. Glyphdraw: Learning to draw chinese characters in image synthesis models coherently. *arXiv preprint arXiv:2303.17870*, 2023.
- [106] Razvan V Marinescu, Daniel Moyer, and Polina Golland. Bayesian image reconstruction using deep generative models. *arXiv preprint arXiv:2012.04567*, 2020.
- [107] David Martin, Charless Fowlkes, Doron Tal, and Jitendra Malik. A database of human segmented natural images and its application to evaluating segmentation algorithms and measuring ecological statistics. In *Proceedings eighth IEEE international conference on computer vision. ICCV 2001*, volume 2, pages 416–423. IEEE, 2001.
- [108] Fanqing Meng, Wenqi Shao, Lixin Luo, Yahong Wang, Yiran Chen, Quanfeng Lu, Yue Yang, Tianshuo Yang, Kaipeng Zhang, Yu Qiao, et al. Phybench: A physical commonsense benchmark for evaluating text-to-image models. *arXiv preprint arXiv:2406.11802*, 2024.
- [109] Alican Mertan, Damien Jade Duff, and Gozde Unal. Single image depth estimation: An overview. *Digital Signal Processing*, 123:103441, 2022.
- [110] Ben Mildenhall, Pratul P Srinivasan, Matthew Tancik, Jonathan T Barron, Ravi Ramamoorthi, and Ren Ng. Nerf: Representing scenes as neural radiance fields for view synthesis. *Communications of the ACM*, 65(1):99–106, 2021.
- [111] Sourav Modak and Anthony Stein. Enhancing weed detection performance by means of genai-based image augmentation. *arXiv preprint arXiv:2411.18513*, 2024.
- [112] Sourav Modak and Anthony Stein. Generative ai-based pipeline architecture for increasing training efficiency in intelligent weed control systems. *arXiv preprint arXiv:2411.00548*, 2024.
- [113] Saman Motamed, Danda Pani Paudel, and Luc Van Gool. Lego: Learning to disentangle and invert concepts beyond object appearance in text-to-image diffusion models. *arXiv preprint arXiv:2311.13833*, 2023.

- [114] Chong Mou, Xintao Wang, Liangbin Xie, Jian Zhang, Zhongang Qi, Ying Shan, and Xiaohu Qie. T2i-adapter: Learning adapters to dig out more controllable ability for text-to-image diffusion models. *arXiv preprint arXiv:2302.08453*, 2023.
- [115] Seungjun Nah, Tae Hyun Kim, and Kyoung Mu Lee. Deep multi-scale convolutional neural network for dynamic scene deblurring. In *Proceedings of the IEEE conference on computer vision and pattern recognition*, pages 3883–3891, 2017.
- [116] Kamyar Nazeri, Eric Ng, and Mehran Ebrahimi. Image colorization using generative adversarial networks. In *Articulated Motion and Deformable Objects: 10th International Conference, AMDO 2018, Palma de Mallorca, Spain, July 12-13, 2018, Proceedings 10*, pages 85–94. Springer, 2018.
- [117] Alexander Nichol, Prafulla Dhariwal, Aditya Ramesh, Pranav Shyam, Pamela Mishkin, Bob McGrew, Ilya Sutskever, and Mark Chen. Glide: Towards photorealistic image generation and editing with text-guided diffusion models. *arXiv preprint arXiv:2112.10741*, 2021.
- [118] Daniel Onoro-Rubio and Roberto J López-Sastre. Towards perspective-free object counting with deep learning. In *European conference on computer vision*, pages 615–629. Springer, 2016.
- [119] Georgios Pavlakos, Jitendra Malik, and Angjoo Kanazawa. Human mesh recovery from multiple shots. In *Proceedings of the IEEE/CVF Conference on Computer Vision and Pattern Recognition*, pages 1485–1495, 2022.
- [120] Lorenzo Pisanello, Riccardo Spezialetti, Barbara Bruno, and Fulvio Mastrogiovanni. Dress code: High-resolution multi-modal fashion image translation. In *Proceedings of the IEEE/CVF Conference on Computer Vision and Pattern Recognition (CVPR)*, pages 12243–12252, 2020.
- [121] Dustin Podell, Zion English, Kyle Lacey, Andreas Blattmann, Tim Dockhorn, Jonas Müller, Joe Penna, and Robin Rombach. Sdxl: Improving latent diffusion models for high-resolution image synthesis. *arXiv preprint arXiv:2307.01952*, 2023.
- [122] Rida Qadri, Piotr Mirowski, Aroussiaak Gabriellan, Farbod Mehr, Huma Gupta, Pamela Karimi, and Remi Denton. Dialogue with the machine and dialogue with the art world: Evaluating generative ai for culturally-situated creativity. *arXiv preprint arXiv:2412.14077*, 2024.
- [123] Xiaojian Qi, Renjie Liao, Zhengzhe Liu, Raquel Urtasun, and Jiaya Jia. Geonet: Geometric neural network for joint depth and surface normal estimation. In *Proceedings of the IEEE Conference on Computer Vision and Pattern Recognition*, pages 283–291, 2018.
- [124] Rui Qian, Robby T Tan, Wenhan Yang, Jiajun Su, and Jiaying Liu. Attentive generative adversarial network for raindrop removal from a single image. In *Proceedings of the IEEE conference on computer vision and pattern recognition*, pages 2482–2491, 2018.
- [125] Yujie Qian, Jiang Guo, Zhengkai Tu, Zhenning Li, Connor W Coley, and Regina Barzilay. Molscribe: robust molecular structure recognition with image-to-graph generation. *Journal of Chemical Information and Modeling*, 63(7):1925–1934, 2023.
- [126] Can Qin, Shu Zhang, Ning Yu, Yihao Feng, Xinyi Yang, Yingbo Zhou, Huan Wang, Juan Carlos Niebles, Caiming Xiong, Silvio Savarese, et al. Unicontrol: A unified diffusion model for controllable visual generation in the wild. *arXiv preprint arXiv:2305.11147*, 2023.
- [127] Xu Qin and Zhilin Wang. Nasnet: A neuron attention stage-by-stage net for single image deraining. *arXiv preprint arXiv:1912.03151*, 2019.
- [128] Xu Qin, Zhilin Wang, Yuanchao Bai, Xiaodong Xie, and Huizhu Jia. Ffa-net: Feature fusion attention network for single image dehazing. In *Proceedings of the AAAI conference on artificial intelligence*, volume 34, pages 11908–11915, 2020.
- [129] Liangqiong Qu, Jiandong Tian, Shengfeng He, Yandong Tang, and Rynson WH Lau. Deshadownet: A multi-context embedding deep network for shadow removal. In *Proceedings of the IEEE conference on computer vision and pattern recognition*, pages 4067–4075, 2017.

- [130] Ruijie Quan, Xin Yu, Yuanzhi Liang, and Yi Yang. Removing raindrops and rain streaks in one go. In *Proceedings of the IEEE/CVF conference on computer vision and pattern recognition*, pages 9147–9156, 2021.
- [131] Yuhui Quan, Zicong Wu, and Hui Ji. Gaussian kernel mixture network for single image defocus deblurring. *Advances in Neural Information Processing Systems*, 34:20812–20824, 2021.
- [132] Yuhui Quan, Zicong Wu, Ruotao Xu, and Hui Ji. Deep single image defocus deblurring via gaussian kernel mixture learning. *IEEE Transactions on Pattern Analysis and Machine Intelligence*, 2024.
- [133] Aditya Ramesh, Prafulla Dhariwal, Alex Nichol, Casey Chu, and Mark Chen. Hierarchical text-conditional image generation with clip latents. *arXiv preprint arXiv:2204.06125*, 2022.
- [134] Anurag Ranjan and Michael J Black. Optical flow estimation using a spatial pyramid network. In *Proceedings of the IEEE conference on computer vision and pattern recognition*, pages 4161–4170, 2017.
- [135] Smitha Raveendran, Mukesh D Patil, and Gajanan K Birajdar. Underwater image enhancement: a comprehensive review, recent trends, challenges and applications. *Artificial Intelligence Review*, 54:5413–5467, 2021.
- [136] Anton Razhigaev, Arseniy Shakhmatov, Anastasia Maltseva, Vladimir Arkhipkin, Igor Pavlov, Ilya Ryabov, Angelina Kuts, Alexander Panchenko, Andrey Kuznetsov, and Denis Dimitrov. Kandinsky: an improved text-to-image synthesis with image prior and latent diffusion. *arXiv preprint arXiv:2310.03502*, 2023.
- [137] Shaoqing Ren, Kaiming He, Ross Girshick, and Jian Sun. Faster r-cnn: Towards real-time object detection with region proposal networks. *Advances in neural information processing systems*, 28, 2015.
- [138] Jaesung Rim, Haeyun Lee, Jucheol Won, and Sunghyun Cho. Real-world blur dataset for learning and benchmarking deblurring algorithms. In *Computer vision–ECCV 2020: 16th European conference, glasgow, UK, August 23–28, 2020, proceedings, part XXV 16*, pages 184–201. Springer, 2020.
- [139] Robin Rombach, Andreas Blattmann, Dominik Lorenz, Patrick Esser, and Björn Ommer. High-resolution image synthesis with latent diffusion models. In *Proceedings of the IEEE/CVF conference on computer vision and pattern recognition*, pages 10684–10695, 2022.
- [140] Olaf Ronneberger, Philipp Fischer, and Thomas Brox. U-net: Convolutional networks for biomedical image segmentation. In *Medical image computing and computer-assisted intervention–MICCAI 2015: 18th international conference, Munich, Germany, October 5–9, 2015, proceedings, part III 18*, pages 234–241. Springer, 2015.
- [141] Nishith Ranjon Roy. *GAN with skip patch discriminator for biological electron microscopy image generation*. University of Arkansas, 2024.
- [142] Tao Ruan, Ting Liu, Zilong Huang, Yunchao Wei, Shikui Wei, and Yao Zhao. Devil in the details: Towards accurate single and multiple human parsing. In *Proceedings of the AAAI conference on artificial intelligence*, volume 33, pages 4814–4821, 2019.
- [143] Nataniel Ruiz, Yuanzhen Li, Varun Jampani, Yael Pritch, Michael Rubinstein, and Kfir Aberman. Dreambooth: Fine tuning text-to-image diffusion models for subject-driven generation. In *Proceedings of the IEEE/CVF Conference on Computer Vision and Pattern Recognition*, pages 22500–22510, 2023.
- [144] Chitwan Saharia, William Chan, Saurabh Saxena, Lala Li, Jay Whang, Emily Denton, Seyed Kamyar Seyed Ghaseimpour, Burcu Karagol Ayan, Tim Salimans, Jonathan Ho, David J Fleet, and Mohammad Norouzi. Photorealistic text-to-image diffusion models with deep language understanding. In *International Conference on Machine Learning (ICML)*, 2022.

- [145] Ranjan Sapkota and Manoj Karkee. Generative ai in agriculture: Creating image datasets using dall. e's advanced large language model capabilities. *arXiv preprint arXiv:2307.08789*, 2023.
- [146] Zehong Shen, Zhi Cen, Sida Peng, Qing Shuai, Hujun Bao, and Xiaowei Zhou. Learning human mesh recovery in 3d scenes. In *Proceedings of the IEEE/CVF Conference on Computer Vision and Pattern Recognition*, pages 17038–17047, 2023.
- [147] Abhishek Kumar Singh and Ioannis Patras. Fashionsd-x: Multimodal fashion garment synthesis using latent diffusion. *arXiv preprint arXiv:2404.18591*, 2024.
- [148] James Seale Smith, Yen-Chang Hsu, Lingyu Zhang, Ting Hua, Zsolt Kira, Yilin Shen, and Hongxia Jin. Continual diffusion: Continual customization of text-to-image diffusion with c-lora. *arXiv preprint arXiv:2304.06027*, 2023.
- [149] Kihyuk Sohn, Nataniel Ruiz, Kimin Lee, Daniel Castro Chin, Irina Blok, Huiwen Chang, Jarred Barber, Lu Jiang, Glenn Entis, Yuanzhen Li, et al. Styledrop: Text-to-image generation in any style. *arXiv preprint arXiv:2306.00983*, 2023.
- [150] Kechen Song and Yunhui Yan. A noise robust method based on completed local binary patterns for hot-rolled steel strip surface defects. *Applied Surface Science*, 285:858–864, 2013.
- [151] Martin Spitznagel, Jan Vaillant, and Janis Keuper. Physicsgen: Can generative models learn from images to predict complex physical relations? *arXiv preprint arXiv:2503.05333*, 2025.
- [152] Astitva Srivastava, Pranav Manu, Amit Raj, Varun Jampani, and Avinash Sharma. Wardrobe: Text-guided generation of textured 3d garments. In *European Conference on Computer Vision*, pages 458–475. Springer, 2024.
- [153] Jiaxiang Tang, Jiawei Ren, Hang Zhou, Ziwei Liu, and Gang Zeng. Dreamgaussian: Generative gaussian splatting for efficient 3d content creation. *arXiv preprint arXiv:2309.16653*, 2023.
- [154] Luming Tang, Nataniel Ruiz, Qinghao Chu, Yuanzhen Li, Aleksander Holynski, David E. Jacobs, Bharath Hariharan, Yael Pritch, Neal Wadhwa, Kfir Aberman, and Michael Rubinstein. Realfill: Reference-driven generation for authentic image completion. *ACM Transactions on Graphics*, 43(4):1–12, July 2024.
- [155] Sanli Tang, Fan He, Xiaolin Huang, and Jie Yang. Online pcb defect detector on a new pcb defect dataset, 2019.
- [156] Maxim Tatarchenko, Stephan R Richter, René Ranftl, Zhiwen Li, Vladlen Koltun, and Thomas Brox. What do single-view 3d reconstruction networks learn? In *Proceedings of the IEEE/CVF conference on computer vision and pattern recognition*, pages 3405–3414, 2019.
- [157] Andrew DH Thomas, Michael G Rodd, John D Holt, and CJ Neill. Real-time industrial visual inspection: A review. *Real-Time Imaging*, 1(2):139–158, 1995.
- [158] Dmitry Tochilkin, David Pankratz, Zexiang Liu, Zixuan Huang, Adam Letts, Yangguang Li, Ding Liang, Christian Laforte, Varun Jampani, and Yan-Pei Cao. Triposr: Fast 3d object reconstruction from a single image. *arXiv preprint arXiv:2403.02151*, 2024.
- [159] Michael Tschannen, André Susano Pinto, and Alexander Kolesnikov. Jetformer: An autoregressive generative model of raw images and text. *arXiv preprint arXiv:2411.19722*, 2024.
- [160] Hung-Yu Tseng, Qinbo Li, Changil Kim, Suhib Alsisan, Jia-Bin Huang, and Johannes Kopf. Consistent view synthesis with pose-guided diffusion models. In *Proceedings of the IEEE/CVF Conference on Computer Vision and Pattern Recognition*, pages 16773–16783, 2023.
- [161] Yuxiang Tuo, Wangmeng Xiang, Jun-Yan He, Yifeng Geng, and Xuansong Xie. Anytext: Multilingual visual text generation and editing. *arXiv preprint arXiv:2311.03054*, 2023.
- [162] Dani Valevski, Danny Lumen, Yossi Matias, and Yaniv Leviathan. Face0: Instantaneously conditioning a text-to-image model on a face. In *SIGGRAPH Asia 2023 Conference Papers*, pages 1–10, 2023.

- [163] Andrey Voynov, Qinghao Chu, Daniel Cohen-Or, and Kfir Aberman. $p+$: Extended textual conditioning in text-to-image generation. *arXiv preprint arXiv:2303.09522*, 2023.
- [164] Ziyu Wan, Bo Zhang, Dong Chen, Pan Zhang, Fang Wen, and Jing Liao. Old photo restoration via deep latent space translation. *IEEE Transactions on Pattern Analysis and Machine Intelligence*, 45(2):2071–2087, 2022.
- [165] Bochao Wang, Huabin Zheng, Xiaodan Liang, Yimin Chen, Liang Lin, and Meng Yang. Towards characteristic-preserving image-based virtual try-on network. In *Proceedings of the European Conference on Computer Vision (ECCV)*, pages 589–604, 2018.
- [166] Jiayu Wang, Yifei Ming, Zhenmei Shi, Vibhav Vineet, Xin Wang, Sharon Li, and Neel Joshi. Is a picture worth a thousand words? delving into spatial reasoning for vision language models. *Advances in Neural Information Processing Systems*, 37:75392–75421, 2024.
- [167] Jifeng Wang, Xiang Li, and Jian Yang. Stacked conditional generative adversarial networks for jointly learning shadow detection and shadow removal. In *Proceedings of the IEEE conference on computer vision and pattern recognition*, pages 1788–1797, 2018.
- [168] Jinbao Wang, Shujie Tan, Xiantong Zhen, Shuo Xu, Feng Zheng, Zhenyu He, and Ling Shao. Deep 3d human pose estimation: A review. *Computer Vision and Image Understanding*, 210:103225, 2021.
- [169] Junxiao Wang, Ting Zhang, Heng Yu, Jingdong Wang, and Hua Huang. Magicgeo: Training-free text-guided geometric diagram generation. *arXiv preprint arXiv:2502.13855*, 2025.
- [170] Xiaolong Wang, David Fouhey, and Abhinav Gupta. Designing deep networks for surface normal estimation. In *Proceedings of the IEEE conference on computer vision and pattern recognition*, pages 539–547, 2015.
- [171] Xinlong Wang, Xiaosong Zhang, Zhengxiong Luo, Quan Sun, Yufeng Cui, Jinsheng Wang, Fan Zhang, Yueze Wang, Zhen Li, Qiying Yu, et al. Emu3: Next-token prediction is all you need. *arXiv preprint arXiv:2409.18869*, 2024.
- [172] Xintao Wang, Ke Yu, Shixiang Wu, Jinjin Gu, Yihao Liu, Chao Dong, Yu Qiao, and Chen Change Loy. Esrgan: Enhanced super-resolution generative adversarial networks. In *Proceedings of the European conference on computer vision (ECCV) workshops*, pages 0–0, 2018.
- [173] Yihan Wang, Muyang Li, Han Cai, Wei-Ming Chen, and Song Han. Lite pose: Efficient architecture design for 2d human pose estimation. In *Proceedings of the IEEE/CVF conference on computer vision and pattern recognition*, pages 13126–13136, 2022.
- [174] Yuan Wang, Bin Zhu, Yanbin Hao, Chong-Wah Ngo, Yi Tan, and Xiang Wang. Cookingdiffusion: Cooking procedural image generation with stable diffusion. *arXiv preprint arXiv:2501.09042*, 2025.
- [175] Zhengyi Wang, Yikai Wang, Yifei Chen, Chendong Xiang, Shuo Chen, Dajiang Yu, Chongxuan Li, Hang Su, and Jun Zhu. Crm: Single image to 3d textured mesh with convolutional reconstruction model. In *European Conference on Computer Vision*, pages 57–74. Springer, 2024.
- [176] Daniel Watson, William Chan, Ricardo Martin-Brualla, Jonathan Ho, Andrea Tagliasacchi, and Mohammad Norouzi. Novel view synthesis with diffusion models. *arXiv preprint arXiv:2210.04628*, 2022.
- [177] Diana Wofk, Fangchang Ma, Tien-Ju Yang, Sertac Karaman, and Vivienne Sze. Fastdepth: Fast monocular depth estimation on embedded systems. In *2019 International Conference on Robotics and Automation (ICRA)*, pages 6101–6108. IEEE, 2019.
- [178] Haiyan Wu, Yanyun Qu, Shaohui Lin, Jian Zhou, Ruizhi Qiao, Zhizhong Zhang, Yuan Xie, and Lizhuang Ma. Contrastive learning for compact single image dehazing. In *Proceedings of the IEEE/CVF conference on computer vision and pattern recognition*, pages 10551–10560, 2021.

- [179] Jianzong Wu, Chao Tang, Jingbo Wang, Yanhong Zeng, Xiangtai Li, and Yunhai Tong. Diffsensei: Bridging multi-modal llms and diffusion models for customized manga generation. *arXiv preprint arXiv:2412.07589*, 2024.
- [180] Gui-Song Xia, Xiang Bai, Jian Ding, Zhen Zhu, Serge Belongie, Jiebo Luo, Mihai Datcu, Marcello Pelillo, and Liangpei Zhang. Dota: A large-scale dataset for object detection in aerial images. In *Proceedings of the IEEE conference on computer vision and pattern recognition*, pages 3974–3983, 2018.
- [181] Zhuofan Xia, Dongchen Han, Yizeng Han, Xuran Pan, Shiji Song, and Gao Huang. Gsва: Generalized segmentation via multimodal large language models. In *Proceedings of the IEEE/CVF Conference on Computer Vision and Pattern Recognition*, pages 3858–3869, 2024.
- [182] Guangxuan Xiao, Tianwei Yin, William T Freeman, Frédo Durand, and Song Han. Fastcomposer: Tuning-free multi-subject image generation with localized attention. *arXiv preprint arXiv:2305.10431*, 2023.
- [183] Jinqi Xiao, Miao Yin, Yu Gong, Xiao Zang, Jian Ren, and Bo Yuan. Comcat: Towards efficient compression and customization of attention-based vision models. *arXiv preprint arXiv:2305.17235*, 2023.
- [184] Xiaodan Xing, Siofra Murdoch, Chunling Tang, Giorgos Papanastasiou, Jan Cross-Zamirska, Yunzhe Guo, Xianglu Xiao, Carola-Bibiane Schönlieb, Yinhai Wang, and Guang Yang. Can generative ai replace immunofluorescent staining processes? a comparison study of synthetically generated cellpainting images from brightfield. *Computers in Biology and Medicine*, 182:109102, 2024.
- [185] Yinghao Xu, Zifan Shi, Wang Yifan, Hansheng Chen, Ceyuan Yang, Sida Peng, Yujun Shen, and Gordon Wetzstein. Grm: Large gaussian reconstruction model for efficient 3d reconstruction and generation. In *European Conference on Computer Vision*, pages 1–20. Springer, 2024.
- [186] Han Xue, Zhiwu Huang, Qianru Sun, Li Song, and Wenjun Zhang. Freestyle layout-to-image synthesis. In *Proceedings of the IEEE/CVF Conference on Computer Vision and Pattern Recognition*, pages 14256–14266, 2023.
- [187] Zhiyuan Yan, Junyan Ye, Weijia Li, Zilong Huang, Shenghai Yuan, Xiangyang He, Kaiqing Lin, Jun He, Conghui He, and Li Yuan. Gpt-imgeval: A comprehensive benchmark for diagnosing gpt4o in image generation. *arXiv preprint arXiv:2504.02782*, 2025.
- [188] Lu Yang, Wenhe Jia, Shan Li, and Qing Song. Deep learning technique for human parsing: A survey and outlook. *International Journal of Computer Vision*, 132(8):3270–3301, 2024.
- [189] Lu Yang, Qing Song, Zhihui Wang, Mengjie Hu, Chun Liu, Xueshi Xin, Wenhe Jia, and Songcen Xu. Renovating parsing r-cnn for accurate multiple human parsing. In *European Conference on computer vision*, pages 421–437. Springer, 2020.
- [190] Lu Yang, Qing Song, Zhihui Wang, and Ming Jiang. Parsing r-cnn for instance-level human analysis. In *Proceedings of the IEEE/CVF conference on computer vision and pattern recognition*, pages 364–373, 2019.
- [191] Lu Yang, Qing Song, Zhihui Wang, Zhiwei Liu, Songcen Xu, and Zhihao Li. Quality-aware network for human parsing. *IEEE Transactions on Multimedia*, 25:7128–7138, 2022.
- [192] Wei Yang, Wanli Ouyang, Xiaolong Wang, Jimmy Ren, Hongsheng Li, and Xiaogang Wang. 3d human pose estimation in the wild by adversarial learning. In *Proceedings of the IEEE conference on computer vision and pattern recognition*, pages 5255–5264, 2018.
- [193] Wenhan Yang, Robby T Tan, Jiashi Feng, Jiaying Liu, Zongming Guo, and Shuicheng Yan. Deep joint rain detection and removal from a single image. In *Proceedings of the IEEE conference on computer vision and pattern recognition*, pages 1357–1366, 2017.

- [194] Zhengyuan Yang, Linjie Li, Kevin Lin, Jianfeng Wang, Chung-Ching Lin, Zicheng Liu, and Lijuan Wang. The dawn of lmms: Preliminary explorations with gpt-4v (ision). *arXiv preprint arXiv:2309.17421*, 9(1):1, 2023.
- [195] Rüveyda Yilmaz, Kaan Keven, Yuli Wu, and Johannes Stegmaier. Cascaded diffusion models for 2d and 3d microscopy image synthesis to enhance cell segmentation. *arXiv preprint arXiv:2411.11515*, 2024.
- [196] Jason J Yu, Fereshteh Forghani, Konstantinos G Derpanis, and Marcus A Brubaker. Long-term photometric consistent novel view synthesis with diffusion models. In *Proceedings of the IEEE/CVF International Conference on Computer Vision*, pages 7094–7104, 2023.
- [197] Jiahui Yu, Yuanzhong Xu, Jing Yu Koh, Han Zhang, Jason Baldridge, and Yonghui Wu. Scaling autoregressive models for content-rich text-to-image generation. *arXiv preprint arXiv:2206.10789*, 2022.
- [198] Ivana Žeger, Sonja Grgic, Josip Vuković, and Gordan Šišul. Grayscale image colorization methods: Overview and evaluation. *IEEE access*, 9:113326–113346, 2021.
- [199] Mingliang Zhai, Xuezhi Xiang, Ning Lv, and Xiangdong Kong. Optical flow and scene flow estimation: A survey. *Pattern Recognition*, 114:107861, 2021.
- [200] He Zhang, Vishwanath Sindagi, and Vishal M Patel. Image de-raining using a conditional generative adversarial network. *IEEE transactions on circuits and systems for video technology*, 30(11):3943–3956, 2019.
- [201] Kai Zhang, Lingbo Mo, Wenhui Chen, Huan Sun, and Yu Su. Magicbrush: A manually annotated dataset for instruction-guided image editing. *Advances in Neural Information Processing Systems*, 36:31428–31449, 2023.
- [202] Lvmin Zhang, Anyi Rao, and Maneesh Agrawala. Adding conditional control to text-to-image diffusion models. In *Proceedings of the IEEE/CVF International Conference on Computer Vision*, pages 3836–3847, 2023.
- [203] Richard Zhang, Phillip Isola, and Alexei A Efros. Colorful image colorization. In *Computer Vision–ECCV 2016: 14th European Conference, Amsterdam, The Netherlands, October 11–14, 2016, Proceedings, Part III* 14, pages 649–666. Springer, 2016.
- [204] Tao Zhang, Xiangtai Li, Hao Fei, Haobo Yuan, Shengqiong Wu, Shunping Ji, Chen Change Loy, and Shuicheng Yan. Omg-llava: Bridging image-level, object-level, pixel-level reasoning and understanding. *Advances in Neural Information Processing Systems*, 37:71737–71767, 2024.
- [205] Weidong Zhang, Ling Zhou, Peixian Zhuang, Guohou Li, Xipeng Pan, Wenyi Zhao, and Chongyi Li. Underwater image enhancement via weighted wavelet visual perception fusion. *IEEE Transactions on Circuits and Systems for Video Technology*, 34(4):2469–2483, 2023.
- [206] Xincheng Zhang, Ling Yang, Guohao Li, Yaqi Cai, Jiake Xie, Yong Tang, Yujiu Yang, Mengdi Wang, and Bin Cui. Itercomp: Iterative composition-aware feedback learning from model gallery for text-to-image generation. *arXiv preprint arXiv:2410.07171*, 2024.
- [207] Yongming Zhang, Tianyu Zhang, and Haoran Xie. Texcontrol: Sketch-based two-stage fashion image generation using diffusion model. In *2024 Nicograph International (NicoInt)*, pages 64–68. IEEE, 2024.
- [208] Yuxin Zhang, Weiming Dong, Fan Tang, Nisha Huang, Haibin Huang, Chongyang Ma, Tong-Yee Lee, Oliver Deussen, and Changsheng Xu. Prospect: Prompt spectrum for attribute-aware personalization of diffusion models. *ACM Transactions on Graphics (TOG)*, 42(6):1–14, 2023.
- [209] Yiming Zhao and Zhouhui Lian. Udifftext: A unified framework for high-quality text synthesis in arbitrary images via character-aware diffusion models. *arXiv preprint arXiv:2312.04884*, 2023.

- [210] Guangcong Zheng, Xianpan Zhou, Xuewei Li, Zhongang Qi, Ying Shan, and Xi Li. Layout-diffusion: Controllable diffusion model for layout-to-image generation. In *Proceedings of the IEEE/CVF Conference on Computer Vision and Pattern Recognition*, pages 22490–22499, 2023.
- [211] Yu Zheng, Jiahui Zhan, Shengfeng He, Junyu Dong, and Yong Du. Curricular contrastive regularization for physics-aware single image dehazing. In *Proceedings of the IEEE/CVF conference on computer vision and pattern recognition*, pages 5785–5794, 2023.
- [212] Zhihang Zhong, Mingdeng Cao, Xiang Ji, Yinqiang Zheng, and Imari Sato. Blur interpolation transformer for real-world motion from blur. In *Proceedings of the IEEE/CVF Conference on Computer Vision and Pattern Recognition*, pages 5713–5723, 2023.
- [213] Bolei Zhou, Hang Zhao, Xavier Puig, Sanja Fidler, Adela Barriuso, and Antonio Torralba. Scene parsing through ade20k dataset. In *Proceedings of the IEEE conference on computer vision and pattern recognition*, pages 633–641, 2017.
- [214] Bolei Zhou, Hang Zhao, Xavier Puig, Tete Xiao, Sanja Fidler, Adela Barriuso, and Antonio Torralba. Semantic understanding of scenes through the ade20k dataset. *International Journal of Computer Vision*, 127:302–321, 2019.
- [215] Feng Zhou, Jianqin Yin, and Peiyang Li. Lifting by image–leveraging image cues for accurate 3d human pose estimation. In *Proceedings of the AAAI Conference on Artificial Intelligence*, volume 38, pages 7632–7640, 2024.
- [216] Hao Zhou, Sunil Hadap, Kalyan Sunkavalli, and David W Jacobs. Deep single-image portrait relighting. In *Proceedings of the IEEE/CVF international conference on computer vision*, pages 7194–7202, 2019.
- [217] Yupeng Zhou, Daquan Zhou, Ming-Ming Cheng, Jiashi Feng, and Qibin Hou. Storydiffusion: Consistent self-attention for long-range image and video generation. *Advances in Neural Information Processing Systems*, 37:110315–110340, 2024.
- [218] Luyang Zhu, Dawei Yang, Tyler Zhu, Fitsum Reda, William Chan, Chitwan Saharia, Mohammad Norouzi, and Ira Kemelmacher-Shlizerman. Tryondiffusion: A tale of two unets. In *Proceedings of the IEEE/CVF Conference on Computer Vision and Pattern Recognition*, pages 4606–4615, 2023.
- [219] Zuo-Liang Zhu, Zhen Li, Rui-Xun Zhang, Chun-Le Guo, and Ming-Ming Cheng. Designing an illumination-aware network for deep image relighting. *IEEE Transactions on Image Processing*, 31:5396–5411, 2022.